



Durham E-Theses

The electrification of ice and water at temperatures around the freezing point

Dawson, Roger

How to cite:

Dawson, Roger (1969) *The electrification of ice and water at temperatures around the freezing point*, Durham theses, Durham University. Available at Durham E-Theses Online:
<http://etheses.dur.ac.uk/8682/>

Use policy

The full-text may be used and/or reproduced, and given to third parties in any format or medium, without prior permission or charge, for personal research or study, educational, or not-for-profit purposes provided that:

- a full bibliographic reference is made to the original source
- a [link](#) is made to the metadata record in Durham E-Theses
- the full-text is not changed in any way

The full-text must not be sold in any format or medium without the formal permission of the copyright holders.

Please consult the [full Durham E-Theses policy](#) for further details.

3

THE ELECTRIFICATION OF ICE AND WATER

AT TEMPERATURES AROUND THE FREEZING POINT.

A thesis presented in candidature for the degree of Doctor

of Philosophy in the University of Durham,

by

Roger Dawson, B.Sc.,
of the Graduate Society.

August, 1969.

The copyright of this thesis rests with the author.
No quotation from it should be published without
his prior written consent and information derived
from it should be acknowledged.



The Electrification of Ice and Water at Temperatures
around the Freezing Point.

R. Dawson

August 1969.

ABSTRACT.

An attempt has been made to see whether there is a basic charge separation process which operates between ice and water when they are moving relative to one another. Measurements have also been made on the potential differences produced between ice and water under a variety of different conditions and the effect on the potential differences of having air bubbles within the ice/water interface has been studied.

Apparatus is described for the measurement of the electrical effects on freezing and melting bulk samples of water. No evidence has been found for a charge separation process which operates only when water moves relative to ice at the freezing point. However, the results show that at freezing rates of $10 \mu\text{m s}^{-1}$ and above that the mechanism proposed by Workman and Reynolds (1950) is responsible for the majority of the net charge separated, whereas, at very low freezing rates or on melting, the Temperature Gradient Mechanism, proposed by Latham and Mason(1961) predominates.

The relevance of the electrification of ice and water to the origin of electrical charges in clouds is discussed, and

explanations of the results of earlier work on simulations of conditions in clouds are put forward, in the light of the results obtained during the experiments with bulk water samples.

FOREWORD.

The S.I. system of units has been used exclusively in the experimental work described in this thesis. Occasionally, other units have been used, for example, in the discussion of the structure of ice and water, but only where comparisons are being made between two values of a parameter in the same units.

I should like to express my sincere thanks to all those people who have assisted me in any way during both the work described in, and the preparation of, this thesis.

In particular, I am indebted to my supervisor for the past two and a half years, Dr. W. C. A. Hutchinson, and to Dr. G. Kohnstam of the Chemistry Department in Durham and the late Professor J. A. Chalmers, who suggested the topic. Thanks are also due to Professor G. D. Rochester, F.R.S., for the provision of the research and other facilities in the Physics Department, to my fellow research students in the Atmospheric Physics Group, for their helpful comments and suggestions, to the technical staff of the Physics and Chemistry Departments, in particular Mr. J. Morajee who was responsible for the construction of most of the apparatus, and to the United States Office of Naval Research, for their financial support during the first year and a half of the work under contracts numbers N62558 - 4299 and F61052 -68-C -0007.

Finally, I must thank Miss G. C. Hedley, for her secretarial help during the preparation of this thesis, Mrs. M. Kimmitt, for her speed and efficiency in the preparation of the typescript, and Mr. J. Normile, who duplicated the completed typescript.

TABLE OF CONTENTS.

ABSTRACT

FOREWORD

CHAPTER I.	INTRODUCTION	page	1
I.1.	The Nature of the Problem		1
I.2.	The Thunderstorm		2
I.3.	Theories of Thunderstorm Electrification.		4
	I.3(a) Dinger and Gunn, 1946		7
	I.3(b) Workman and Reynolds, 1948		7
	I.3(c) The theory of Reynolds, Brook and Gourley, 1957		9
	I.3(d) The theory of Latham and Mason, 1961		10
	I.3(e) Reiter's theory, 1965		10
I.4.	The Electrification of Non-stormy Clouds		11
	I.4(a) The nimbo-stratus cloud		11
	I.4(b) Trade-wind cumulus clouds		12
	I.4(c) Minor shower clouds		13
	I.4(d) Other cloud studies		13
CHAPTER II.	THE STRUCTURE OF ICE AND WATER	page	14
II.1.	The Structure of Ice		14
II.2.	The Structure of Water		16
II.3.	Charge Transport in Water		17
II.4.	Charge Transport in Ice		19.

CHAPTER III.	THE ELECTRIFICATION OF ICE AND WATER	page 21
III.1.	Charge Separation in Ice	21
III.1(a)	Electrification directly associated with temperature gradients in ice	21
III.1(b)	Electrification associated with the evaporation of an ice surface	24
III.1(c)	Charge separation associated with the cracking and fracturing of ice	25
III.2.	The Separation of Electric Charge in Melting Ice	25
III.3.	Charge Separation in Water	26
III.3(a)	Spraying, splashing and bubbling phenomena	26
III.3(b)	Solid/liquid interfacial phenomena	26
III.3(c)	Temperature gradients in solutions	29.
III.4.	Charge Separated by the Freezing of Water	29.
CHAPTER IV.	LABORATORY SIMULATIONS OF CONDITIONS IN CLOUDS AND THE ELECTRIFICATION OF HAIL AND SNOW	page 32
IV.1.	The Electrification of Single Water Drops	32
IV.1(a)	The work of Mason and Maybank	33
IV.1(b)	The work of Kachurin and Bekryaev	34
IV.1(c)	The work of Hutchinson, Evans and Stott	35
IV.1(d)	The work of Rogers.	35

IV.2.	Hail and Simulated Hailstones	page 36
IV.2(a)	The electrification of hail and snow by collision with droplets.	37
IV.2(b)	The electrification of hail and snow by collision with ice particles.	42
IV.2(c)	Electrification on melting	43
IV.3.	Electrification Associated with the Formation of Spongy Ice on Hail.	45
CHAPTER V.	EXPERIMENTAL INVESTIGATION OF THE ELECTRICAL EFFECTS AT ICE/WATER INTERFACES	46
V.1.	Experiments with Ice-coated Balls	46
V.2.	The Rotating Tube Experiment	49
V.3.	Electrical Measurements with Ice Tubes	54
V.3(a)	Experiments with unsupported ice capillary tubes.	56
V.3(b)	The perspex tube experiments	59
CHAPTER VI.	THE FREEZING POTENTIAL MEASUREMENTS	63
VI.1.	The Design of the Apparatus	63
VI.1(a)	The size of the freezing cell	63
VI.(b)	The method of cooling the freezing face	64
VI.1(c)	The nature of the electrodes	65
VI.2.	Early Experiments with the Freezing Cells	67
VI.2(a)	General experimental method	67
VI.2(b)	Observations	67

VI.3.	The Effect of Air Bubbles on the Freezing Potentials	page 70
VI.4.	The Effect of the Freezing Rate on the Freezing Potential	72
VI.4(a)	The effect of the supercooling on the freezing potentials	73
VI.4(b)	The instantaneous relationship between freezing potential and freezing rate	74
VI.4(c)	The effect on the freezing potentials of stirring the solutions	77
VI.4(d)	A possible explanation for the shape of the voltage against time graphs	80
VI.5.	The Effect of Impurities on the Freezing Potentials	82
VI.5(a)	Changes in pH	82
VI.5(b)	Changes in conductivity	84
VI.5(c)	Changing the electrode material	85
VI.6.	Other Experiments with the Freezing Cells	86
CHAPTER VII.	THE ELECTRIFICATION OF WATER FLOWING THROUGH AN ICE TUBE SUPPORTED IN A GLASS COOLING-JACKET.	87
VII.1.	The Design of the Apparatus	88
VII.1(a)	The basic apparatus	88
VII.1(b)	Experimental method and early results	90

VII.2. The Controlled-Environment Box	page 96
VII.2(a) The purity of the water	100
VII.2(b) Experimental details	102
VII.2(c) The graphs of voltage against time for the freezing tube	105
VII.3. Conclusions	107
CHAPTER VIII. CONCLUSIONS AND POSSIBLE APPLICATIONS TO CLOUD PHENOMENA	110
VIII.1. Conclusions which can be drawn from the Freezing Experiments	110
VIII.2. Possible Applications of the Results to Cloud Electrification Phenomena	113
VIII.2(a) The electrification of simulated hailstones	113
VIII.2(b) The charge separated on melting	119
VIII.3. The Electrification of Melting Snow on the Ground	120
CHAPTER IX. SUGGESTIONS FOR FURTHER WORK	122
APPENDICES.	
REFERENCES.	

CHAPTER I.

INTRODUCTION

I. 1. The Nature of the Problem.

Electrical activity in thunderclouds seems to arise as soon as the ice phase is detected and hail often accompanies thunderstorms. The sign of the charge on falling snow and, according to Bent and Hutchinson (1965) on lying snow, changes when melting occurs.

In endeavouring to reconcile the widely differing laboratory results of Reynolds, Brook and Gourley (1957) and Latham and Mason (1961 B) on the electrification of hail, Church (1966) detected a separation of electric charge when a simulated hailstone moving at terminal velocity in air was struck by uncharged water droplets which shattered on impact leaving a glassy surface on the hailstone and producing several smaller droplets. In general, the simulated hailstone became negatively charged on encountering droplets whose temperatures were below $+2^{\circ}\text{C}$ and positively charged on encountering droplets whose temperatures were above $+2^{\circ}\text{C}$. He found that the charge separated was a maximum for droplets at -3°C .

Bent and Hutchinson (1965) investigated the electric space charge density at heights of 1 m and 2 m over lying snow and found an unusual effect on rapid melting of a snow surface over which a wind was blowing with velocity 7 to 14 m s^{-1} . The space charge density at 2 m was $+6.3\text{ pC m}^{-3}$ and at 1 m was -9.4 pC m^{-3} . Normally the upper collector registered the same sign of electric charge as the lower collector.

These results may, perhaps, be explained in terms of either a charge separation mechanism which operates when liquid water moves relatively to ice or some modification of recognised charge separation processes



caused by motion of the water. It is the purpose of the present work to investigate these possibilities.

I. 2. The Thunderstorm.

The electric charge separation processes in thunderclouds are more effective than in other types of cloud. Many of the laboratory experiments on charge separation processes have attempted to simulate conditions in clouds and, in order to compare the results of the laboratory experiments with measurements made on natural clouds, it is necessary to have some idea of the prevailing conditions. Since there is a wide variation in the characteristics of, and conditions within, thunderstorms, great care should be exercised in applying results obtained during one particular storm to thunderstorms in general.

The most intensive study of cumulonimbus clouds which developed into thunderstorms was that of Braham and Byers (1949). Using both radar and aircraft measurements, they showed that a cumulonimbus cloud consists of one or more localised regions of pronounced precipitation, vertical wind velocity and electrical activity. These active regions or cells varied in size from 0.5 km to 10 km in horizontal extent, although Kuettner (1950) has proposed the existence of sub-cells which may be only of the order of 100 m diameter. According to Byers and Braham the cells go through three stages of evolution.

- (i) A cumulus phase, with updraughts throughout.
- (ii) A mature phase, when a strong updraught is surrounded by a region of down-draughts and there is intense precipitation and electrical activity.
- (iii) A dissipating stage, when the down-draught spreads throughout the entire cell.

Workman and Holzer (1942) reported that the updraught sometimes displays a pulse-like nature and may have a velocity of up to 50 m s^{-1} , although 10 m s^{-1} is said to be more typical.

Hail may fall from regions of the cell where the updraught is too weak to support it and may reach the ground either as hail or rain. Usually, the hail is in the form of rounded or conical shapes of from 4 to 6 mm across, although very large hailstones do occur, particularly in association with very active thunderclouds. Rates of precipitation of hail of up to 5 cm hr^{-1} have been reported. During the later stages of the storm, the hail may give way to snow.

Most thunderclouds are characterised by their great vertical depth, which may be up to 10 km and the wide temperature range which this must necessarily involve. The bases are normally warmer than 0°C and the tops may extend beyond the -40°C isotherm. Often the cloud top consists of an anvil-shaped mass of ice crystals but Moore (1965) has reported lightning activity from clouds having different physical dimensions and appearances from this picture and whose tops were said to be warmer than 0°C .

Many models have been proposed for the distribution of charges within a thundercloud. Wilson (1925) showed that the cloud may be regarded as a simple dipole with the positive pole uppermost, provided that it is observed from a horizontal distance much greater than the height of the cloud and the separation of the charges. Simpson and Robinson's results (1940) also suggested that the cloud is usually of positive polarity but they found some evidence for a region of positive charge in the base. The exact location of the positive charge is said,

by Williams (1958), to be in the updraught of the front of the cloud and close to the sharp boundary of the front of the precipitation zone, occupying a width of the order of 1 km in the direction of motion of the cloud.

The precise locations of the main upper positive and lower negative centres of charge are not known. Malan and Schonland (1951) used five different methods to show that successive lightning strokes come from charge centres lying at increasing heights, probably in the same vertical column but Brook (1969) states that the evidence for a vertical distribution of charge centres is not conclusive and that there is some evidence to suggest that the position of the charge centres depends on the direction of motion of the cloud and the angle of the main up- and down-draughts to the vertical. Browning (1968) has shown that the up- and down-draughts are often not vertical and may be at different inclinations to each other. However, it is generally true that the positive charge centre lies at a higher altitude than the negative. (See Table I.1)

I.3. Theories of Thunderstorm Electrification.

Many theories of thunderstorm electrification have been proposed. They may be divided into three main classes according to the way in which the charges are separated.

- (i) Classical; in which the charge is separated by the interaction of initially neutral cloud particles.
- (ii) Influence; in which the positive and negative charges are available as atmospheric ions.
- (iii) Convection; in which the origin of the charges is outside the cloud.

	SIMPSON & ROBINSON (1940.)		GISH & WAIT (1950.)		MALAN (1952)	
	charge	height	charge	height	charge	height
UPPER + CHARGE.	+24C	6 km	+39C	9.5km	+40C	10 km
- CHARGE CENTRE	-20C	3 km	-39C	5km	-40C	5 km
LOWER + CHARGE.	+4C	1.5Km			+10C	2 Km

TABLE I.1. Charge Distribution in
Thunderclouds.

Theories have also been proposed which are combinations of these mechanisms.

The viability of many of these theories depends on whether the electrification is caused by precipitation. In observations on twelve thunderstorms, Workman and Reynolds (1949) observed that radar returns indicating the presence of large particles within the cloud occurred several minutes before precipitation was visible or electrical activity was evident. They also noted that the top of the "radar cloud" descended at about the time electrical activity, i.e. lightning discharges, began. However, Moore (1965 A & B), while agreeing that a radar echo can always be detected in clouds before the occurrence of lightning, states that the strength of the echo indicates that precipitation is only present with equivalent intensities of, typically, 1 to 3 mm hr⁻¹ in stagnant air. Since the rain echo strength increases a hundred- or a thousand-fold within 10 to 20 s after the lightning discharge, he infers that lightning is the cause rather than the result of the intense precipitation. This is obviously an issue which will not be finally settled without many more investigations.

Chalmers (1965) states that if it is accepted that precipitation plays a necessary part in the process of separation of the main charges in the thundercloud, any theory to account for this must satisfy certain conditions.

- (i) The process must give a positive upper and a negative lower charge.
- (ii) The process must give a rate of separation of charge of up to several amperes.
- (iii) The process must operate at temperatures below the freezing point.

(iv) The process must be connected with precipitation in the solid form.

(v) If the same process operates in nimbo-stratus clouds, it must do so much less effectively than in cumulo-nimbus clouds.

From these requirements and from the need for any process suggested to fit in with existing knowledge of cloud phenomena, including the initiation of precipitation, certain general results can be deduced.

In the gravitational separation in space, for the heavier particles, which must carry down negative charge, requirement (iv) suggests that these must be solid precipitation particles. The lighter particles, carrying a positive charge, must move upwards in the rising air of the storm and might be ions in the air, or cloud droplets, or fragments of water or ice smaller than the precipitation particles.

In order to account for (v) above, it is necessary to postulate some property of the cloud, important in charge separation, that differs between cumulo-nimbus and nimbo-stratus clouds.

The following is a list of the names of those who have proposed theories of cloud electrification during this century.

1905	Gerdien	1948	Rossmann
1909	Simpson	1948	Workman & Reynolds
1913	Elster & Geitel	1948	Wall
1929	Wilson	1955	Vonnegut
1935	Gunn	1956	Wilson
1937	Simpson & Scrase	1957	Reynolds, Brook & Gourley
1940	Findeisen	1961	Latham & Mason
1944	Frenkel	1961	Sartor

1946	Dinger & Gunn	1963	Magono & Takahashi
1947	Grenet	1965	Reiter.

A brief outline of some of these theories involving the presence of both ice and water is set out below.

I. 3(a). Dinger and Gunn, 1946

In experiments on the electrification of water and ice on freezing and melting, Dinger and Gunn reported a charge separation of $4.2 \times 10^{-10} \text{ C g}^{-1}$ of ice melted with the water becoming positive and the released air bubbles becoming negatively charged. This rate of charge separation may be sufficiently large to explain electric fields as great as those commonly encountered in thunderstorms but the polarity is of the wrong sign to explain the origin of the main thunderstorm dipole. However, it has been suggested that the charge acquired by melting hail contributes to the lower positive charge in thunderclouds.

I. 3(b). Workman and Reynolds, 1948.

Costa Ribiero (1945) discovered that large potential differences were set up between ice and water on freezing dilute aqueous solutions. Workman and Reynolds (1948-50) also studied the effect and applied their results to electrification of clouds. They envisaged that an ice crystal, formed by sublimation near the top of the cloud, would fall and encounter supercooled droplets at a sufficiently low temperature to form a rime ice-pellet or graupel. Growth by this process would continue until a level of about -10°C or -15°C was reached, where glaze ice would form upon the pellet. It would grow by this process and its rate of fall would increase relative to the suspended, or perhaps ascending, super-

cooled waterdrops. In the region of about -10°C , if conditions were favourable, these drops should impinge upon the cold, glazed pellet, and a portion of the water should freeze to its surface in a thin layer. The remaining portion of the water, because of splash effects and the velocity of the hail pellet relative to air, would become detached in small drops carrying positive charges which would be transported into the cloud above. Eventually the degree of supercooling of the impinging droplets would decrease to the extent that the hailstone would cease its growth and start melting, whereupon it should share its negative charge with the impinging droplets and ultimately the charge would be reduced toward zero. The negatively charged droplets would then encounter more hailstones and their previously acquired negative charge should make it possible for the new hail pellets to acquire still bigger charges and so on. This theory, therefore, predicts that the cloud will have positive polarity, that the negative charge centre will remain at about a constant height and it requires that the cloud must extend below the 0°C isotherm.

However, laboratory experiments by Reynolds et al (1957) and Latham and Mason (1961 B) have failed to confirm that sufficient charge can be separated by collisions between a wet, simulated hailstone and supercooled water droplets but Church (1966) observed that a rotating, iced probe became negatively charged on encountering droplets whose temperature was below $+2^{\circ}\text{C}$ and positively charged on encountering droplets whose temperature was above $+2^{\circ}\text{C}$. He also noted that the amount of charge separated on these occasions was not significantly affected by heating the probe with an infra-red lamp. This theory and these results

will be discussed more fully at a later stage.

I. 3(c). The theory of Reynolds, Brook and Gourley, 1957.

From their laboratory measurements, Reynolds et al. (1957) estimated that when ice crystals collided with hailstones in the presence of water droplets, the mean charge separated by a rebounding ice crystal was 0.17 pC leaving the hailstone negatively charged. Applying this result to a model thundercloud containing a liquid water content of 1 g m^{-3} and a crystal concentration of 10^4 m^{-3} , they showed that hail in concentrations of 10 g m^{-3} , falling at 10 m s^{-1} relative to the ice crystals, was capable of producing a 20 C discharge in a cell 1 km in diameter in about 14 minutes. In a thundercloud of volume 50 km^3 , sufficient charge would be separated to account for the repetition of lightning discharges.

Latham and Mason (1961 B) performed similar experiments and concluded that the electrification of hailstones by ice crystals was five orders of magnitude less than the results of Reynolds et al., clearly indicating that the mechanism was insufficient to explain thunderstorm electrification. Church (1966) found a charge separation between these two values which was two orders of magnitude less than the results of Reynolds et al.. These results could not be quantitatively explained in terms of the "Temperature Gradient Theory" (Latham and Mason 1961 A) although the sign of the charge separation was as predicted by this theory. Church states that any attempt to produce closer correspondence with the results of Reynolds et al. would be based on speculation. Clearly, further work is required in this direction.

I. 3(d). The Theory of Latham and Mason, 1961.

Latham and Mason (1961 B) investigated the charge separated by the shattering of supercooled water droplets on hailstones. They concluded that the electrification of the average thundercloud could be explained by the splintering of droplets with diameters in the range 0.04 mm to 0.1 mm on hailstones. They estimated that charge would be segregated at a rate of $1 \text{ C km}^{-3} \text{ min.}^{-1}$. However, this rate of charge separation may only be 1% of that found in violent thunderstorms and this has not been satisfactorily explained.

I. 3(e). Reiter's theory, 1965.

A subsidiary charge separation mechanism was proposed by Reiter (1965). It is claimed that a charge separation of $15 \text{ C km}^{-3} \text{ min}^{-1}$ will result.

Reiter showed that appreciable quantities of nitrate ions are produced in clouds by silent electrical discharges and that the greater the degree of atmospheric instability, the greater the number of ions produced. Laboratory experiments showed that when ice particles, grown by sublimation, broke away from a cold plate they carried 10 to 50 times more charge when they had been grown in an atmosphere containing nitrous gases than when they had been grown in ordinary air. He applied these results to thunderclouds and suggested that some atmospheric feedback process was operating in which the charge separation mechanism was the fragmentation of crystal dendrites, needles and splinters from the surface of hailstones in a nitrous atmosphere. He believed that these charged particles could be separated in a way which would increase both

the field and the nitrate ion concentration, leading to an increase in the charge separated on fragmentation.

Many of the questions posed by this theory remain unanswered. The degree of fragmentation of ice particles in thunderclouds is unknown. No inhibiting process preventing charge build-up in other forms of clouds up to the point where discharges occur has been proposed and no explanation is given of how the charges are segregated so as to enhance the field.

These few examples illustrate the wide divergency of approach to the problems of thundercloud electrification and the difficulties which must be overcome in proposing a viable theory.

I. 4. The Electrification of Non-stormy Clouds.

The study of the electrical effects of non-stormy clouds has been somewhat neglected compared with the study of the more intense effects in thunderclouds.

I. 4(a). The nimbo-stratus cloud

In the absence of any measurements with airborne instruments, such as the alti-electrograph, in nimbo-stratus clouds, the only information available is that which has been obtained from currents and potential gradients at the earth's surface. Chalmers (1965), assuming a quasi-static state during continuous, steady precipitation when the total vertical current density would be the same at all levels, states that there must be a negative current downwards so that the conduction current above the cloud brings down negative charge. Therefore, the potential of the top of the cloud must be above that of the electrosphere, i.e. greater than $+ 2.9 \times 10^5$ V with respect to earth.

Measurements at the ground indicate that the polarity of a nimbo-stratus snow cloud is the same as that of the main charges in a thundercloud.

In the nimbo-stratus rain cloud there appear to be two processes at work. It is reasonable to suppose, in view of the great vertical depth of these clouds, that, in the main, the raindrops falling from these clouds will have been in the solid state for part of their previous history. It is fairly certain, therefore, that there occurs within the cloud the same process as for the snow cloud. Since results show that in the rain cloud the total charge separation is usually in the opposite direction to the snow cloud, there must be some other process of charge separation giving negative above and positive below. Chalmers (1965) points out that since we know that there must be two processes operating in thunderclouds to produce the main dipole and the lower positive charge and since, in both cases, the direction of the separation of charge is the same, it is very tempting to suggest that the same processes are at work, on a different scale of intensity, in both types of cloud.

I. 4(b). Trade-wind cumulus clouds.

Fitzgerald (1956) and Fitzgerald and Byers (1958) investigated the electrical structure of small cumulus clouds. Their results showed that these clouds had an excess negative charge of 10^{-3} C with indications of a positive charge in the upper part of the clouds when no ice was present. The negative charge was centred on regions of high liquid water content. As soon as solid precipitation was observed, a positive charge appeared of greater magnitude than the negative charge in all-

water clouds.

I. 4(c). Minor shower clouds.

Tamura (1956) investigated clouds of dimensions of the order of 2 to 3 km which gave potential gradients in the range $\pm 2 \text{ kV m}^{-1}$. In seven out of ten cases the polarity of the clouds was negative so that the separation of charge is in the opposite direction to that in the typical thunderstorm. Usually the showers were mainly of snow and were caused by convection.

I. 4(d). Other cloud studies.

Several workers have investigated the charges on cloud particles in non-precipitating clouds. In general it appears that the larger droplets have positive charges and smaller droplets have negative charges. Where ice is present, it is usually negatively charged. (See Chalmers (1965) Section 13. 8.)

CHAPTER II.

THE STRUCTURE OF ICE AND WATER.

In order to understand the processes by which charge is separated in ice and water, it is necessary to have some knowledge of the structure. Ice is dealt with first, as its structure is the more fundamental and the better characterised.

II.1. The Structure of Ice.

Ice may exist in many crystalline forms which are produced either by high pressures or low temperatures. (See Fig. II.1.) The diagram shows that the only stable form in conditions which usually prevail in the atmosphere is the hexagonal Ice I.

Within this structure, each oxygen atom is surrounded by four hydrogen atoms in a tetrahedral arrangement. (See Fig. II.2.). Bernal and Fowler (1933) proposed three "rules" governing the structure.

- (i) The hydrogen atoms lie at equilibrium positions along lines joining neighbouring oxygen atoms.
- (ii) There is only one hydrogen atom on each such linkage, forming a "hydrogen-bond".
- (iii) Each oxygen atom has two near hydrogen atom neighbours, thus preserving the structure of the water molecule.

The "hydrogen-bond" in ice has a free-energy of formation which is about one tenth of the energies of formation of normal covalent or ionic bonds. Pauling (1949) considered a simplified model $O - H \cdots O$, and disregarded all other electrons except two for the bond $O - H$ and two for a "lone-pair", i.e. a non-bonding pair of electrons, on

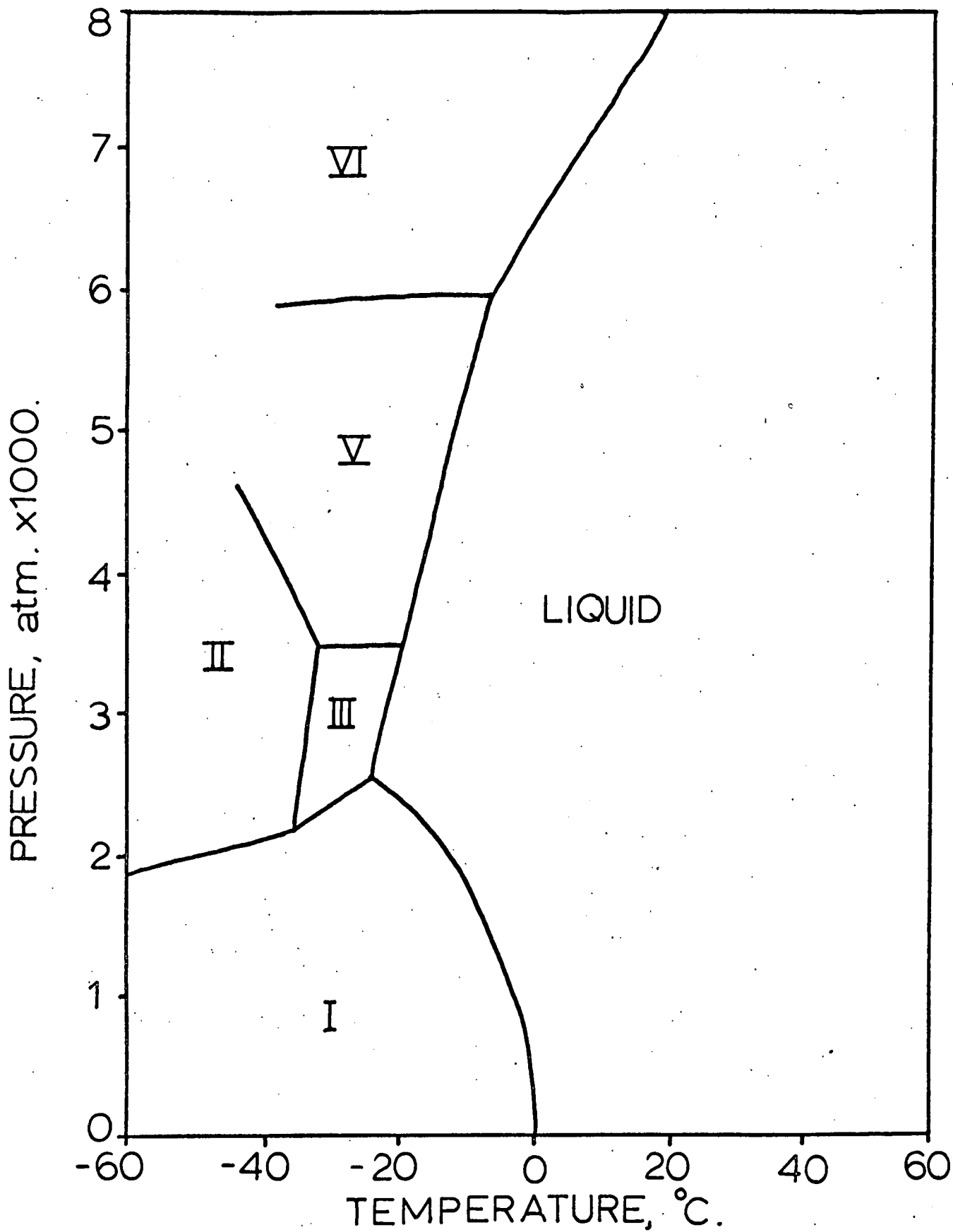
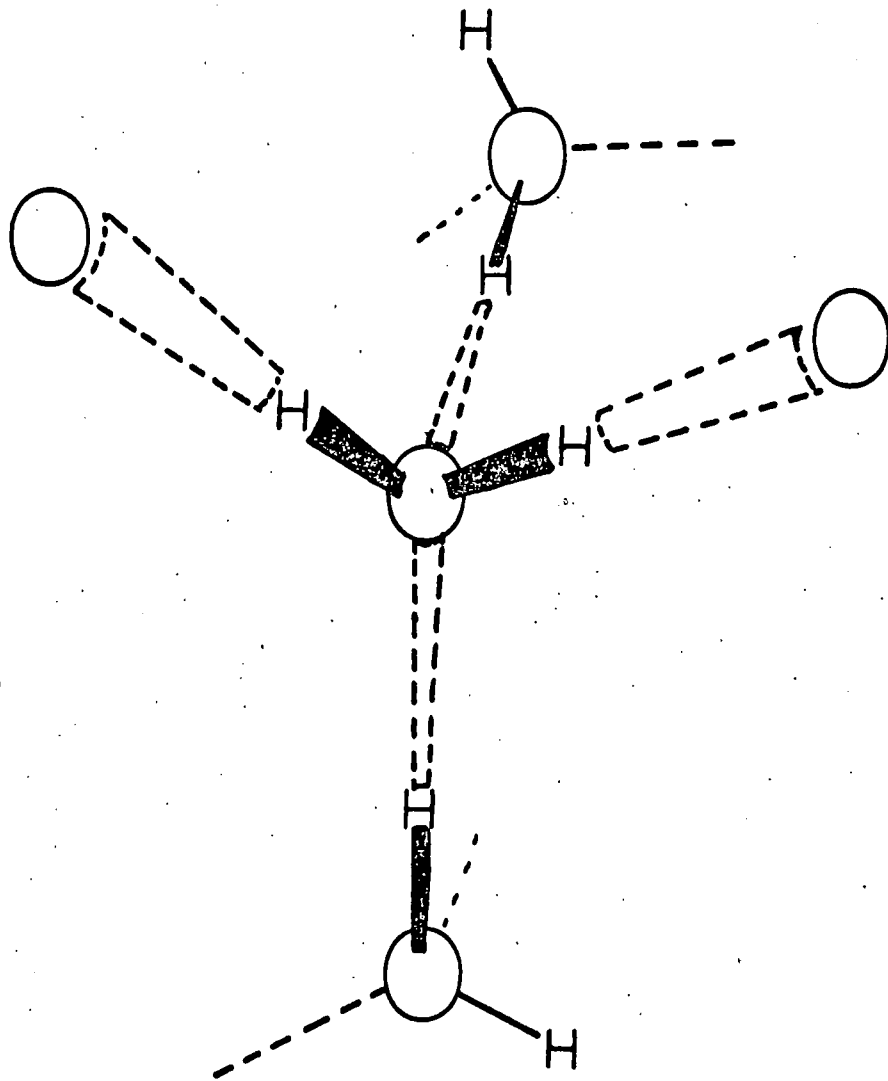


Fig. II.1. the polymorphism of ice.

----- hydrogen-bond.

— co-valent bond.



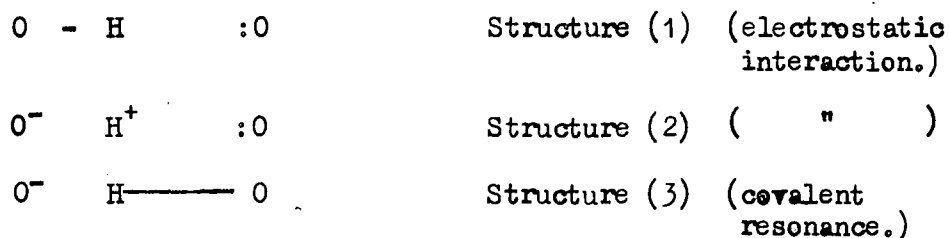
O—H bond length = 1.0 \AA

O---H bond length = 1.76 \AA

Fig. II.2.

the Bernal-Fowler model of
the structure of ice.

the other oxygen atom. He anticipated that the following structures are likely to contribute to some extent.



(The energy necessary for the production of divalent hydrogen is far too high for it to contribute in any way to the true structure.)

Coulson and Danielsson (1954) have considered the free-energy of each structure and from a knowledge of the O - H and H ---O distances have deduced that Structure (1) contributes 65%, Structure (2) contributes 31% and Structure (3) contributes 4% to the equilibrium configuration of O - H ---O. Coulson (1961) derived a theoretical dissociation energy for ice from this model and obtained a value of 8.6 k cal. mole⁻¹. (The experimental value is 6.1 k cal. mole⁻¹.) He says it is perfectly clear that in this particular case no completely satisfactory account of the nature of the bond can be given without including several factors not normally requiring consideration in the explanation of the structure of conventional bonds. Nevertheless, the good qualitative agreement shows that the concept of an electrostatic "hydrogen-bond" in ice is acceptable.

Pauling (1935) pointed out that an ordered arrangement of the hydrogen atoms according to the Bernal and Fowler Rules would be inconsistent with the finite zero point entropy which had been observed by Giauque and Ashley (1933). However, if the hydrogen atoms were free to move between two different equilibrium positions along the lines joining oxygen atoms and spent half of their time in each position, the entropy

introduced into the model would correspond well with the zero point entropy found in practice. (See Pauling (1960).) Pauling's model (see Fig. II.3.) is well supported by data from X-ray and neutron diffraction studies, which give oxygen - oxygen inter-atomic distances of 2.76 \AA and oxygen-hydrogen inter-atomic distances of about 1 \AA along lines joining the oxygen atoms.

II. 2. The Structure of Water.

The structure of water has presented much more of a problem. Water has an extremely high boiling point when compared with its homologues, hydrogen sulphide, H_2S , hydrogen selenide, H_2Se , and hydrogen telluride, H_2Te , all of which are gases at room temperature. Clearly, therefore, the molecules must be highly associated in water but not in H_2S , H_2Se or H_2Te . One way in which molecules containing a very electronegative atom plus hydrogen atoms can become associated is by means of hydrogen-bonding. Hydrogen-bonding also occurs in hydrogen chloride and hydrogen fluoride and it is reasonable to assume water molecules are associated by this means. However, only a statistical proportion of the molecules will be associated at any one time.

Bernal and Fowler (1933) suggested that, between 4°C and 200°C water has a tetrahedrally hydrogen-bonded structure with a lattice similar to that of quartz, while below 4°C , the structure is similar to the tridymite form of silica. Pauling proposed a pentagonal dodecahedral structure in which hydrogen-bonding is of prime importance. Van Panthaleon van Eck et al. (1958) have suggested that the arrangement of molecules involves, essentially, a six-fold co-ordination of water molecules with four short OH ---- O hydrogen-bonds of the order of 2.9 \AA length and two long O----O

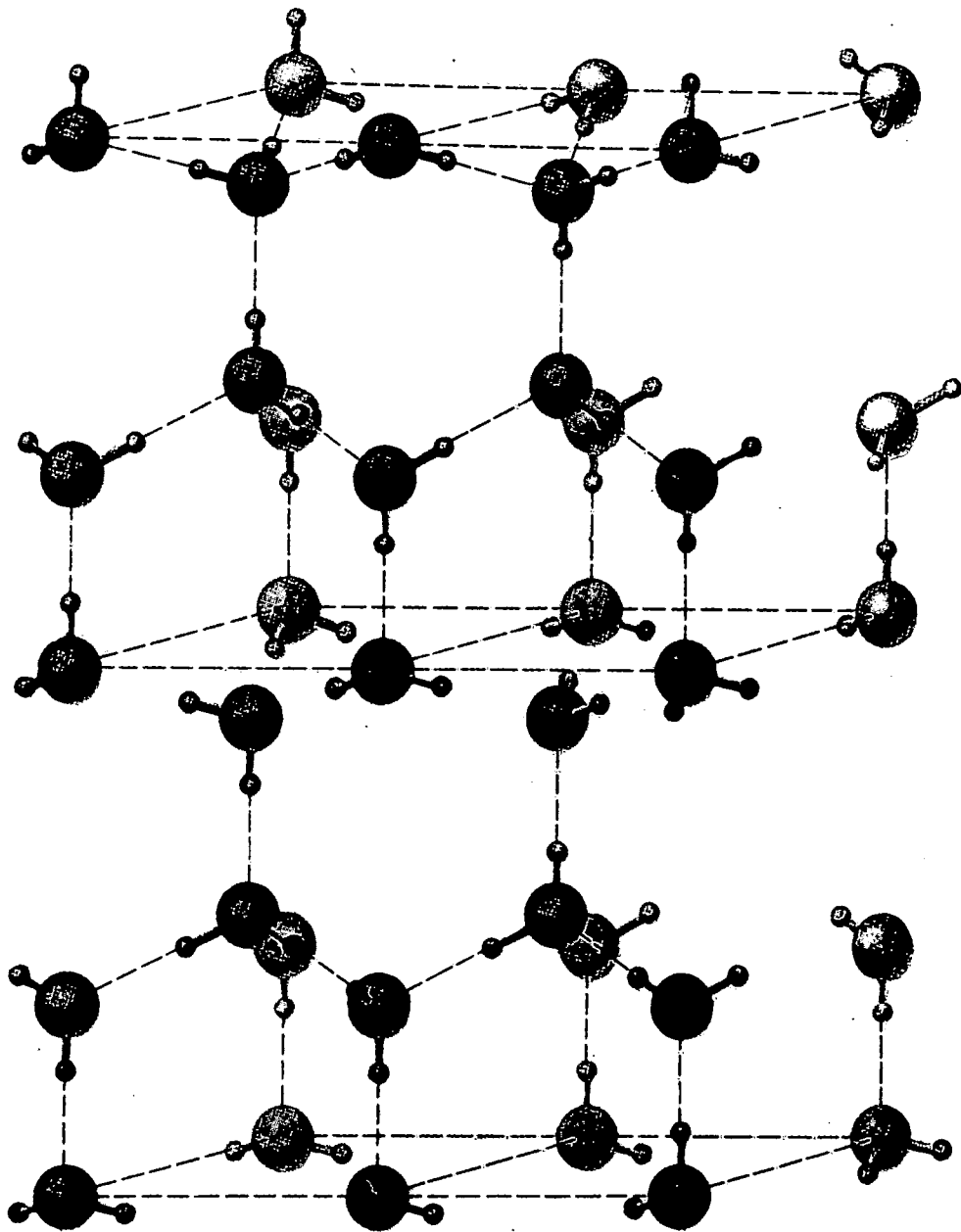


Fig.II.3. The arrangement of molecules in the ice crystal. The orientation of the water molecules as represented in the drawing is arbitrary; there is one proton along each oxygen-oxygen axis, closer to one or the other of the two oxygen atoms. [Linus Pauling, *The Nature of the Chemical Bond*, Cornell University Press, 1960]

contacts of about 3.6 Å length. An ice-like structure might also contribute to some extent to the ordered portion of the liquid. However, Frank (1958) postulates that bonded, flickering clusters of ice-like material are surrounded by, and alternate roles with, disordered fluid, which makes up the rest of the sample.

Experiments have been described by Walrafen (1968) of Raman studies using an argon-ion laser on solutions of HDO in H₂O. His results indicated that the two-state mixture model involving "flickering clusters" was most likely to be correct. The addition of dimethyl sulphoxide to the solution appeared to increase the proportion of clusters, whereas increasing temperature and pressure, which encourages "structure break-up", appeared to reduce the proportion of clusters.

Yet another model is due to Pople (1951). He proposed that there might be a distribution of bond energies which is said by Wall and Hornig (1965) to give better agreement with infra-red data. This has led Perram and Levine (1968) to believe that the effects of hydrogen-bonding in the phase behaviour of water are restricted only to the elevation of the transition temperatures and to the increase of latent heat relative to normal liquids.

One thing which is agreed by most authorities is that the degree of order within liquid water is determined by a statistical process which is dependent on temperature, increasing with decreasing temperature.

II.3. Charge Transport in Water.

Since there are no free electrons in water, its electrical conductivity must be explained in terms of ions.

Water is said to dissociate according to the equation:



although this is an over-simplification since both these ions are highly solvated by neutral water molecules. The mobilities of these ions at 25°C have been calculated to be:

$$\begin{array}{llll} \text{H}_3\text{O}^+, & 36.2 \times 10^{-8} & \text{m s}^{-1} & \text{per V m}^{-1} \\ \text{OH}^-, & 19.8 \times 10^{-8} & \text{m s}^{-1} & \text{per V m}^{-1}, \end{array}$$

which are much higher than those of other univalent ions in water, e.g.

$$\begin{array}{llll} \text{Li}^+, & 3.0 \times 10^{-8} & \text{m s}^{-1} & \text{per V m}^{-1} \\ \text{Cl}^-, & 7.9 \times 10^{-8} & \text{m s}^{-1} & \text{per V m}^{-1} \end{array}$$

and this discrepancy cannot be explained by differences in the degree of solvation of the ions. The existence of some special charge transport mechanism is indicated. Heuckel (1928) suggested that a proton could jump from molecule to molecule, a mechanism which is still considered to explain satisfactorily the conductivity of water. (See Fig. II.4).

Eigen and De Maeyer (1958) considered the two possibilities proposed by Gierer and Wirtz (1949) that either

(i) the proton jump within the hydrogen-bond is rate determining, or.

(ii) the proton passes quickly through a chain of bonds at the end of which it has to wait until a new hydrogen-bond is formed, and therefore, the formation of hydrogen-bonds is rate determining.

In the light of all the available experimental evidence, they came to the conclusion that the rate of formation of hydrogen-bonds is the rate-determining step in the transport of charge in water.

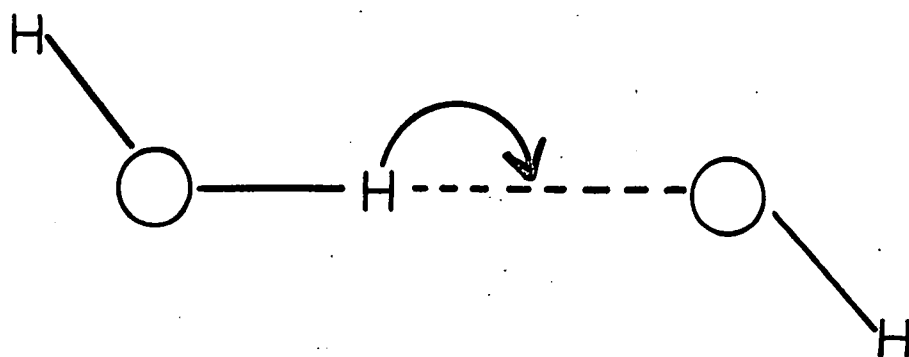
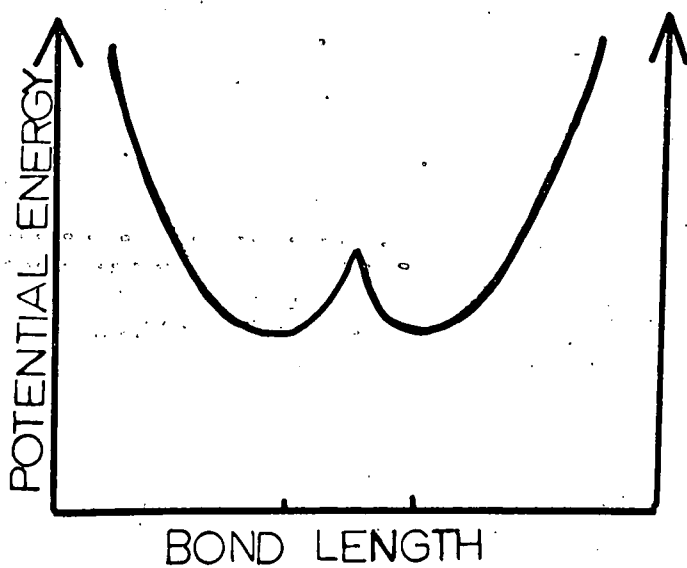
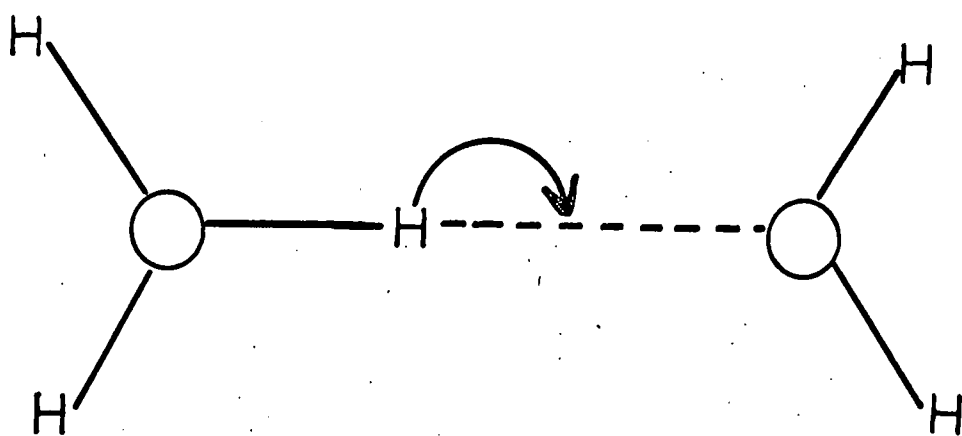


Fig. II.4. the "Proton-jump"
mechanism of charge transport in
water.

II.4. Charge Transport in Ice.

The electrical conductivity of ice has been measured by several workers, e.g. Siksna (1957), Bradley (1959), and shows a marked temperature dependence. According to Bradley (1959) the conductivity is given by $2340 \cdot \exp(-12300/RT) \Omega^{-1} \text{ m}^{-1}$, where R is the gas constant and T is the absolute temperature. The absolute values for the specific conductivity depend to a large extent on the impurities within the sample as these govern the number of ions and defects present in the ice structure. However, in general there are fewer ions per unit volume in ice than in water.

Decroly et al. (1957) have shown that the static conductivity of ice is purely ionic and Graenicher (1958) points out that the conductivity can be explained if ionised states exist in the lattice. But since the direct current conductivity does not vary with time, even when sufficient time should have elapsed for all the original ion-states to be removed, it can be seen that the existence of ion-states alone cannot adequately explain the conductivity of ice. It was Bjerrum (1951) who postulated that the generation and migration of lattice defects would allow ion-states to be regenerated to diffuse through the molecule more than once.

Despite there being fewer ions in ice, the specific conductivity of ice is of the same order of magnitude as that of water, when both are at temperatures very near the freezing point. Clearly, therefore, the mobility of the proton within ice is much higher than in water. This higher mobility is readily explained when one appreciates that the rate-determining step in the charge transfer process

cannot be the formation of hydrogen-bonds, as ice has virtually a fully-hydrogen-bonded structure, but must be the proton-jump within the hydrogen-bond. The marked decrease in conductivity with falling temperature is explained by Eigen and De Maeyer (1958) by the increase in the activation of this transition at lower temperatures resulting in a corresponding decrease in the probability of quantum mechanical tunnelling.

The ion-states present in ice are the hydroxonium ion, H_3O^+ and the hydroxylion, OH^- . The manner in which they diffuse through the lattice is shown in Fig.II.5. It can be seen from this diagram that the diffusion results in a re-orientation of molecule B so that no further diffusion of ion-states is possible. Although it is not shown in this diagram, the OH^- ion diffuses in a similar manner.

The production and migration of Bjerrum defects is shown in Fig.II.6. The production of such defects violates the second Bernal and Fowler Rule, but Bjerrum considered that the defects might be created by a thermally excited proton rotating about its oxygen atom to another equilibrium position in a neighbouring bond. Each such transition generates one doubly-occupied and one vacant bond, known as D- and L-defects respectively. It is the migration of the D- defect which is shown in Fig.II.6, but the L-defect migrates in a similar manner. A comparison with Fig.II.5, shows that the migration of defects has the effect of re-orientating the molecules (note particularly molecule B) so as to allow further ionic diffusion.

Table II.1 compares some of the properties of ion - states and Bjerrum defects, in so far as they are known.

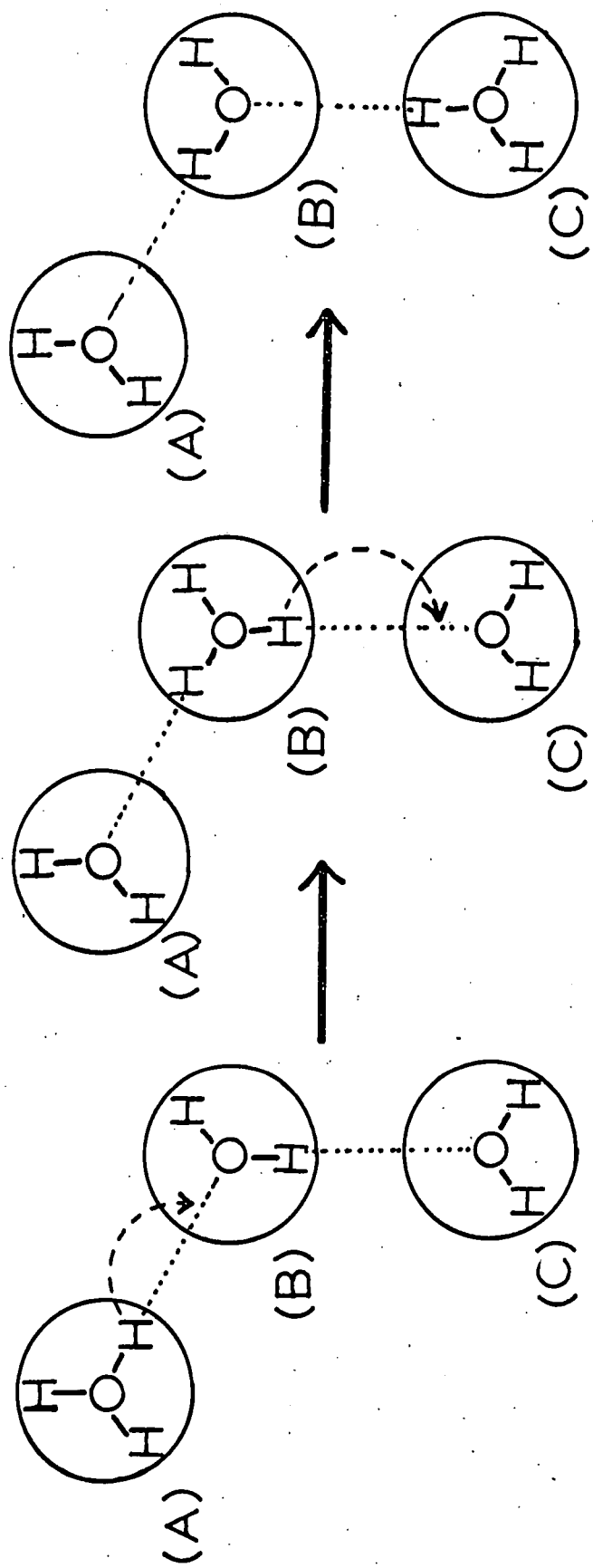


Fig. II. 5. CHARGE TRANSPORT IN ICE, the diffusion of the H_3O^+ ion.

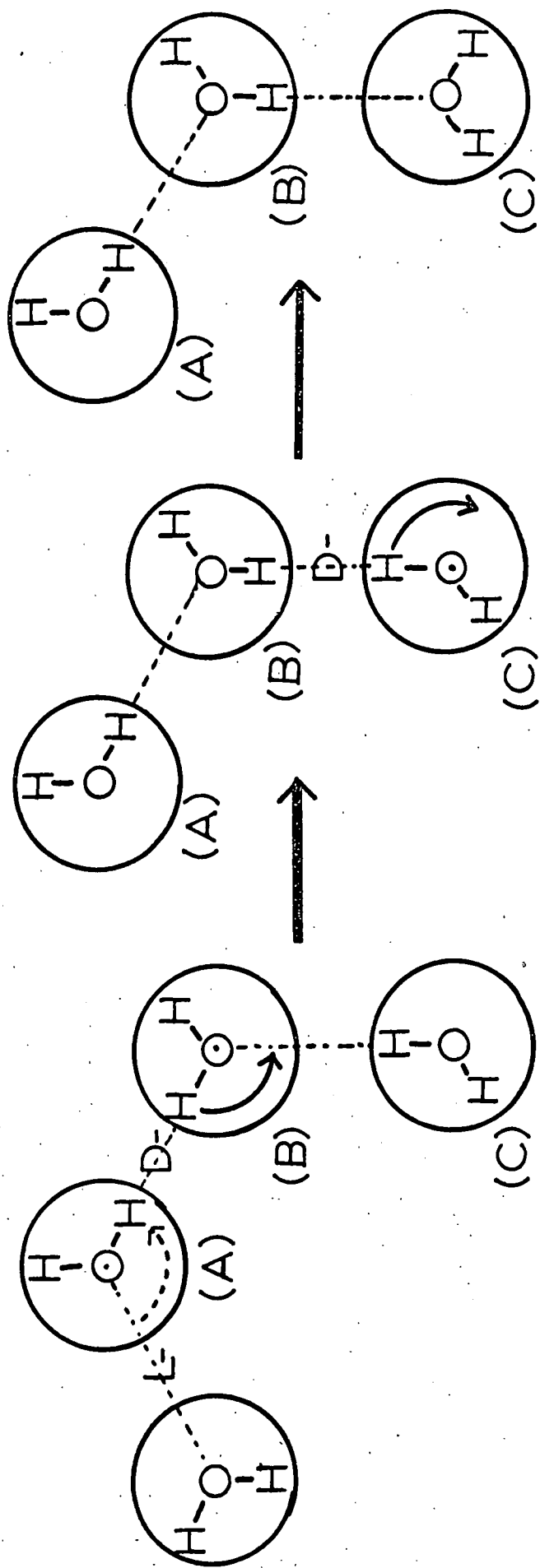


Fig. II.6. the generation & migration of Bjerrum defects in ice.

	Ion-states.	Bjerrum Defects.
Energy of Formation.	1.2 ± 0.1 eV.	0.68 ± 0.04 eV.
Concentration.	$8 \times 10^{14} \text{ m}^{-3}$	$7 \times 10^{19} \text{ m}^{-3}$
Transition Probability.	$6 \times 10^{13} \text{ s}^{-1}$	$2 \times 10^{11} \text{ s}^{-1}$
Mobility (in m s^{-1} per Vm^{-1})	$\mu_+ = 7.5 \times 10^{-6}$	$\mu_L = 2 \times 10^{-8}$
Mobility - ratio.	$\frac{\mu_+}{\mu_-} = 10^0 \text{ to } 100$	$\frac{\mu_L}{\mu_D} \approx 1$
Activation-energy of Diffusion.	0 (tunnelling)	0.235 ± 0.01 eV

TABLE II.1. A Comparison of the Properties of Ion-states and Bjerrum Defects in Pure Ice at -10°C .

CHAPTER III

THE ELECTRIFICATION OF ICE AND WATER.

The principal mechanisms of charge separation in water and ice, and the results and theories of previous workers in this field are summarised briefly.

III. 1. Charge Separation in Ice.

III. 1(a). Electrification directly associated with temperature gradients in ice.

When two pieces of identical insulating material are rubbed together asymmetrically, they acquire equal and opposite charges. Henry (1952) suggested that a temperature gradient effect might be responsible as the rubber and the rubbed material will be warmed by friction in different ways. Reynolds, Brook and Gourley (1957) stroked two ice-coated metal rods together asymmetrically so that a small, fixed area of one rod was rubbed over a similar area along the whole length of the other. They noted that the rubber always became negatively charged and that the rubbed rod acquired an equal and opposite charge, which was attributed to the former rod being made warmer by the rubbing.

Transient contacts between two ice specimens were made by Brook (1958), who observed that the colder of two identical specimens always became positively charged. He also noted that ice made from 10^{-4} molar sodium chloride solution always became negatively charged on making contact with pure ice, even when the specimens differed in temperature by several degrees. He concluded that his results showed that the potential difference between two pieces of ice in contact was a sensitive function of their temperature difference but the experiments with sodium

chloride-doped ice indicated that another source of e.m.f. might also have been operative.

A theory of proton diffusion to explain the appearance of a potential difference between the ends of an ice specimen subjected to a steady temperature gradient was developed by Latham and Mason (1961A). The theory depends upon the properties of ice mentioned in Chapter II, viz:

- (a) the concentrations of H_3O^+ and OH^- ions rise quite rapidly with increasing temperature, and
- (b) the mobility of the H_3O^+ ion is at least ten times greater than that of the OH^- ion.

Therefore, the establishment of a temperature gradient in an ice specimen will be accompanied by the setting up of a concentration gradient of ions of both signs. The more rapid initial diffusion of the H_3O^+ ion down the temperature gradient will lead to a separation of charge with a net excess of positive charge at the colder end of the ice. The resulting space-charge distribution will be such as to oppose the further separation of charge and under the influence of a steady temperature gradient, eventually a steady state will be reached in which no net flow of current occurs. At this time a steady potential difference will have been established between the ends of the specimen, with the cold end positively charged and the warm end negatively charged. Assuming that the charge is concentrated on opposite faces of the ice, the predicted charge separation is given by

$$\sigma = \frac{\epsilon_0 \epsilon k \left(\frac{\mu_+}{\mu_-} - 1 \right) \left(\frac{\Phi}{kT} + 1 \right)}{2e \left(\frac{\mu_+}{\mu_-} + 1 \right)} \cdot \frac{dT}{dx}$$

- where σ = the surface charge density on the ends of the ice.
 ϵ_0 = the permittivity of free space.
 ϵ = the dielectric constant of ice.
 k = Boltzmann's constant.
 e = the electronic charge.
 Φ = the activation energy for the dissociation of ice.
 T = the absolute temperature.
 μ_+/μ_- = the mobility ratio for H_3O^+ and OH^- ions.

Substituting typical values in this equation gives

$$\sigma = 1.65 \times 10^{-10} (dT / dx) \text{ C m}^{-2}.$$

This corresponds to a potential of $1.86 \Delta T$ mV across a specimen whose faces are at temperatures differing by ΔT deg.C.

Latham and Mason measured the potentials between opposite faces of an ice disc and found very good agreement with the calculated values for temperature differences of up to 10 deg.C. provided that the warmer face of the specimen was below -7°C . At temperatures above this, larger potential differences were measured than predicted by the simple theory but Latham and Mason believed that these could be explained by the variations in the conductivity of ice found by Bradley (1957). The presence of impurities in the ice had only a very slight effect on the measured potential differences. Sodium chloride caused the potentials to be reduced whereas hydrofluoric acid caused them to be increased. It was also shown that when transient contact was made between ice specimens initially having different temperatures, the charge separated could be explained by the Temperature Gradient Theory and that it was dependent on the time of contact, the maximum separation being after a contact

time of 0.01 s.

Jaccard (1963) has considered the effect of the Bjerrum defects on the thermoelectric power of ice. Allowing for the fact that the effective charge carried by each defect is less than the unit electronic charge, he showed that the predicted value would agree with Latham and Mason provided that the mobility ratio of the Bjerrum defects is 1.2.

Latham (1964 A) has also shown that the separation of charge can be detected by an induction method using a single ice crystal suspended only by a fibre, thus eliminating sources of possible spurious effects.

III. 1(b). Electrification associated with the evaporation of an ice surface.

Measurements have been made of the electrification on evaporation of ice from an ice-coated copper sphere of radius 15 mm by Latham and Stow (1965). The sphere was maintained at -20°C and dry nitrogen was blown over its surface at temperatures between 0 and -40°C . They found that for nitrogen temperatures between 0 and -10°C , the sphere became positively charged and for temperatures below -10°C the sphere became negatively charged. In a subsidiary experiment, the variation of the temperature difference in the iced surface between nitrogen and the interior was found and they showed that the electrification on evaporation could be qualitatively explained in terms of the Temperature Gradient Theory but quantitative agreement would not be expected in the absence of detailed knowledge of the spacial distribution of charge caused by temperature gradients.

Recently, Cross (1969) has examined evaporating ice surfaces under a scanning electron microscope and has shown that polycrystalline

ice develops a fragile, fibrous surface. He suggests that the breaking off of ice splinters from such a surface could explain the electrification observed by Latham and Stow. Each splinter will be colder than the large ice mass and, on breaking away, will carry positive charge into the airstream, as described by Latham (1963).

III. 1(c). Charge separation associated with the cracking and fracturing of ice.

This appears to be the result of the mechanical separation of ice fragments in which a charge separating process, e.g. the Temperature Gradient mechanism, had previously been operating.

III. 2. The Separation of Electric Charge in Melting Ice.

Dinger and Gunn (1946) detected a charge separation of up to $4.2 \times 10^{-10} \text{ C g}^{-1}$ of ice melted. The air above the sample acquired a negative charge and the water, a positive charge. They noted that the presence of dissolved gases was essential for the observed charging effects to occur and related the charging mechanism to earlier experiments on the cataphoresis of gas bubbles. In a later paper, Dinger (1965) has reported charges as high as $2.2 \times 10^{-9} \text{ C g}^{-1}$ for triply distilled water when great care was taken to avoid surface contamination.

The magnitude of the effect is very sensitive to the presence of small amounts of impurities and the failure of Matthews and Mason (1963) to detect even one hundredth of the charge separation reported by Dinger and Gunn was attributed to the presence of high concentrations of carbon dioxide in the vicinity of the apparatus (Dinger, 1964).

III.3. Charge Separation in Water.

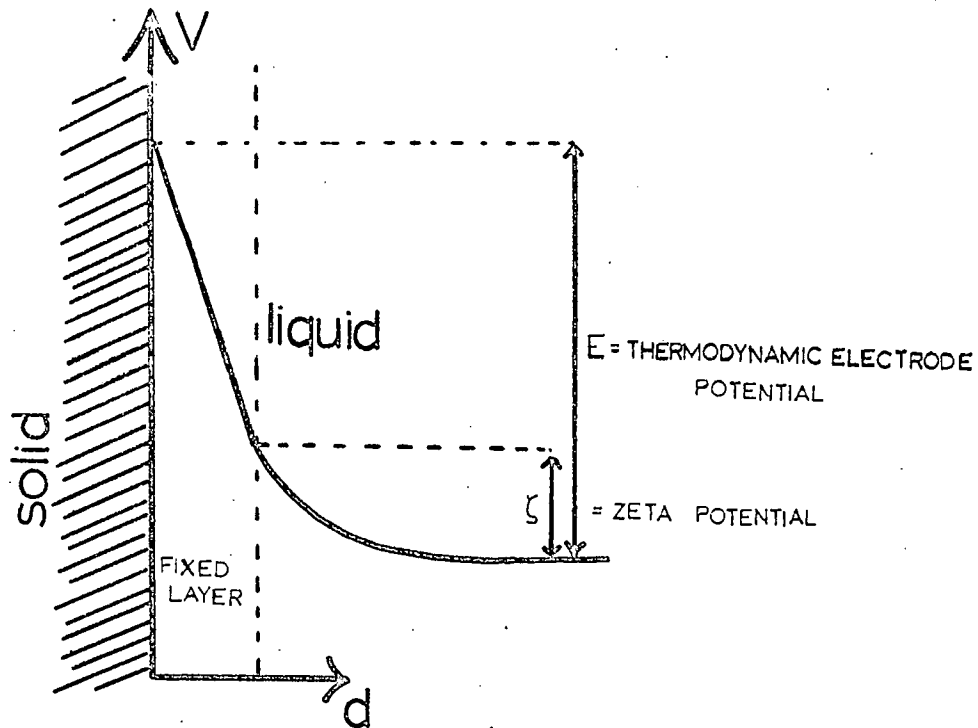
III.3.(a). Spraying, splashing and bubbling phenomena.

Neglecting chemical electrode potentials of metals in aqueous solutions of their ions, these phenomena probably represent the main ways in which charge is separated in water. Loeb (1958) gives a detailed account of these phenomena, which, in contrast to the charge separation mechanisms in ice, are mainly due to the presence of impurities and the existence of an electric double layer at the liquid/air interface.

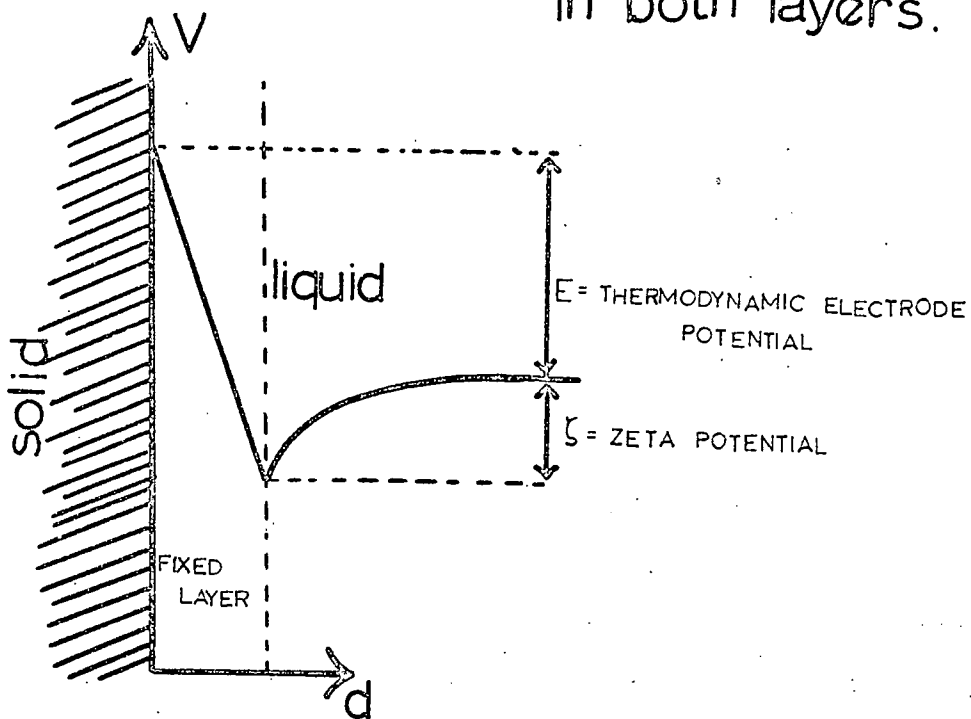
Mason and Iribarne (1967) have looked in detail at the charge separated by bubbles bursting at the air/water interface and have found that the charge separated depends upon the bubble radius, the impurities in the water, the composition of the gas in the bubble and the life-time of the bubble before bursting. In order to obtain reproducible results, they ensured that the water surface, at which the bubble burst, was continuously renewed and they confined their measurements to bubbles which burst immediately on arrival at the surface. The results obtained under these conditions were consistent with a theory based on the rupture of an electric double layer. Droplets from bursting bubbles of nitrogen, which had had radii in the region 20 to 200 μm , carried away net negative charge of up to 3×10^{-13} C per bubble from solutions with ionic concentrations of less than 10^{-4} molar.

III.3 (b). Solid/liquid interfacial phenomena.

It is convenient at this point to examine the charge separation which may result when a liquid moves relatively to a solid



(a) ions of same sign in both layers.



(b) ions of opposite sign in each layer.

Fig. III.1. THE ELECTRIC DOUBLE LAYER.

with which it is in contact.

The concept of differently charged layers, i.e. an electric double layer, at a solid/liquid boundary was proposed by Helmholtz in 1879. The original picture has been modified by Gouy (c.1909) and more recently by Stern (1924). According to Stern the double layer is in two parts: one, which is approximately a single ion in thickness, remains almost fixed to the solid surface: the other extends some distance into the liquid phase and is diffuse. (See Fig.III.1.) In this second region, thermal agitation permits the free movement of the particles but the electrostatic field at the surface may result in preferential attraction of those of opposite sign. In this region the potential falls gradually to the level in the bulk of the liquid where the charge distribution is uniform. The overall fall in potential between the solid and the liquid represents the thermodynamic Electrode Potential. The potential difference between the fixed layer and the bulk liquid is known as the Zeta Potential, ζ .

In order that simple mathematical considerations may be applied to electrokinetic phenomena, it is necessary to assume that the diffuse double layer is equivalent to a parallel plate condenser, with a separation between the plates of d carrying a charge of q per square metre. Then

$$\zeta = qd / D\epsilon_0$$

where D is the dielectric constant of the medium between the plates and ϵ_0 is the permittivity of free space (See Glasstone, 1962, page 1220 onward.).

Let us consider the case of a liquid flowing through a capillary tube, radius r . The velocity of the liquid varies with the distance, x , from the centre of the tube and is equal to $P(r^2 - x^2)/4\eta l$ for laminar flow, where P is the pressure difference between the ends of the tube of length, l and η is the viscosity of the liquid. The moving part of the double layer is at a distance $r - d$ from the centre of the tube and so its velocity, v , is given by:

$$v = \frac{rdP}{2l\eta}$$

(the very small quantity d^2 can be neglected in comparison with $2rd$)

If one side of the double layer is forced past the other, the strength of the current, I , produced is given by

$$I = 2\pi r q v = \pi r^2 q \frac{dP}{l\eta}$$

If k is the specific conductivity of the liquid used, then the conductivity of the liquid in the tube is $\pi r^2 k/l$ and if S is the "streaming" or flow potential, i.e. the potential measured between the ends of the tube, it follows from Ohm's law, that

$$S = I l / \pi r^2 k \\ = q dP / k \eta$$

Hence, we see that a value for the Zeta potential between the liquid and the material comprising the tube can be obtained by measuring the potential produced between the ends of a tube through which the liquid is forced.

The validity of the expression derived using the above simplifying assumptions has been justified by the close correspondence between the values of ζ obtained from different methods. (e.g. see Glasstone, 1962, page 1225). Traditionally such exper-

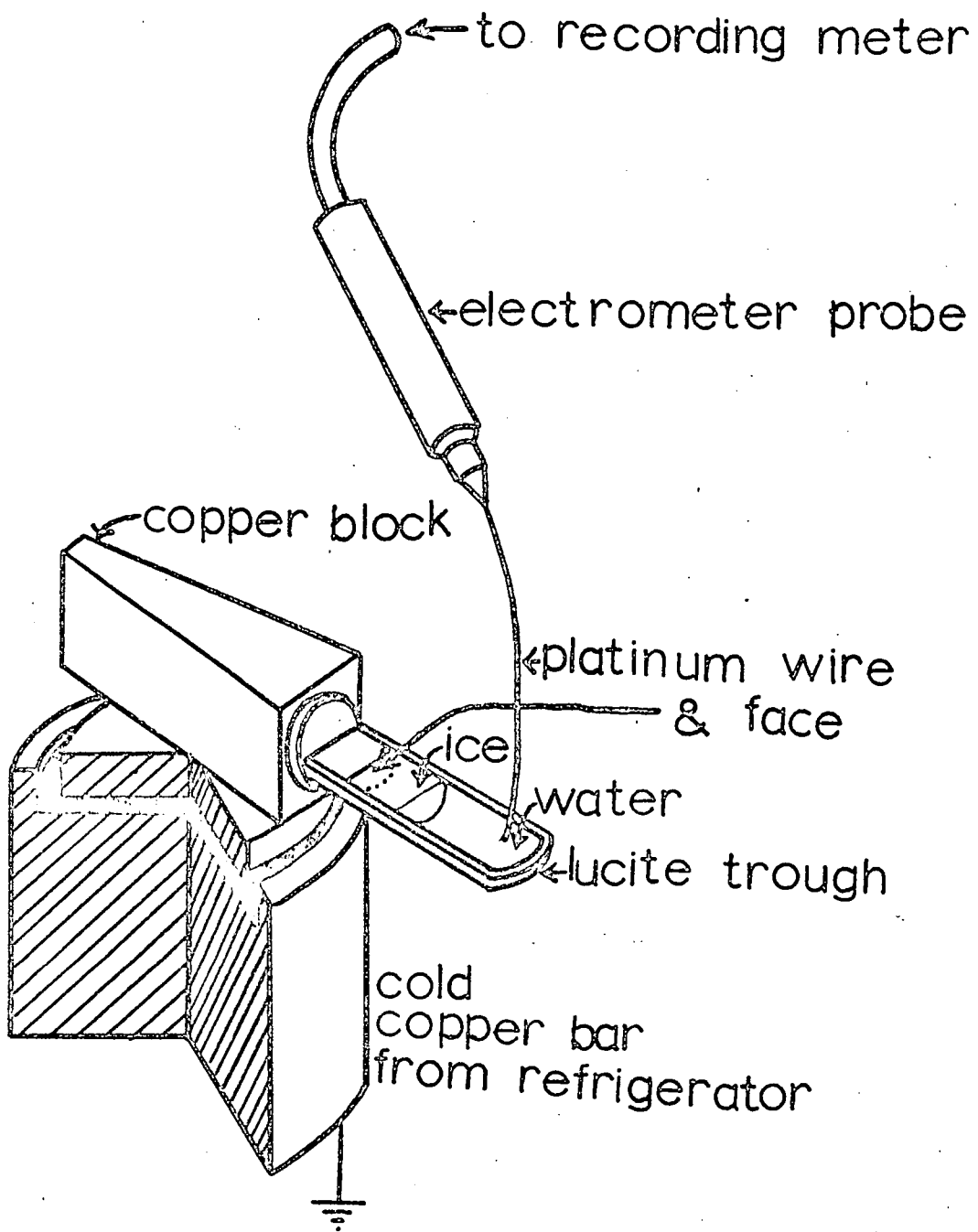


Fig. III.2.

Workman and Reynolds' apparatus for the measurement of freezing potentials

iments have been carried out on aqueous solutions of ionic salts in glass tubes, but charge can be separated by many low conductivity liquids on flowing through tubes of various materials.

III. 3(c). Temperature gradients in solutions.

Latham (1964 B) has reported that temperature gradients in ionic solutions give rise to electric potentials. The colder portions of potassium and sodium chloride solutions acquired net positive charge. The results were said to be explicable in terms of a mechanism similar to that responsible for the charge transfer produced by temperature gradients in ice.

III. 4. Charge Separated by the Freezing of Water.

In 1946 Workman and Reynolds began a series of laboratory experiments in the hope of discovering a physical process which might be basic in the generation of thunderstorm electricity. Using the apparatus shown in Fig.III.2, with copper block temperatures of - 5 to - 30 °C, they found that the water froze in an orderly manner from the platinum face outwards.

Relatively large potential differences were developed between the water and ice when dilute ionic solutions were used. The charge separation started when freezing began and stopped when freezing ceased. The potentials were measured using shunts of from 10^6 to $10^8 \Omega$ across the electrometer to ground. Workman and Reynolds also observed that a reverse potential was not realised on melting. They attributed this to prior neutralisation through the poorly conducting ice. They also

noted that in their measurements, the magnitude of the open circuit potentials was independent of the freezing rates over a wide range, and they stated that the potentials only appeared variable to the extent that internal leakage currents reduced the measurable potentials for slow rates of freezing and crystal disorientation reduced them at very high rates of freezing. These authors also reported that when random crystal orientation resulted from spontaneous freezing of supercooled solutions, hardly any charge separation was observed. However, Pruppacher, Steinberger and Wang (1968) have observed charge separation on spontaneous freezing and potential differences within an order of magnitude of those obtained by Workman and Reynolds at lower freezing rates.

The actual values of the freezing potentials were highly dependent on very small concentrations of ionic solutes, e.g. 3×10^{-5} molar ammonia solutions gave - 232 V with the water negatively charged, 2×10^{-5} molar sodium fluoride solutions gave + 21 V with the water positive, and 10^{-4} molar sodium chloride solutions gave + 30 V. This led them to suspect that the - 40 V, approximately, obtained on freezing distilled water of conductivity $10^{-4} \Omega^{-1} \text{ m}^{-1}$ was due to the presence of ammonia, and when care was taken to eliminate ammonia as a contaminant, the potentials in distilled water were reduced to a few volts.

The ionic character of the effect was demonstrated by partially freezing a 7×10^{-5} molar sodium chloride solution in an atmosphere of helium with an electrometer shunt of $2 \times 10^7 \Omega$. The pH of the solution before freezing was 6.3, that of the unfrozen water

was 6.2 and that of the re-melted ice was 7.0, showing that the chloride ions were selectively trapped in the ice. Calculations showed that the differences in pH corresponded to a charge separation of $3.4 \times 10^{-5} \text{ C g}^{-1}$ compared to the $3.0 \times 10^{-5} \text{ C g}^{-1}$ measured by the electrometer. Allowing for the leakage currents this represented excellent agreement, and, although Workman and Reynolds (1950) admitted that such good agreement was probably fortuitous, they considered that their interpretation was justified.

Various aspects of the Workman and Reynolds Effect have been examined by Gill (1953), Lodge et al. (1956), Heinmets (1962), Gross (1965), Pruppacher et al. (1968) and others. In general, the findings of Workman and Reynolds have been confirmed although no one has succeeded in producing such large potentials. More detailed discussion of these results is to be found in Chapter VI.

CHAPTER IV.

LABORATORY SIMULATIONS OF CONDITIONS IN CLOUDS AND THE ELECTRIFICATION OF HAIL AND SNOW

IV. 1. The Electrification of Single Water Drops.

Charge separation due to the freezing of single water drops occurs when the drop shatters. However, Rogers (1967) and Johnson and Hallett (1968) have shown that single drops are unlikely to shatter in conditions of free fall in the atmosphere. Nevertheless, shattering of small droplets on hailstones may occur and therefore the results of work on single drops may be applicable to the electrification of hail.

When a water drop is being frozen, spicules and bulges often appear on its surface. Dorsey (1948) proposed that these could be explained if the surface of the drop froze first, so that subsequent freezing resulted in a build-up of pressure inside the drop which ultimately caused the ice shell to rupture. A jet of water would then be ejected and would freeze on the outside, producing either a spicule or a bulge. Blanchard (1951) investigated the growth of spicules on freezing drops of 8 mm diameter which were freely supported in a vertical wind tunnel. He verified the mechanism suggested by Dorsey and in a subsequent paper, Blanchard (1955), he reported that the manner in which the drops froze depended upon their temperatures at the time of freezing. At temperatures above about -5°C a shell of clear ice formed at the bottom of the drop and grew over the whole surface. Thin planes of ice also grew from the base of the drop into the interior. At temperatures below -5°C , the freezing occurred nearly simultaneously over the entire surface of

the drop, causing the drop to become opaque due to the presence of small air bubbles forced out of the solution as the water froze.

IV. 1(a). The work of Mason and Maybank.

Mason (1956) had noticed that the bursting of freezing water drops produced small ice crystals. Mason and Maybank (1960) investigated the freezing of drops with diameters in the range 0.6 to 2 mm suspended on fibres. The drops were allowed to supercool to a known temperature and then they were nucleated with either silver iodide crystals or small ice particles. These authors reported that drops supercooled to about -15°C froze in two stages. The first stage was the rapid formation of an opaque outer shell of ice containing many small air bubbles. Liberation of latent heat then warmed the drop up to 0°C and the liquid interior froze slowly. During this second stage, some of the water from the drop interior seeped slowly through the ice shell and froze on the surface. When drops were nucleated at temperatures just below the freezing point, a thin, transparent ice shell spread slowly over the entire surface of the drop. Freezing then progressed towards the interior and at this stage spicules were often produced. Mason and Maybank also showed that the amount of air dissolved in the drop was important in determining whether spicules were produced. The pressure build-up resulting from the freezing of the water is more easily accommodated by air bubbles, and shattering and splinter production are reduced if air bubbles are present. They also noted that the presence of small amounts

of dissolved salts (less than 0.2 molar) did not affect the way in which the drops froze.

Mason and Maybank examined the electrification of freezing drops nucleated at a temperature of -1°C and then placed in an environment temperature of -10°C . No charge was detected until shattering occurred and, in general, the major drop residues became negatively charged, while the minor drop residues became positively charged. They explained their results in terms of a temperature gradient which they assumed to exist between layers in the ice shell of a partially frozen drop.

IV. 1(b). The work of Kachurin and Bekryaev

Kachurin and Bekryaev (1960) investigated the electrification of freezing drops with diameters between 0.2 and 2 μm over a temperature range -3 to -20°C . The drops were suspended, at the focus of a microscope, on a fine wire eyelet which could be connected to either an electrometer or an oscilloscope. By filming the freezing they were able to correlate variations in the charges on the drops with particular events in the freezing sequence. A typical oscillogram trace is shown in Fig. IV.1. Peak A is said to be associated with the breaking off of small ice particles as fissures form in the ice shell. Peaks B, C and D were associated with the breaking off of negatively charged ice particles from the spicules, while the general negative trend on the record was due to the ejection of streams of positively charged microscopic water droplets.

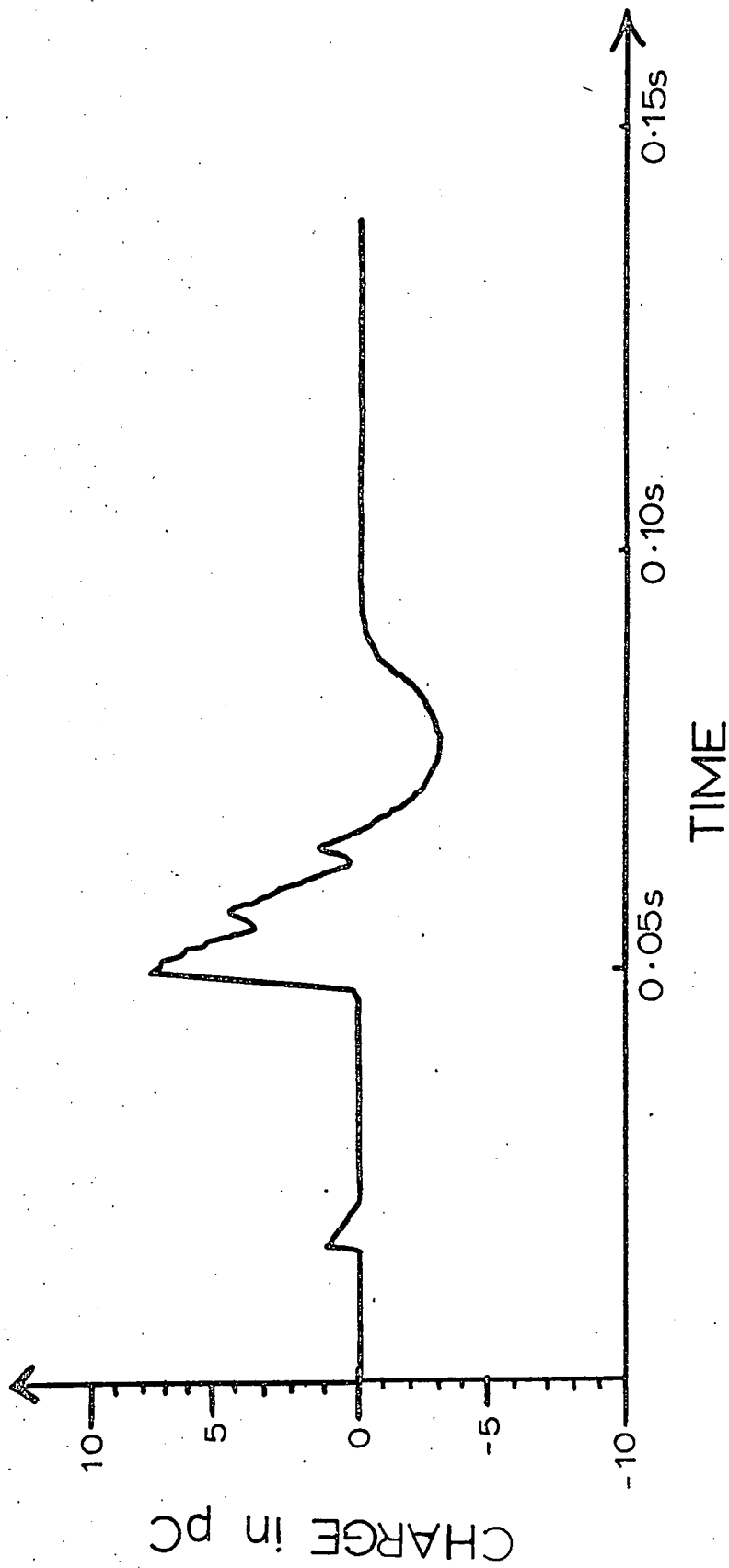


Fig. IV.1. A typical oscillogram of the charge on a freezing water drop (after Kachurin & Bekryaev).

IV. 1(c). The work of Hutchinson, Evans and Stott.

Evans and Hutchinson (1963) and Stott and Hutchinson (1965) examined the freezing of supercooled drops of 0.9 to 1.7 mm diameter suspended on an insulating fibre. The drops were nucleated by a cloud of small ice crystals, produced by small pieces of solid carbon dioxide, when they had become supercooled by 1 to 2 deg.C and then they were lowered quickly into a refrigerated cell with an environment temperature of -15°C . Stott and Hutchinson (1965) summarised all the results obtained.

The results were in agreement with those of Kachurin and Bekryaev for the sign of the charge separation, but the charge separated by shattering drops was, in many cases, too large to be explained in terms of the Temperature Gradient Theory. Stott and Hutchinson pointed out that their results, and those of Kachurin and Bekryaev, and Evans and Hutchinson, were consistent with a theory involving a substantial charge separation across the water/ice boundary in the solidifying drop. The charge separation mechanism proposed by Workman and Reynolds would, it was thought, separate sufficient charge to explain the results.

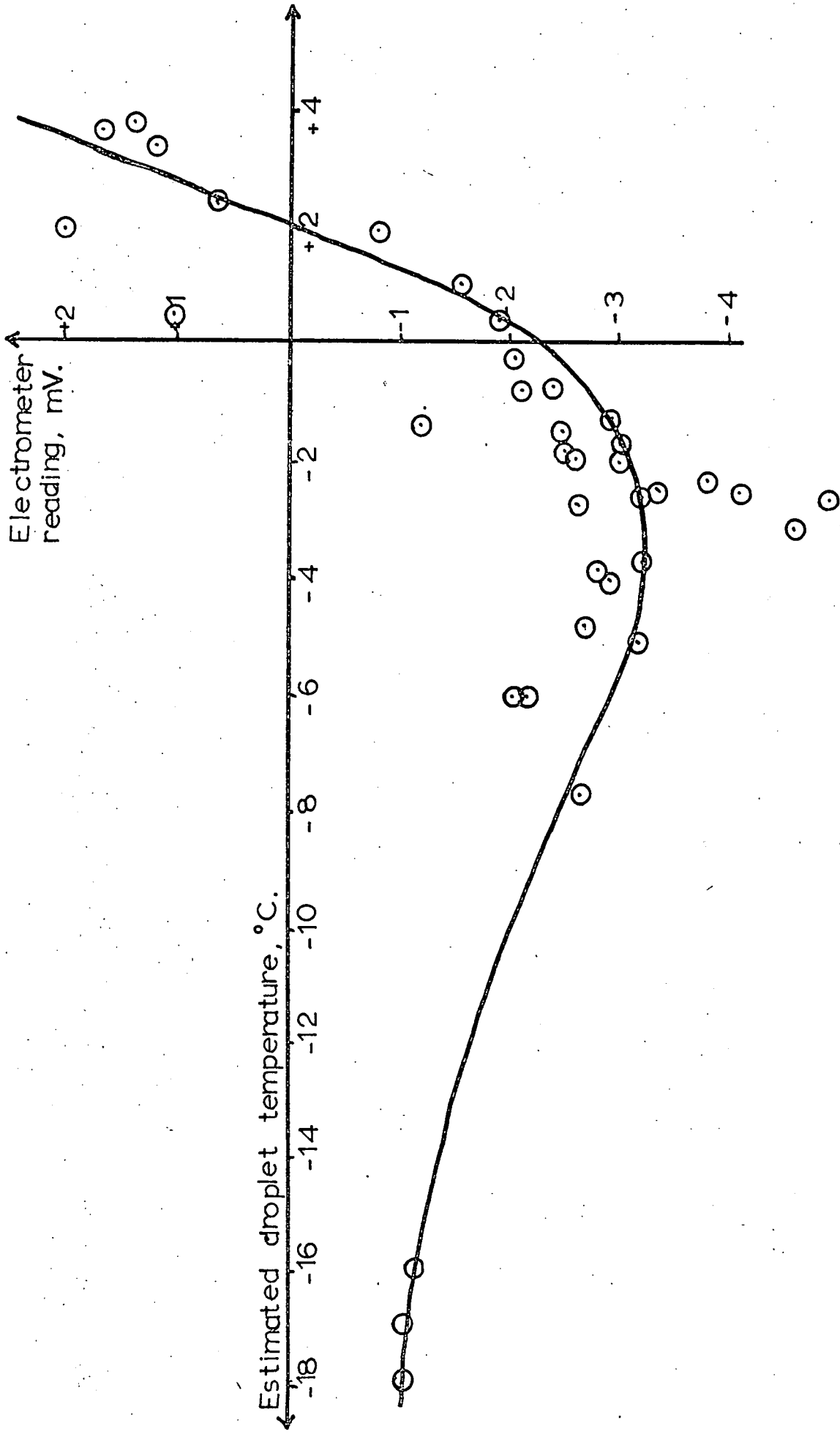
IV. 1(d). The work of Rogers.

Rogers (1967) supported water drops, with diameters in the range 3 to 5 mm, on an air-stream, and by noting the time taken for freezing to commence, he calculated the degree of supercooling of the drop when freezing was initiated. In measurements on 150 drops

separated. They explained their results in terms of the Temperature Gradient Theory.

Church (1966) performed experiments designed to investigate discrepancies in the results of these previous workers. He found no significant charging when a 4 mm diameter phosphor-bronze ball, coated with ice 0.5 to 0.75 mm thick, was rotated at a tangential velocity of 10 m s^{-1} in a cloud of supercooled water droplets at $-18 \text{ }^\circ\text{C}$. The forward face of the balls became coated with hard, opaque ice but he could find no evidence of splinter production or splashing, which might explain why no charge was separated both in his experiment and the experiment of Reynolds et al. (1957). However, when the cloud was seeded by introducing either a few small fragments of solid carbon dioxide or a rod, cooled in liquid nitrogen, into it, immediate, strong electrification was produced. Although Church does not describe the appearance of the "hailstone" under these conditions, Berriman (private communication), using a modification of Church's apparatus, observed that a rimed surface was produced under somewhat similar conditions, suggesting that splintering was a possible explanation for Church's results.

The electrification on shattering of larger water drops, having diameters in the range 50 to $150 \mu\text{m}$, on encountering a rotating ice-coated rod of 4 mm diameter, was also studied by Church. The surface of the rod became rippled and glassy and only droplets of about $10 \mu\text{m}$ upwards had been flung off the probe. The variation of charging with droplet temperature is shown in Fig. IV.2. He suggested that the results might be explicable in terms of the Workman and Reynolds Effect



Variation of the charging of the probe with droplet temperature, (after Church).

Fig. IV.2.

by assuming that a small fraction of the droplet froze on touching the "hailstone". Charge might be separated across the resulting ice/water interface and this charge separation would be registered as an electrometer deflection when the droplet was flung off. However, he was unable to explain either the reduction in negative charging when the temperature became lower or the positive charging caused by the warmer droplets.

Rogers (1967) investigated the electrification of ice-spheres of 15 mm diameter, freely supported on an air-jet. When a sphere was accreting droplets in the range 5 to 100 μm diameter, it became negatively charged at temperatures of above -10°C and positively charged at temperatures of -12°C and below. He believed this change in sign could, in part, be attributed to a difference in the way in which droplets froze. (See Section IV. 1.) He suspected that water droplets might be flung off at temperatures above -10°C , whereas ice splinters would be ejected at lower temperatures. The sign of the charge separation was opposite to that found by Magono and Takahashi (1963) who noted that the charge acquired by a riming probe depended on the temperature of the probe and the riming rate. Magono and Takahashi, however, explained their results in terms of collisions between ice crystals and the probe, the riming due to supercooled droplets being of importance only in determining the nature of the probe surface. In Rogers' experiments, no ice crystals were detected in the air-jet and he assumed, therefore, that a different charge generating mechanism was operating from that proposed by Magono and Takahashi.

IV. 2(b) The electrification of hail and snow by collision with ice particles.

We have already seen that the electrification of hail on collecting water droplets is enhanced by the presence of ice crystals in the cloud. (See Section IV. 2(a).) Reynolds, Brook and Gourley (1957) explained the negative charging of their spheres in terms of the temperature gradient between the "hailstone", warmed by the latent heat released from the freezing of the droplets, and the cold, rebounding ice crystals. They also reported that very little charge was separated if no droplets were present in the cloud or if the cloud particles and the simulated hailstone were at the same temperature.

Latham and Mason (1961 B) measured the electrification of an iced probe by the passage of a stream of ice crystals in the absence of liquid water. The probe consisted of an insulated metal cylinder covered with a thin coating of ice and mounted on a copper rod. The surface temperature of the probe could be raised, by means of a small, internal electric heater, and lowered, by placing a cylinder containing solid carbon dioxide at various positions along the copper rod. Probe temperatures as low as -30°C were obtainable. A stream of $20\ \mu\text{m}$ ice crystals was drawn past the probe for a known time and the quantity of charge acquired by the probe was measured by placing the probe in an induction can attached to an electrometer. Latham and Mason found that the charge separated varied linearly with the temperature difference between the probe and the crystals. However, for a temperature difference of $5\ \text{deg. C}$, the average charge separated per crystal collision was $1.7 \times 10^{-18}\ \text{C}$ which was a factor of 10^5 less

than that found by Reynolds et al. (1957).

Church (1966) repeated the work of Latham and Mason using somewhat different apparatus. The charging measured by Church was greater by a factor of 50 than that measured by Latham and Mason and did not appear to vary linearly with the measured temperature gradient. He was unable to account for these discrepancies completely but attributed them to differences between his probes and those used by Latham and Mason. Recently, there has been much discussion on the possible enhancement of the Temperature Gradient Effect under conditions different from those for which the quantitative theory was worked out, (e.g. Latham and Stow, Discussion, Quart. J. Royal Met.Soc., Vol. 94, page 415 (1968.)) and it appears certain that quite large variations from the calculated values may be possible in some cases.

IV. 2(e). Electrification on melting.

From their results on the melting of ice specimens, Dinger and Gunn (1946) predicted that melting hail would become positively charged.

Drake (1968) observed the melting of small frozen water drops with diameters of "a few millimetres", supported by a wire loop connected to an electrometer. The temperature, humidity and velocity of the gas flow around the specimen were carefully controlled. No charging was recorded until the specimens began to melt. Strong, positive charging coincided with the onset of strong convection in the melt-water and continued until the last traces of ice disappeared. The separation of charge was due to the presence of air bubbles in the

sample, which burst on reaching the water surface. Convection in the melt-water would have the effect of continuously renewing the water surface which might otherwise have become contaminated. Such contamination has the effect of reducing the charge separated by bursting bubbles.

Using an air-jet for supporting ice spheres of 15 mm diameter, Rogers (1967) also found positive charging on melting. However, when small water droplets were flung off the melting simulated hailstone, it became negatively charged. He postulated this might explain the field measurements of MacCready and Proudfit (1965) who found negative charges on melting hail in the +2 to + 8 °C region.

The electrification on melting of falling snow crystals has been investigated by Magono and Kikuchi (1965) and Kikuchi (1965). They found that natural snow crystals acquired positive charge on melting, usually sufficient to overcome their original negative charge.

They found that the charge acquired was approximately proportional to the air bubble concentration contained in the snowflakes, although large air bubbles did not appear to contribute to the charging. Magono and Kikuchi noted that the snowflakes under observation melted to form a single drop and did not break up.

In general, these results seem to indicate that melting under quiet, non-turbulent conditions leaves the pellet with a positive charge, whereas melting which involves the loss of water from the surface of the ice pellet would leave it with a net negative charge.

IV. 3. Electrification Associated with the Formation of Spongy Ice on Hail.

When supercooled water droplets freeze, they do so very quickly, much more quickly than the water is frozen in, for example, Workman and Reynolds-type experiments. Therefore, measurements made at lower freezing rates may not be applicable under the conditions of accretion of supercooled droplets by hail in the atmosphere.

Macklin and Ryan (1962) and (1965) and Pruppacher (1967) have established that ice crystals grow in supercooled water by multiple branching, thereby producing an interwoven network of dendritic ice structures which are capable of retaining considerable amounts of liquid water. List (1960) and Macklin (1961) have shown that if the rate at which supercooled cloud droplets impinge on an ice pellet is sufficiently large, the heat of fusion released during the freezing cannot be dissipated sufficiently rapidly and an ice-water mixture, or spongy ice, is deposited on the growing ice particle. The enhanced water retention in the production of spongy ice compared with, say, the production of glaze ice, may result in a difference in the mechanism of charge separation which can operate under these different conditions.

The results of laboratory investigations, summarised briefly above, clearly show the variation in experimental results which may be obtained by slightly changing the experimental conditions. It is hoped that the experimental work described below may show which of these conditions are likely to be of major importance in determining the electrification of ice particles and water droplets.

CHAPTER V.

EXPERIMENTAL INVESTIGATION OF THE ELECTRICAL EFFECTS AT ICE/WATER INTERFACES.

We have seen in the preceding chapters that many of the processes thought to be of importance in the electrification of clouds, hail, rain and snow involve charge separation mechanisms which operate at air/water or water/ice interfaces. Many workers have studied the air/water interface and a considerable amount of theoretical and experimental work has been directed towards determining the properties of, and structure within, the interface, but comparatively few attempts have been made to investigate the nature of the ice/water interface.

The experiments described in the following chapters were designed with the object of characterising the electrokinetic, or zeta potential, should one exist, between ice and very dilute aqueous solutions, and to see if the results could be in any way related to the charge separation mechanisms already known to exist in ice/water systems.

V. 1. Experiments with Ice-coated Balls.

Church (1966) observed that a moving ice-coated brass rod of 4 mm diameter became charged when droplets splashed from its surface. (See Fig. IV.2.). The appearance of the resultant ice surface suggested that the droplets had spread out on impact and had flowed over the surface of the ice to form a liquid layer which had then frozen. However, portions of the liquid layer had been lost before freezing, perhaps due to the centrifugal force exerted by the rotating rod, or the configuration of the air flow around the rod. In order to be able

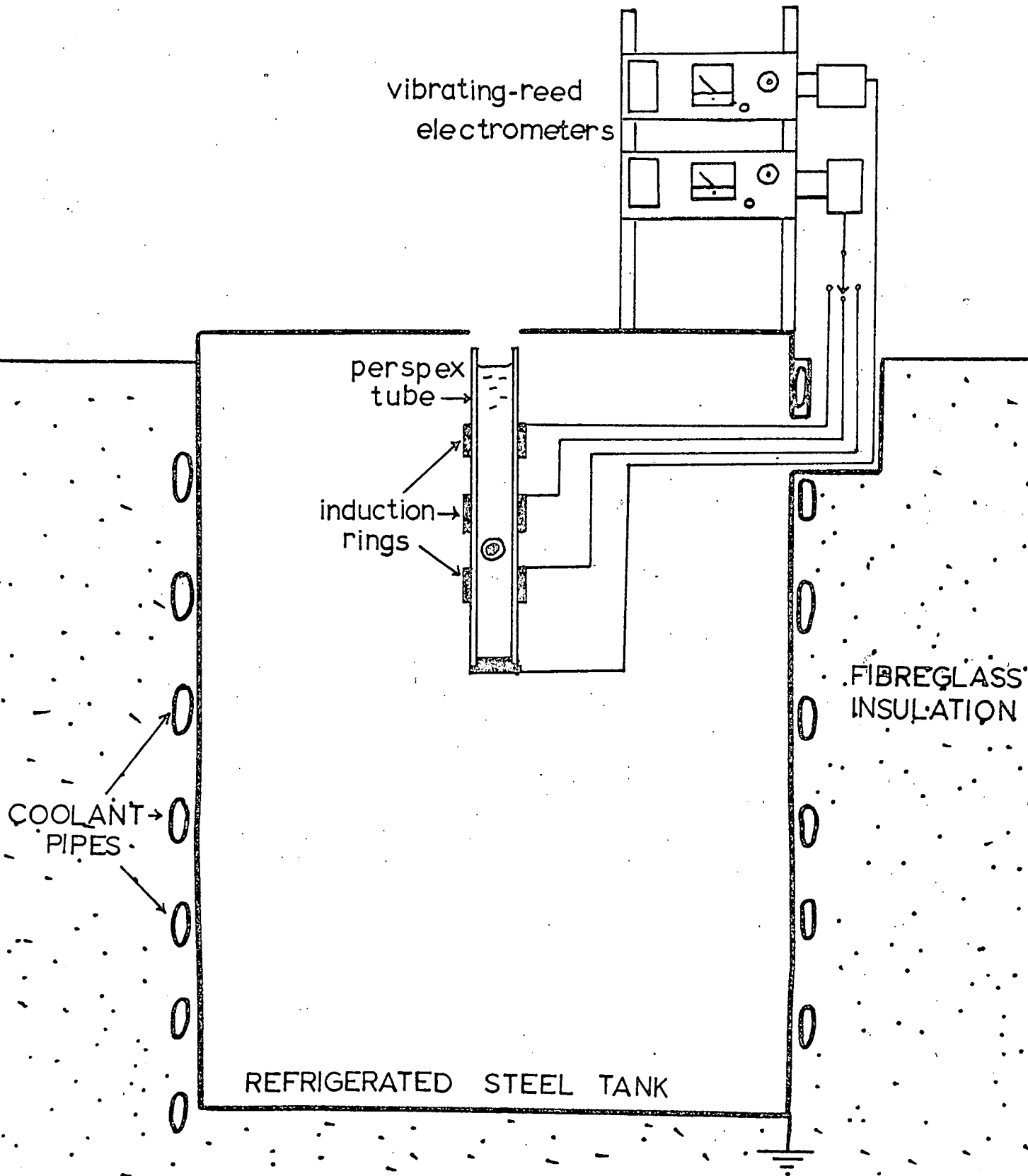


Fig. V.1. APPARATUS FOR DETERMINING THE CHARGE ON ICE-COATED SPHERES, FALLING THROUGH WATER.

to compare directly the amount of charge which had been acquired by the rod and the charge which might be separated at the ice/water interface as a result of the motion of the water over the ice, I decided to try to investigate the charge acquired by ice-coated brass spheres of 4 mm diameter on falling through water at 0 ° C.

A perspex tube, internal diameter 25 mm, external diameter 32 mm and 245 mm long, was suspended vertically in an earthed, stainless steel, refrigerated tank, 0.56 m deep and 0.43 m in diameter, maintained at temperatures below 0 ° C. (See Fig. V.1.) The bottom 5 mm of the tube were plugged with a brass disc, connected to an ECKO N616B Vibrating-reed Electrometer. (The electrometer is described in more detail in Appendix 1.) Three brass induction rings, of 32 mm internal diameter and 18 mm in depth were attached to the outside of the tube and could be connected to a second electrometer individually or in parallel. To prevent condensation from shorting out the induction rings or the brass plug, the whole tube assembly was sprayed with "Damp Start", a quick-setting plastic in an aerosol can used to protect high-tension leads on petrol engines.

The detection system was tested by dropping 4 mm nylon spheres down the tube. These spheres almost always carried a charge which was registered as electrometer deflections both by the electrometer connected to the induction rings and the electrometer connected to the brass base of the cylinder. The maximum sensitivity of the electrometers was limited by the background noise level to about 10^{-14} C for the electrometer connected to the brass plug and considerably less than this for the electrometer connected to the induction

rings, because the response time of the electrometer is of the order of 1 s for full scale deflection. A rough calibration showed that the maximum sensitivity of the induction ring system was for charges of about 10^{-9} C, i.e. about half of the charge separation detected by Church at 0° C.

De-mineralised water at the melting point was poured into the cylinder and the electrometers were switched on. The 4 mm brass spheres were coated with ice by cooling them to about -30° C in a second refrigerator compartment and dropping them into a tray of freezing water on the compartment floor. A smooth ice-shell formed over the surface of the spheres, with the exception of a point where a sphere rested on the ice-covered floor of the tray. The spheres were broken away from the ice with tweezers and any holes in the ice-shells were filled by re-cooling the spheres and dropping cold water on to them. Using earthed tweezers, the simulated hailstones were transferred to the perspex tube and released just above the surface of the water.

The electrometer detected no charge as the sphere fell through any of the induction rings. However, when the spheres hit the base of the tube, both electrometers registered deflections. Uncoated brass spheres gave similar deflections and it was concluded that they were due to piezo-electric charging of the perspex tube. The failure of the induction ring system to detect any charge on the spheres could perhaps be attributed to the higher dielectric constant of water compared with that of air. The time taken for the charge on the spheres to be induced

onto the ring would be increased and it is possible that only a small fraction of the charge on the sphere would be induced before it fell out of the ring. The method also suffered from other disadvantages:

- (i) the water in the tube tended to warm up, even when ice was forming on the brass base, so the ice on the sphere was melting as it fell through the water and it was uncertain whether or not the sphere was still completely covered with ice when it arrived at the bottom of the tube: and,
- (ii) the presence of ice on the brass plug might invalidate direct readings of the charge on the sphere, since charge was possibly being separated by the Workman and Reynolds Effect or the Temperature Gradient Effect.

Accordingly, further experiments of this type were discontinued in favour of experiments which might give a less ambiguous result.

V. 2. The Rotating Tube Experiment.

When a horizontal cylinder containing a liquid and a gas is rotated about its long axis, the liquid is centrifuged to the walls of the cylinder and the gas takes up a position in the centre of the tube along the axis of rotation. This principle was used by McTaggart (1914 and 1922) and Alty (1924 and 1929) to determine the charges on gas bubbles in liquids. A small gas bubble was introduced into a glass tube full of liquid. The tube was rotated by an electric motor and the bubble took up a position along the axis of rotation. When a potential difference was applied between electrodes at the ends

of the tube, the bubble moved along the tube and the charge on the bubble was deduced by considering the bubble velocity, the viscous drag opposing migration along the tube and the force on the bubble due to the electric field. McTaggart found it necessary to use as smooth and regular a tube as possible to prevent, or at any rate reduce, the tendency of the bubbles to take up an equilibrium position along the axis of rotation of the tube corresponding to the maximum internal diameter of the tube.

This system should work for any material in a denser fluid and it was decided to attempt to align an ice particle along the axis of a rotating tube filled with water at 0 °C. If it acquires a charge as a result of the motion of the water it should be possible to apply an electric field and move the particle in the same way as was done for air bubbles.

Glass was not thought to be a suitable material for the tube since the equipment would be run at low temperature and there would always be a risk of the enclosed water freezing and fracturing the tube. Perspex or better still, clear polystyrene might be more suitable, but commercially produced tubes were found to vary in internal diameters by 5 to 10% from their nominal bores. However, it was found that perspex tubing could be turned on a lathe and re-polished with an abrasive metal polish to give a good transparent finish without much difficulty and it was less likely to crack, warp or melt under these conditions than polystyrene. Therefore, it was decided to use perspex, but since it is quite brittle, the additional precaution of sealing the ends of the tube with tight push-fit, brass electrodes was

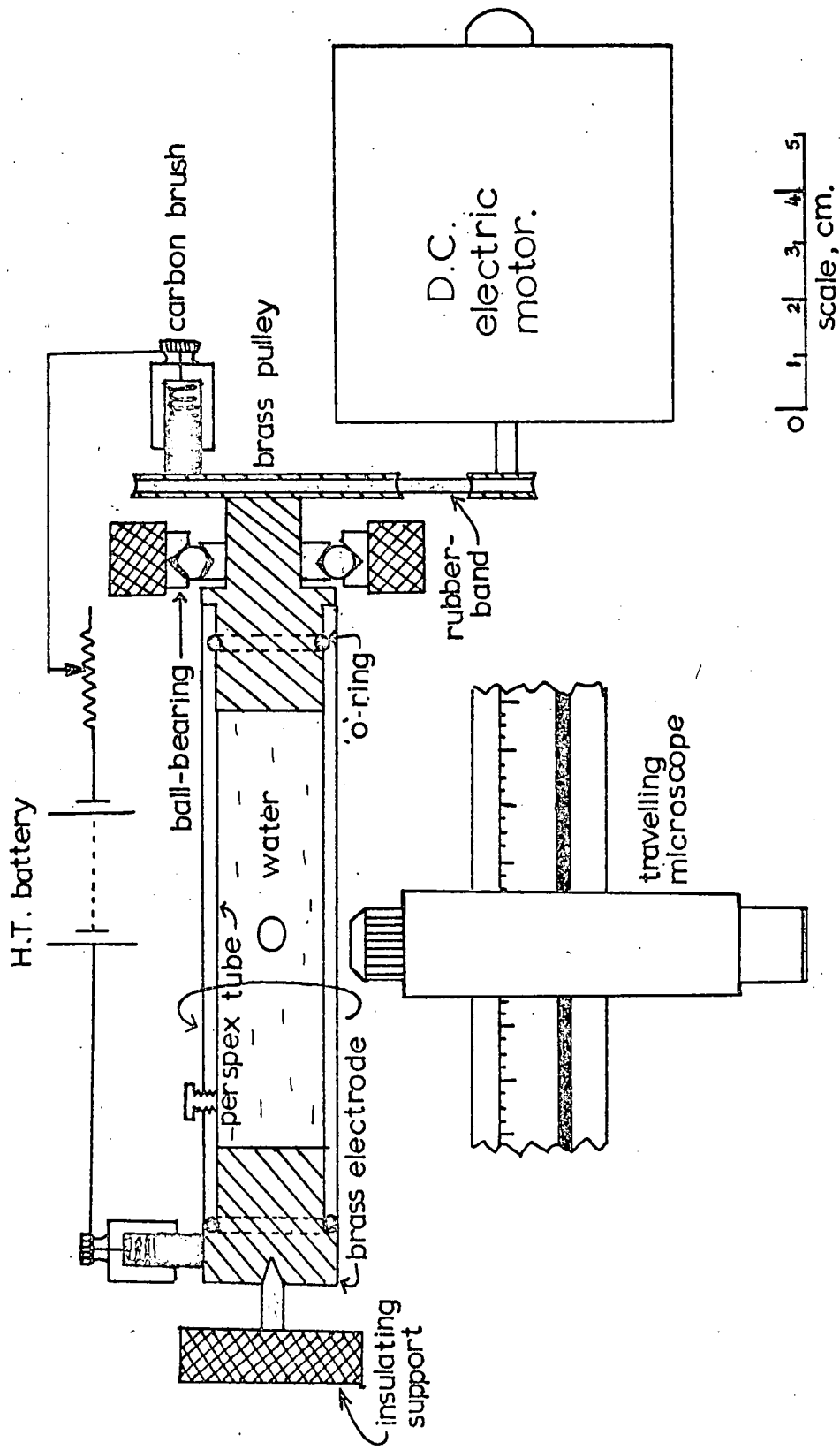


Fig. V.2. THE ROTATING TUBE APPARATUS.

taken. In practice, the tube never fractured due to the expansion of the contents on sudden freezing, and the increase in volume was taken up by movement of the electrodes.

The tube, see Fig.V.2., was made from nominally 19 mm internal diameter perspex tubing which was carefully reamed out to 22.2 mm on a lathe using paraffin as a lubricant for the reaming tool. The outside of the tube was also turned down slightly to prevent distortion of the field of view when the tube was viewed through a microscope due to slight irregularities on the tube's outer surface. Both surfaces of the tube were then carefully polished with metal polish to restore the original glassy finish. The ends of the tube were sealed with brass electrodes, as described above, but it was found to be necessary to fit neoprene 'O'-rings (as shown in Fig.V.2.) to seal the tube, so as to prevent water from being centrifuged out from the very narrow gaps between the electrodes and the tube. Loss of water from the tube allows microscopic air bubbles to appear in the tube, interfering with the measurements.

The pulley-driven electrode is mounted in a ball bearing supported on an insulating tufnol block bolted to a base board. The other electrode is supported on a tapered, steel "centre" also mounted on a tufnol block. The position of the "centre" is adjustable so that play in the bearing can be taken up. Before measurements are made the "centre" is fixed by means of a lock-nut. A potential difference can be applied between the electrodes using carbon brushes rubbing on their exposed surfaces.

The tube may be filled with liquid through a taper-tapped,

4 B.A. hole which is then sealed by a 4 B.A. nylon bolt.

Before commencing the experiments, the tube and electrodes were dismantled and scrubbed in a soap solution. They were then thoroughly washed in de-mineralised water and allowed to stand overnight in a 2 litre beaker full of de-mineralised water before re-assembly. The tube was filled with water by inserting the tip of the needle of a hypodermic syringe into the filling hole and slowly pumping water into the tube, tilting the tube so as to allow all the small air-pockets and bubbles, which were inclined to be trapped inside the tube, to escape through the filling hole. When all the air had been expelled, the tube was filled to overflowing and the nylon bolt was inserted, taking care not to introduce any air bubbles. The whole apparatus was then transferred to a cold-room maintained at between -1 and -3 °C.

The cold-room had a working space measuring 1.4 m long by 0.9 m wide by 2.4 m in height and was fitted with a perspex window through which the tube could be observed. Trap-doors were fitted to this window to enable adjustments to be made to the apparatus without entering the room, so that the temperature of the environment within the cold-room could be maintained.

Eventually, ice began to form on the surface of the electrodes. Usually, this took the form of a thin sheet of glaze ice which could be removed by switching the electric motor on for a few minutes to bring the warmer water in the middle of the tube into contact with the electrodes; but occasionally all the water became supercooled and froze suddenly producing a spongy-ice and water mixture in the tube.

When this happened, the tube was rotated and gently warmed with warm air from a hair-dryer until the last traces of ice had just disappeared.

Having by these means obtained a tube full of water at a temperature very close to the freezing point, the nylon stopper was removed and a small sliver of ice was introduced into the tube. Any air which had also entered was removed as before using a hypodermic syringe. The syringe was kept outside the cold-room to prevent the water in the needle from freezing, but could be introduced into the cold room through one of the trap doors when required.

The stopper was replaced in the tube and the motor was switched on. The ice particle took up a position along the axis of the tube, but at this point difficulties arose.

(i) The ice particle was never exactly spherical and usually it was long, thin and angular. When it took up a position along the axis of the tube, its centre of gravity may have been exactly on the axis of rotation of the tube. However, although there was some tendency for the ice to line up with its longest axis along the tube, this was not very marked and usually the particle precessed about the axis of rotation. This made observation of the particle through the travelling microscope difficult.

(ii) Despite the precautions taken to ensure that the water was as near 0° C as possible, it was always slightly above the melting point and the ice splinters were all slowly melting. Usually, less than two minutes of observation of the

particles was possible.

(iii) Although only ice specimens which were as free of air bubbles as possible were introduced into the tube, they always contained a few microscopic bubbles. On melting of the ice, the bubbles were released into the water and took up a position along the axis of rotation. The air bubbles tended to give an impulse to the ice as they were released, causing the ice particle to move sharply along the tube each time a bubble was released. Often the ice particle was forced off the tube axis when bubbles were released. Electrical measurements were impossible under these conditions and an attempt to segregate ice particles and air bubbles, by varying the speed of rotation of the tube was unsuccessful.

Therefore, another approach to the problem of measuring a zeta potential was tried.

V. 3. Electrical Measurements with Ice Tubes.

The relationship between the potential difference produced between the ends of a capillary tube and the zeta potential between the material of the tube and the liquid flowing through it was derived in Section III.3. Therefore, if it is possible to measure a potential difference between the ends of an ice tube through which water, or a dilute aqueous solution, is flowing and provided that this potential is caused by the movement of a portion of the electric double layer, it will be possible to calculate a value for the zeta potential.

In discussing the mechanics of flow-charging of liquids flowing through tubes, Loeb (1958) states that only limited charge separation would be possible if the resistance of the solution return path was so low that the charge leakage rate nearly equalled the generation rate. Flow electrification in large tubes and for bulk movement has been observed to be confined to liquids having a volume resistivity in excess of $10^7 \Omega \text{ m}$. Water and dilute ionic solutions with resistivities in the range 10^3 to $10^4 \Omega \text{ m}$ would not be expected to give detectable electrification under such conditions, but Loeb points out that in glass tubes of 10^{-7} m radius, even 10^{-2} molar potassium chloride solution with a resistivity of about $10 \Omega \text{ m}$ should give electrification. Therefore, it should be possible to detect any flow electrification produced by very dilute ionic solutions in a tube with an internal diameter of about 1 mm or less and a length of at least 10 mm.

It is also essential in streaming, or flow, potential measurements that the resistance of the tube itself should be large, so that the charge separated does not leak away through the solid. The resistivity of ice at temperatures near freezing is about two orders of magnitude greater than that of water. Therefore, provided that the cross sectional area of the ice tube is not greater than 100 times that of the liquid column, the charge separated should still be detectable. Thus it appears that it should be possible to detect a streaming potential produced by water flowing through an ice tube.

V. 3(a). Experiments with unsupported ice capillary tubes.

If it were possible to manufacture an ice capillary tube which was supported at each end only by an electrode, many sources of spurious charges generated by changes of temperature and mechanical shocks on the insulating material of a support tube would be eliminated. Tests with various types of mould showed that it was possible to produce capillary tubes of about 100 mm length, with an internal diameter of 1.5 mm and an external diameter of 10.8 mm, complete with brass electrodes by the following method.

A brass mould, of the type shown in Fig.V.3., was dismantled, washed in a soap solution, rinsed thoroughly with de-mineralised water and re-assembled. It was then filled with water, using a hypodermic syringe, taking care to ensure that no air bubbles were left in the mould. The mould was transferred to a refrigerator and left there until the water froze.

If the refrigerator was maintained at a temperature of about -30°C , the resulting ice tube was opaque and contained many small air bubbles. These ice tubes were very fragile. However, if the refrigerator was at between 0°C and -5°C and the mould was left at this temperature for about a week before it was opened, a clear, strong ice tube was produced which was composed of only a few large crystals and contained fewer, but larger, air bubbles.

While they were still in the refrigerator, the ice tubes were removed from the moulds in the following way. Firstly, the stainless steel wire was rotated to free it from the ice and then it was smoothly withdrawn from the mould. Secondly, one of the end

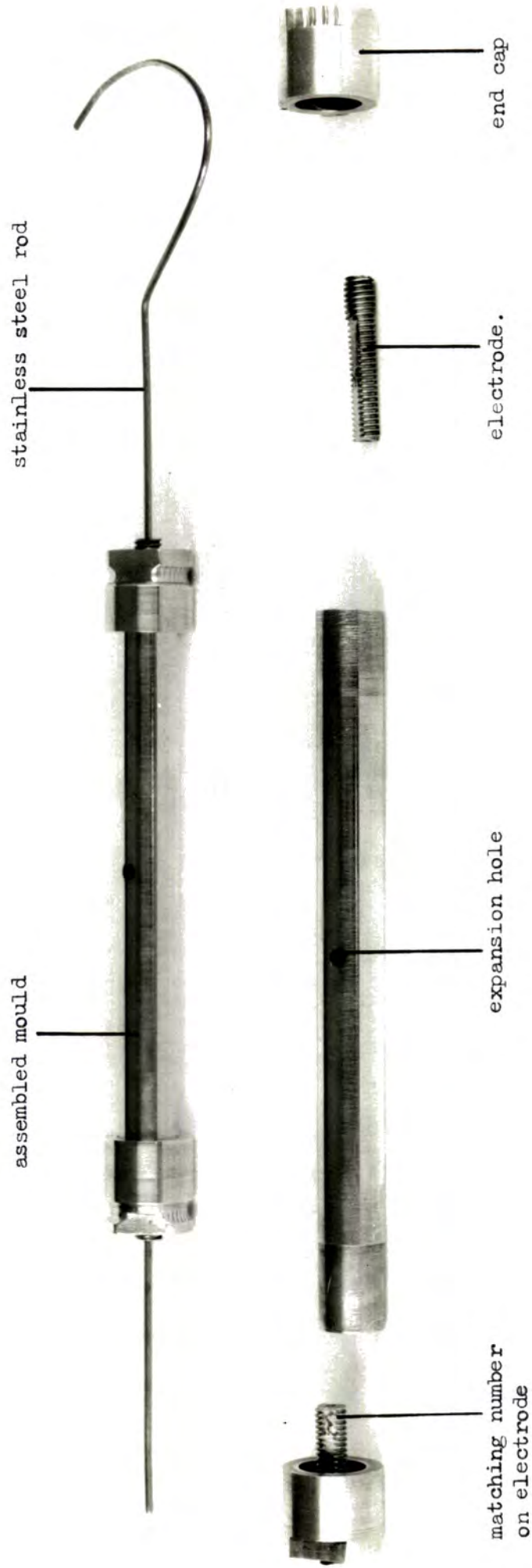


Fig.V.3 The Ice Tube Moulds.

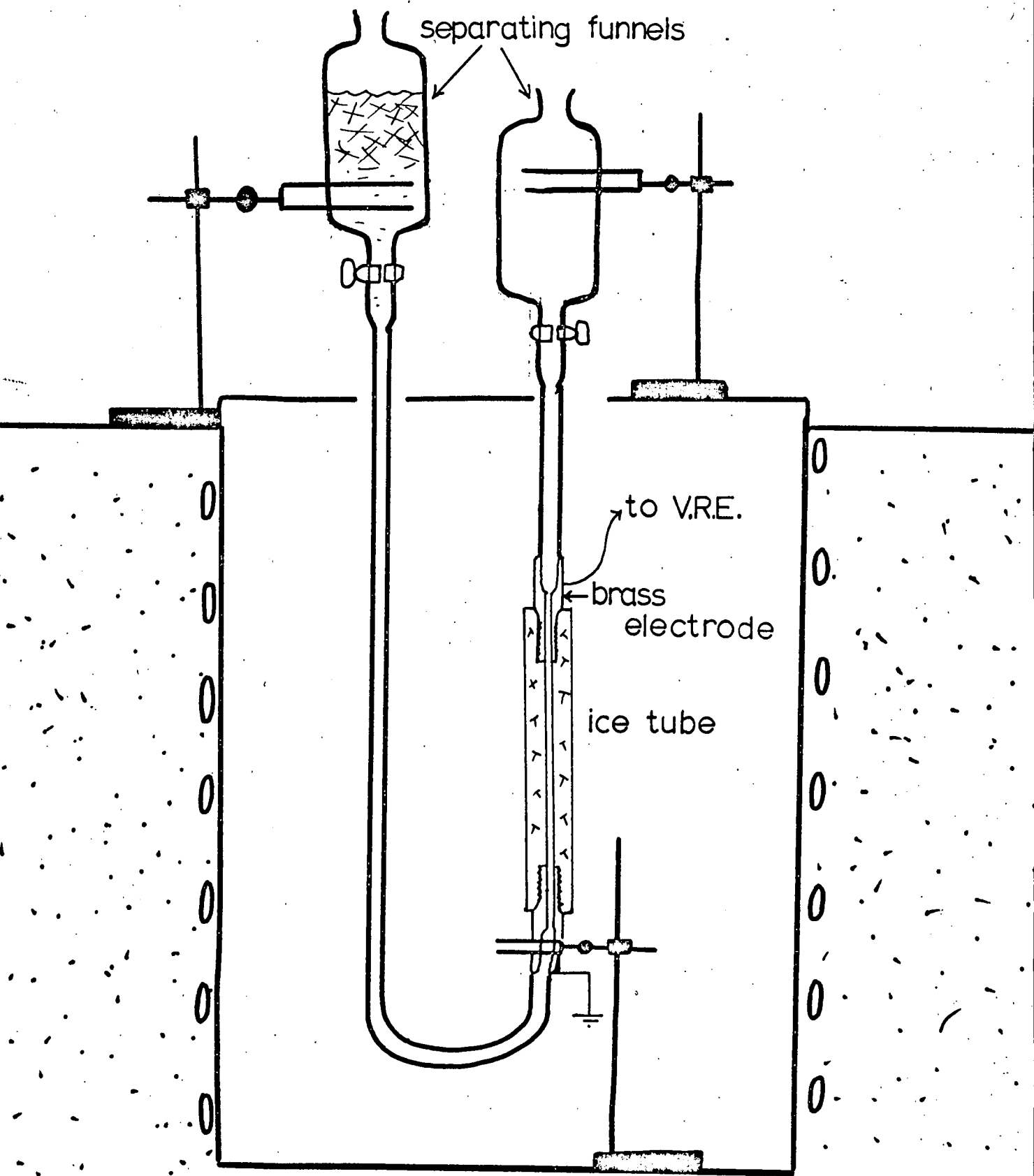


Fig. V.4. EXPERIMENTAL ARRANGEMENT FOR UNSUPPORTED ICE CAPILLARY TUBES.

caps was removed by warming it gently by holding it in the hand for a second or two and then quickly unscrewing it from the electrode. The filling hole was checked to ensure that it was free of ice and the brass body of the mould was withdrawn from the ice tube by warming it gently by hand and slowly easing the ice out by pulling on the remaining end cap. Finally the end cap was unscrewed from the electrode.

About one capillary tube in five could be successfully obtained by this procedure. The remainder shattered or cracked on removal from the mould or else the capillary became blocked as a result of a small drop of water finding its way into an electrode and freezing there.

In order to measure streaming potentials, the tube was mounted vertically in the refrigerator with short lengths of brass tubing screwed onto the electrodes. The lower tube was connected to earth and clamped, the upper tube was connected to a vibrating-reed electrometer. Short lengths of clear 10 mm P.V.C. tubing were attached to the brass tubes and pyrex separating funnels were inserted into the open ends of the tubing. (See Fig.V.4.) The electrometer was used without a shunting resistance across its input. On the first occasion that this was done a steady deflection of about 30 mV was obtained which was eventually traced to using electrodes made from different pieces of brass. Thereafter, all electrodes were made in matching pairs from the same piece of brass and standing electrode potentials were reduced to a few millivolts.

A mixture of crushed ice and water was poured into the upper separating funnel and the taps were opened. Depending on the refrigerator temperature, one of two things happened. Either the water froze in the tube, blocking it completely, or the lower electrode quickly became warmed, melted the surrounding ice and became detached from the ice tube. In both cases, the potentials measured by the electrometer were erratic and of the order of tens of millivolts.

In all these experiments, it had proved to be impossible to control the temperature of the water or ice sufficiently well to ensure that the conditions were stable for long enough to measure an electrokinetic effect. In an attempt to produce water continuously at 0°C , water was made to flow through clear, P.V.C. tubing, with an internal diameter of 10 mm, which was immersed in a refrigerated tank filled with methylated spirit, maintained at a temperature of -25°C . The water which emerged never quite reached 0°C and eventually the flow ceased. When the tube was examined it was seen to have become blocked with ice containing many small air bubbles. These appeared to be arranged in streams beginning at the walls of the tube, but on nearing the centre of the tube, they had bent over towards the direction of the flow until they had joined to form a thin column along the axis of the tube about 0.5 mm in diameter. This indicated that ice had first formed on the walls of the tubing and had gradually become thicker until a capillary tube was formed. It appeared that this method could be used to make an ice capillary tube in situ in an insulating support tube. Further, by changing the temperature of the coolant, the temperature of the water or the rate of flow of the coolant, the freezing rate could be changed.

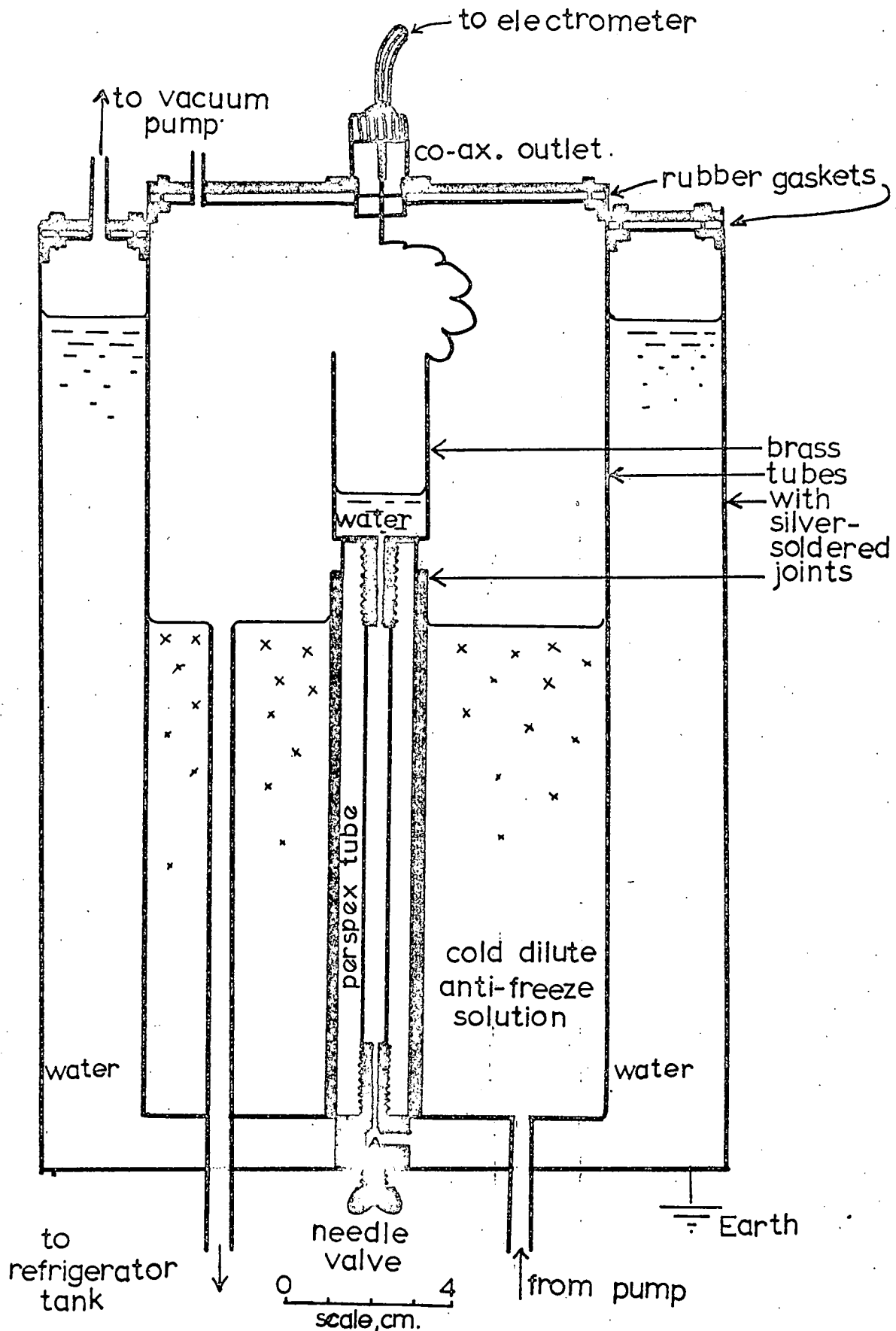


Fig.V.5. APPARATUS FOR MEASURING THE ELECTRIFICATION OF WATER ON FLOWING THROUGH A PERSPEX-SUPPORTED ICE TUBE.

In this way, the required degree of temperature stability for the measurement of an electrokinetic effect might be obtained. The first piece of apparatus built to test this idea did not work in quite the desired way, but did provide some interesting results.

V. 3(b) The perspex tube experiments.

The perspex tube 135 mm long with an internal diameter of 5.3 mm and an external diameter of 12.5 mm is mounted inside three co-axial brass cylinders as shown in Fig.V.5. All the joints between these cylinders, the end plates and fittings were silver-soldered to ensure good electrical contact at low temperatures. (See Appendix 2.) A small, brass cup is fitted to the upper electrode and connected, via a co-axial lead, to a vibrating-reed electrometer.

A 33% aqueous anti-freeze solution (containing ethylene glycol and methanol) was pumped into the space between the inner two brass tubes to a level determined by the exit tube. The innermost, earthed, brass tube was found to be necessary to eliminate charging of the perspex tube by the anti-freeze solution. The anti-freeze solution was returned to a 65 litre-capacity refrigerated tank, maintained at -15°C , from which it was re-circulated by a Stewart and Turner centrifugal pump, with a maximum pumping rate of 6.5 litres per minute.

De-mineralised water was poured into the space between the outer two brass cylinders, with the needle valve below the earthed electrode in the closed position. When ice started to form on the inner wall of the water reservoir the outer lid was fixed in position

and the needle valve was opened. Water flowed into the perspex tube and, after one or two minutes, the vacuum pump was switched on and the water flowed out of the tube back into the reservoir. Thereafter, the vacuum pump was switched on and off at between one and two minute intervals.

When there was no ice present in the tube, the electrometer readings followed the characteristic pattern shown in Fig.V.6. The upper trace was obtained with the lid of the middle tube removed, the lower trace, with the lid in position. The various points marked along the trace correspond to operations which were performed, and visual observations made, at that time. Fig.V.6. shows that when water was in the perspex tube, in the absence of ice, there was a small standing potential of - 10 mV which was not affected by the presence of the operator when the lid was removed. Subsequent "runs" were made with the lid removed so that visual observations could be made.

When the water had been forced backward and forward through the tube three or four times, an abrupt change was observed on the electrometer trace. (See Fig.V.7.) By stopping the experiment at this point on other occasions, this change was correlated with the appearance of ice in the tube. The appearance of a negative peak on the recorder trace was always seen to be followed by the appearance of an air bubble of about 1 mm diameter in the brass cup above the electrode. At about this time, the liquid column in the tube must have become blocked, because the liquid level in the cup was seen to have stopped rising or falling. If the tube was dismantled at this stage, an ice rod was found

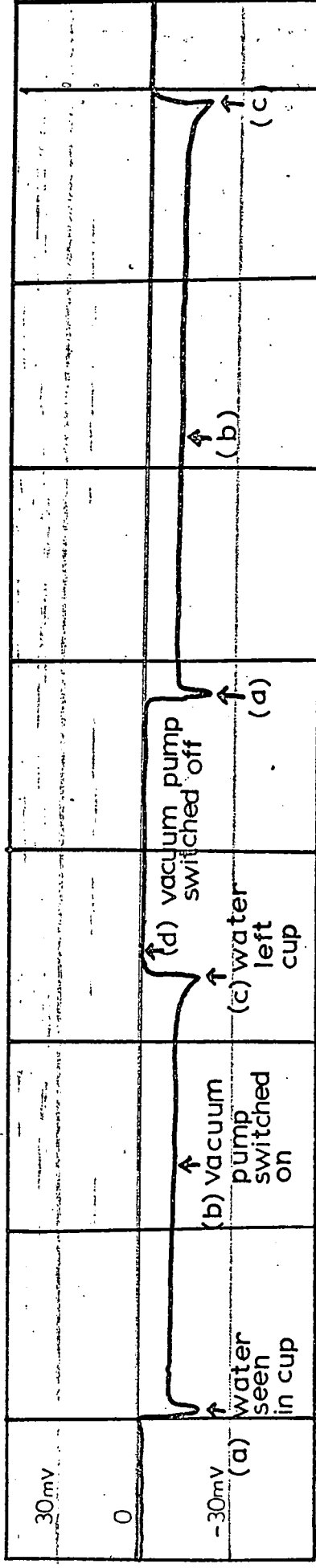
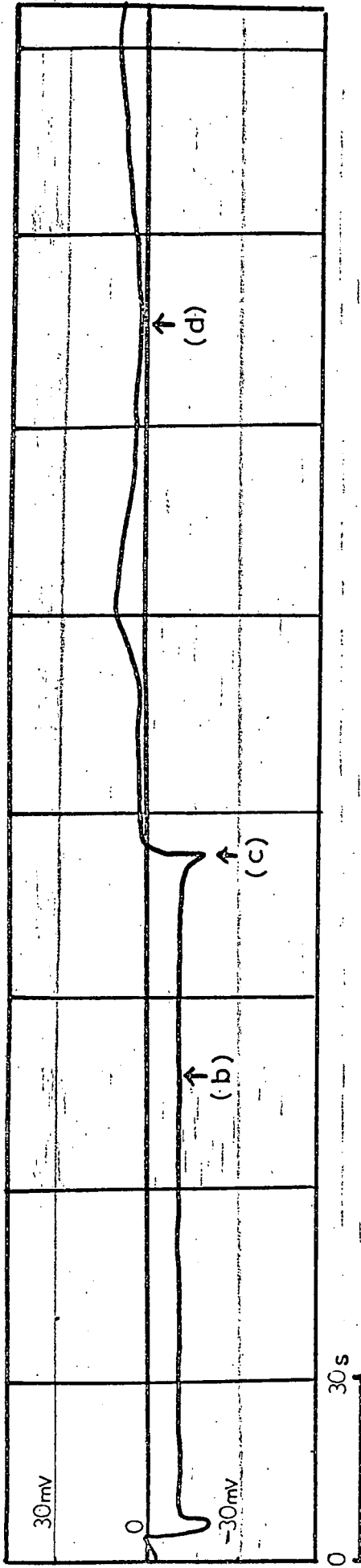


Fig. V. 6. ELECTRIFICATION OF THE PERSPEX TUBE IN THE ABSENCE OF ICE

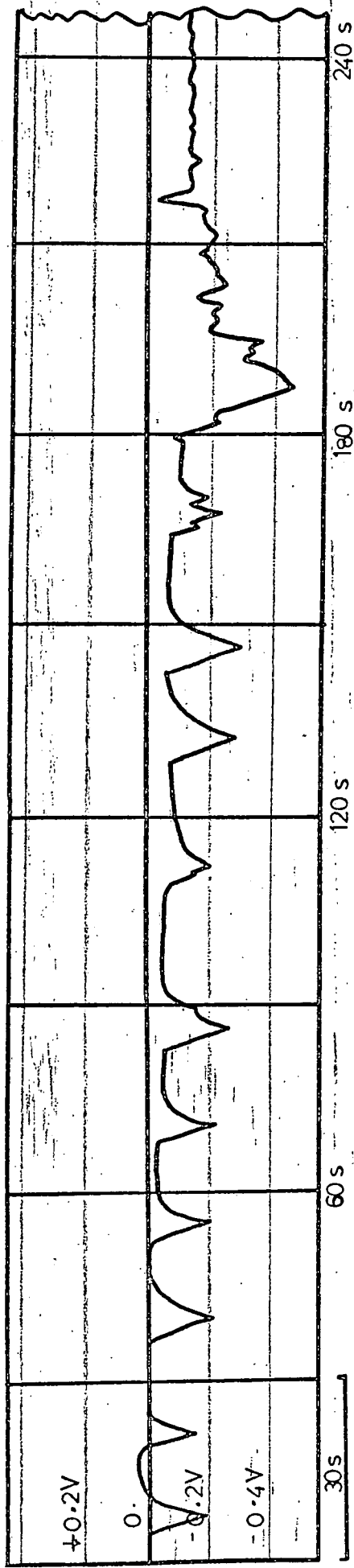


Fig.V.7. A TYPICAL RECORDER TRACE ,SHOWING THE AIR BUBBLE EFFECT IN THE PERSPEX TUBE.

to be filling the perspex tube and examination of this rod showed that it had been formed co-axially. When the large, broad, negative peak had been recorded by the electrometer, the anti-freeze pump was switched off and the anti freeze solution drained quickly out of the apparatus. The electrometer reading gradually fell toward zero and, about one minute later, more peaks and bubbles were observed, but this time the peaks were positive and sharper than the negative peaks had been. The positive peaks eventually became less frequent and ultimately, died away altogether. At this time, the water was seen to be moving in the cup once more.

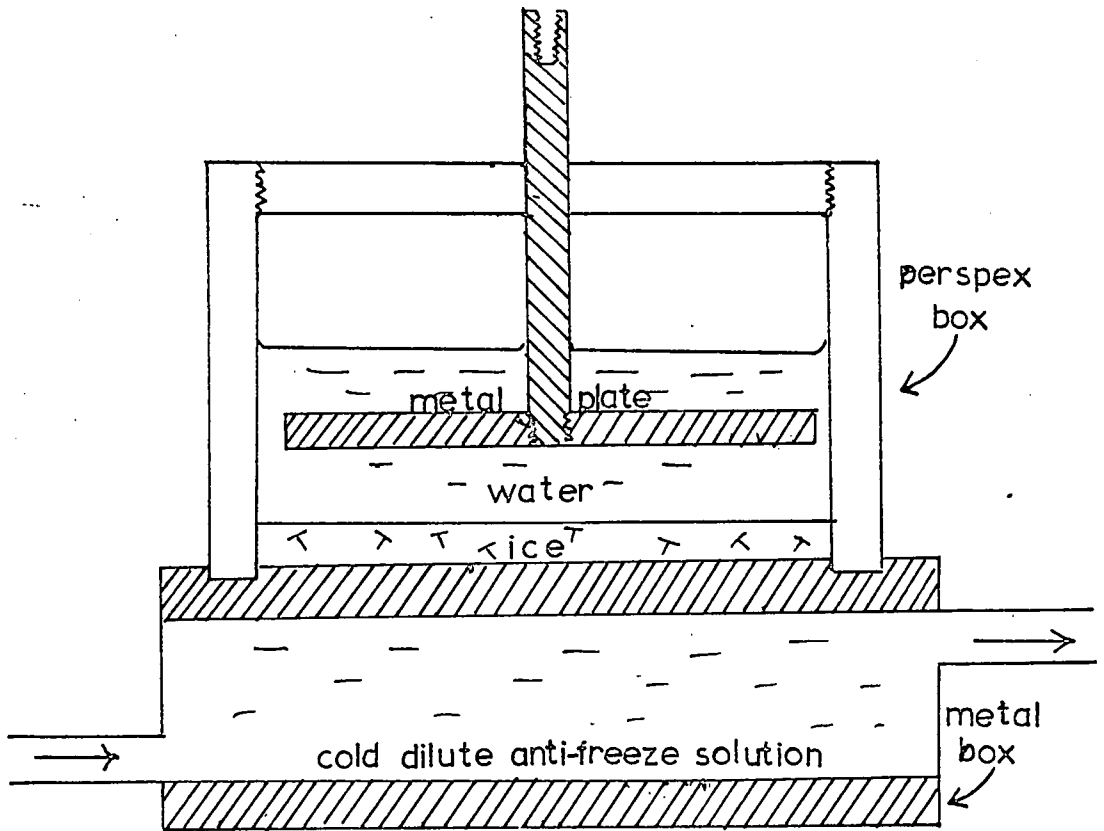
The recorder used in these experiments was a Watanabe Miniwriter, type 201 L. Unfortunately, it was not available for most of the period during which these experiments were being performed, and no other recorder available at the time responded quickly enough to the changes in potential for all the detailed features to be recorded. However, although only four traces have been obtained, (see Appendix 3), the characteristic patterns were observed on each of ten occasions over a period of one month, using samples of demineralised water from the same bottle.

These results could not be explained at the time, but since they appeared to be associated with the freezing and melting of water and ice, and with the production of air bubbles, two other series of experiments were performed:

- (i) Workman and Reynolds-type experiments to measure freezing potentials, and

(ii) the measurement of the electric potential differences developed between water entering into, and emerging from, the ends of an ice tube supported in a glass tube.

These experiments are reported in Chapters VI and VII respectively, and a discussion of the results obtained in the experiment described above in V. 3(b). is deferred until Chapter VII.



THE BASIC FREEZING CELL.

Fig. 7.1.

CHAPTER VI.

THE FREEZING POTENTIAL MEASUREMENTS.

VI. 1. The Design of the Apparatus.

During the course of the work, the fittings on the freezing cell were altered as particular aspects of freezing phenomena were investigated. In its final form the freezing cell is shown in Fig. VI.7 and Fig. VI.8, but the perspex cylinder with its lid, the metal cooling chamber and the flat upper electrode were common to all modifications of the apparatus. The basic freezing cell is shown in Fig. VI.1.

VI. 1(a) The size of the freezing cell.

Workman and Reynolds (1950) state that the charge separation mechanism operating when dilute aqueous solutions are frozen is that ions of one sign are preferentially incorporated into the ice, leaving an excess of ions of the opposite sign in the water. A given rate of incorporation of the ions into the ice will lead to a particular rate of charge separation. However, the potential difference between the ice and the water is not solely a function of the charge separation rate, it is also a function of the charge neutralisation rate, which is principally governed by the leakage resistance of the ice/water interface. If the area of the interface is doubled, for a particular rate of transfer of ions per unit area, the charge separated will be doubled. But since, at the same time, the interfacial resistance will be halved, the potential difference will be unchanged.

Using a larger interfacial area has the advantage that any

possible edge effects, at the walls of the cell, would be reduced. A freezing cell of 76 mm diameter was used, which would hold a maximum of about 100 ml of solution. This cell is rather larger than that used by most other workers.

VI. 1(b). The method of cooling the freezing face.

The method used by Workman and Reynolds was to cool a large copper block in a refrigerator and rely on the heat capacity of the block to cool the freezing face in the freezing cell. (See Fig. III.2.) The principle of using a massive, metal heat-sink has since been used by most workers in this field. In the hope of being able to obtain much more rapid changes in the temperature of the freezing face, it was decided to use only a relatively small, metal heat-sink and to pump a liquid coolant around it. The rate of freezing could then be changed during the course of a "run", by changing either the rate of flow of the coolant past the freezing face or the temperature of the coolant. Methylated spirit or paraffin oil could have been used as the coolant but both suffer from disadvantages. Berriman (private communication) has noticed that the appearance of ice crystals growing by sublimation is modified by the presence of paraffin vapour, and paraffin has an appreciable vapour pressure at temperatures below 0° C. Condensation of paraffin vapour onto the surface of water in the freezing cell would affect the solubility of air in the water and might affect the crystal structure of the ice produced. Methylated spirit is also volatile and tests showed that 0.5 ml of methylated spirit per 100 ml of water changed the appearance of the

ice produced in a freezing cell from a hard, coherent coating to a soft mass of needle-shaped crystals. It also has the disadvantage of being highly flammable and additional precautions must be taken if it is to be pumped around the laboratory. A 33% aqueous, anti-freeze solution has fewer disadvantages, because, although it contains ethylene glycol and methanol to depress the freezing-point of the water, the partial vapour pressures of the volatile constituents are considerably reduced by the presence of the water and, therefore, the laboratory air is less likely to become contaminated. The solution is non-flammable and can be safely pumped with an unprotected pump. When it is used as a coolant, temperatures as low as -30°C can be achieved.

A comparison of the heat capacities and specific heats of the lower electrode and of ice, showed that the temperature drop across the lower electrode was negligible once there was more than 1 mm of ice covering the electrode.

VI. 1(c) The nature of the electrodes.

Five freezing cells were made in all, one with aluminium electrodes, one with stainless steel electrodes and two with brass electrodes. The remaining cell also had brass electrodes, but before the perspex cylinder was fixed in position, gold was evaporated onto the electrode surfaces. This cell was never used in the measurement of freezing potentials because even gentle cooling of the lower face caused the gold coating to peel off. However, it was useful as a check to see whether the change in conductivity of the solutions, with time, was a function of the

electrode material. (See Section VI. 5(b).)

All the cells were the same size and each pair of electrodes was made from the same piece of metal to eliminate electrode potentials. All the electrodes were highly polished. The upper electrode consists of a metal disc, 74 mm in diameter and about 5 mm thick, mounted on a metal rod by means of a no. 0 B.A. tapped hole through its centre. The lower electrode comprises the upper surface of the cooling chamber, through which the anti-freeze solution is pumped. This electrode is 102 mm in diameter and 5 mm thick and, in the case of all except the aluminium electrode, it is silver-soldered to the rest of the cooling chamber. The aluminium cooling chamber is bolted together with brass, 6 B.A. bolts.

Various methods of attaching the perspex tube to the lower electrode were tried. The problem was to bond perspex to a metal in a way which would not break when the metal contracted on cooling. The following method was found to be satisfactory, even when the cell was cooled rapidly from + 30 °C to - 25 °C.

A 6.4 mm wide ring, with an internal diameter of 76 mm, was cut into the lower electrode to a depth of 2 mm. The perspex tube was cemented into this ring with Araldite, an epoxy-resin. Care was taken to ensure that all traces of resin were removed from the electrode surface and the resin was cured at 50 °C for 24 hours before use.

Before each new solution was put into a freezing cell, the electrode surfaces were polished to remove oxide films. All

traces of metal polish were removed by washing thoroughly with a liquid detergent and rinsing with de-mineralised water until no change in the conductivity of the water was detectable.

VI.2. Early Experiments with the Freezing Cells.

VI. 2(a) General experimental method.

The cleaned cell was filled with a solution made from de-mineralised water of resistivity $10^4 \Omega \text{ m}$ or more. The upper electrode and lid were fixed in position, taking care to ensure that no air bubbles were trapped under the electrode. This electrode was connected to the electrometer, which was given an input impedance of $10^{10} \Omega$. Gill (1953) reports that such an impedance allows the measurement of true open circuit potentials, and in fact tests showed that there was no difference in electrometer reading when it was not shunted, but spurious effects, e.g. piezo-electric effects in the coaxial cable, increased in magnitude. The lower electrode was earthed. The electrometer readings were recorded by a Watanabe Miniwriter 201 L, single-channel, potentiometric recorder.

The anti-freeze solution was pumped from the bottom of an 80 litre-capacity, refrigerated tank, through the cooling chamber and back to the top of the tank. The maximum obtainable, coolant flow rate was about 10 litres per minute.

VI. 2(b) Observations.

When ice appeared on the surface of the lower electrode, the electrometer registered a deflection, which might be anything

from about 100 mV to 15 V, with the water positive with respect to the ice in almost every case. (See Fig.VI.2.) The potential differences usually fell away as time increased and sometimes the water became negative with respect to the ice, but there were exceptions to this and some of the voltage-against-time graphs showed two or three maxima. When the ice reached the upper electrode, positive potentials fell away to zero and were replaced by negative potentials, which persisted even when the upper electrode was submerged in the ice and all the water was frozen. These negative potentials were of the order of - 100 mV. Perhaps the most significant observation in these early experiments, was that the potential differences were not reproducible, even when repeated measurements were made on the same solution or when different portions of the same solution were used.

However, the voltage-against-time graphs appeared to become more reproducible after the first few freezings and meltings with the same sample of water on the same day. Two parameters are likely to change after two or three freezings.

- (i) the amount of air dissolved in the water, and
- (ii) the freezing rate.

That the freezing potential depends on the freezing rate was demonstrated by partially restricting the flow of coolant during the course of a freezing run. A fall in the positive freezing potentials was noted. When the flow rate was increased, the freezing potentials increased.

The conclusion that the amount of air in the water would

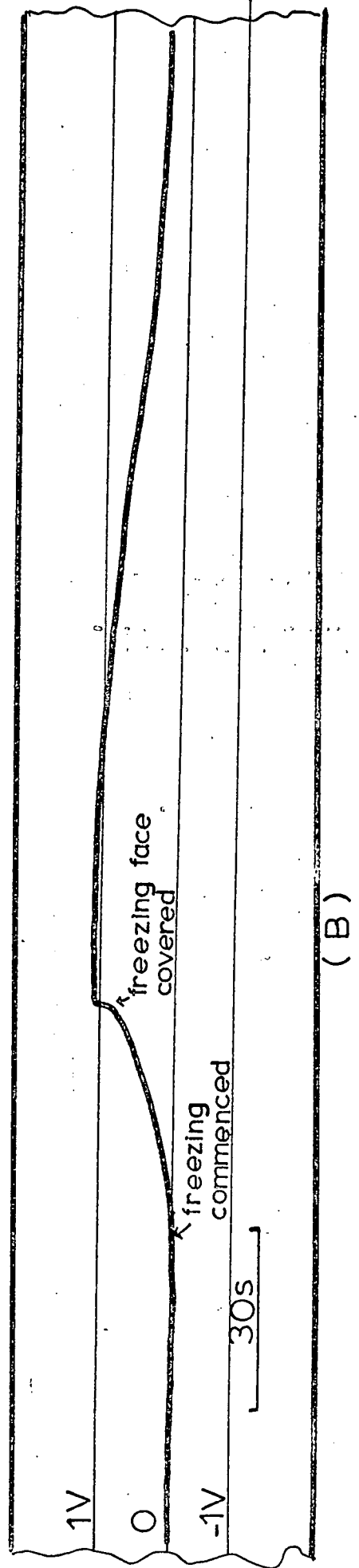
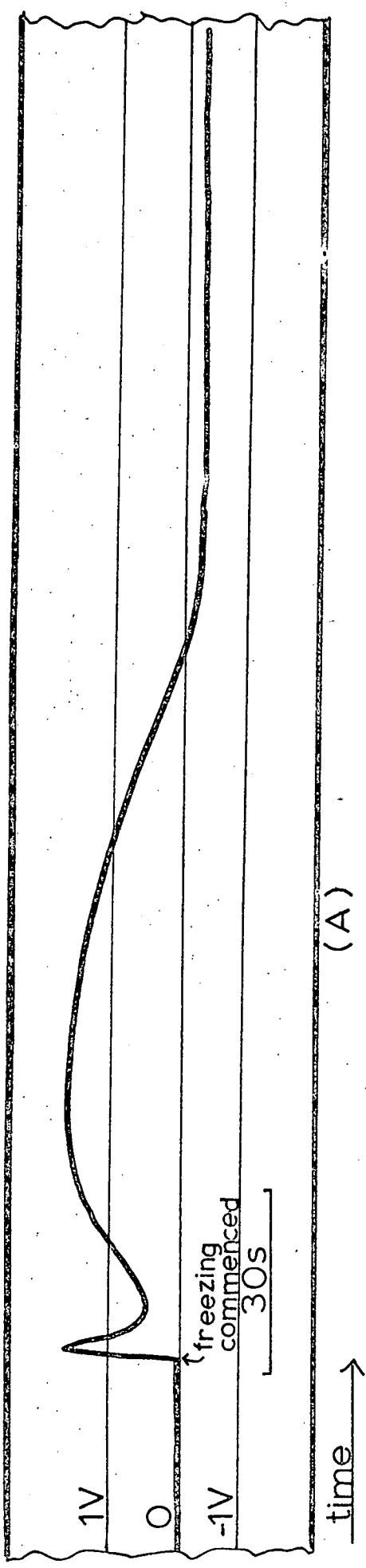


Fig. VI.2. TYPICAL RECORDER TRACES SHOW THE VARIATION IN FREEZING POTENTIAL WITH TIME.

change, and that this alters the freezing potentials may be justified in the following way. Air is much less soluble in ice than in water; therefore, when a saturated solution of air in water is frozen, the air is forced out of solution and air bubbles are produced at the water/ice interface. Some of these bubbles rise up through the solution and are either collected by the upper electrode or float past the electrode to burst at the water surface. However, most of the air is held, by surface tension, to the water/ice interface and, as the ice surface advances it tends to overtake the bubbles. Therefore, the bubbles become elongated in the direction of motion of the interface and, ultimately, they become trapped in the ice phase. When air-free water is allowed to stand in air, it slowly absorbs air until an equilibrium is established between the pressure and temperature of the air and the water, and the amount of air dissolved. Therefore, water which has been in contact with air overnight will be in equilibrium with the surrounding air. When this sample of water is frozen, some of the air will be expelled from solution and on melting the ice, air will begin to be re-absorbed into the water. If insufficient time is allowed to elapse for equilibrium to be re-established before the solution is frozen again, the solution will have less air dissolved in it than on the previous occasion. Therefore, when this solution is frozen, fewer bubbles will be released in the interface and the interfacial resistance will be lower. Hence, the leakage current will be increased and the resultant freezing potential, for the same rate of charge separation, will be

lower.

Experiments were designed to investigate these effects.

VI. 3. The Effect of Air Bubbles on the Freezing Potentials.

A convenient way of disturbing the air-water-ice equilibrium is to change the pressure of the air above the liquid. This was done by partially evacuating the air-space in the freezing cell.

The lid of a basic, brass-electrode freezing cell was fitted with an air-bleed valve and was connected to a vacuum pump. (See Fig. VI.3.) The screw threads in the lid of the cell were sealed with poly-tetrafluoro-ethylene (P.T.F.E.) ribbon on assembly. About 50 ml of de-mineralised water were used in these experiments and it was found that precise control of the air pressure within the cell was not possible, owing to the relatively small volume of air in the cell compared to the capacity of the vacuum pump. On the other hand a high capacity pump was needed, in order that rapid changes in pressure could be made when necessary. An Edwards E.S.³ 43 vacuum pump, capable of pumping 47 litres of air per minute, at atmospheric pressure, was used and the results are characterised as those obtained, "under normal pressure" and those obtained "under reduced pressure".

Case 1. If the air pressure was reduced before ice was present in the cell, very little change was noted in the freezing potentials. (See Fig.VI.4.) There was some evidence that the potential differences were less than under normal pressure, but the differences were less than the normal variations in consecutive

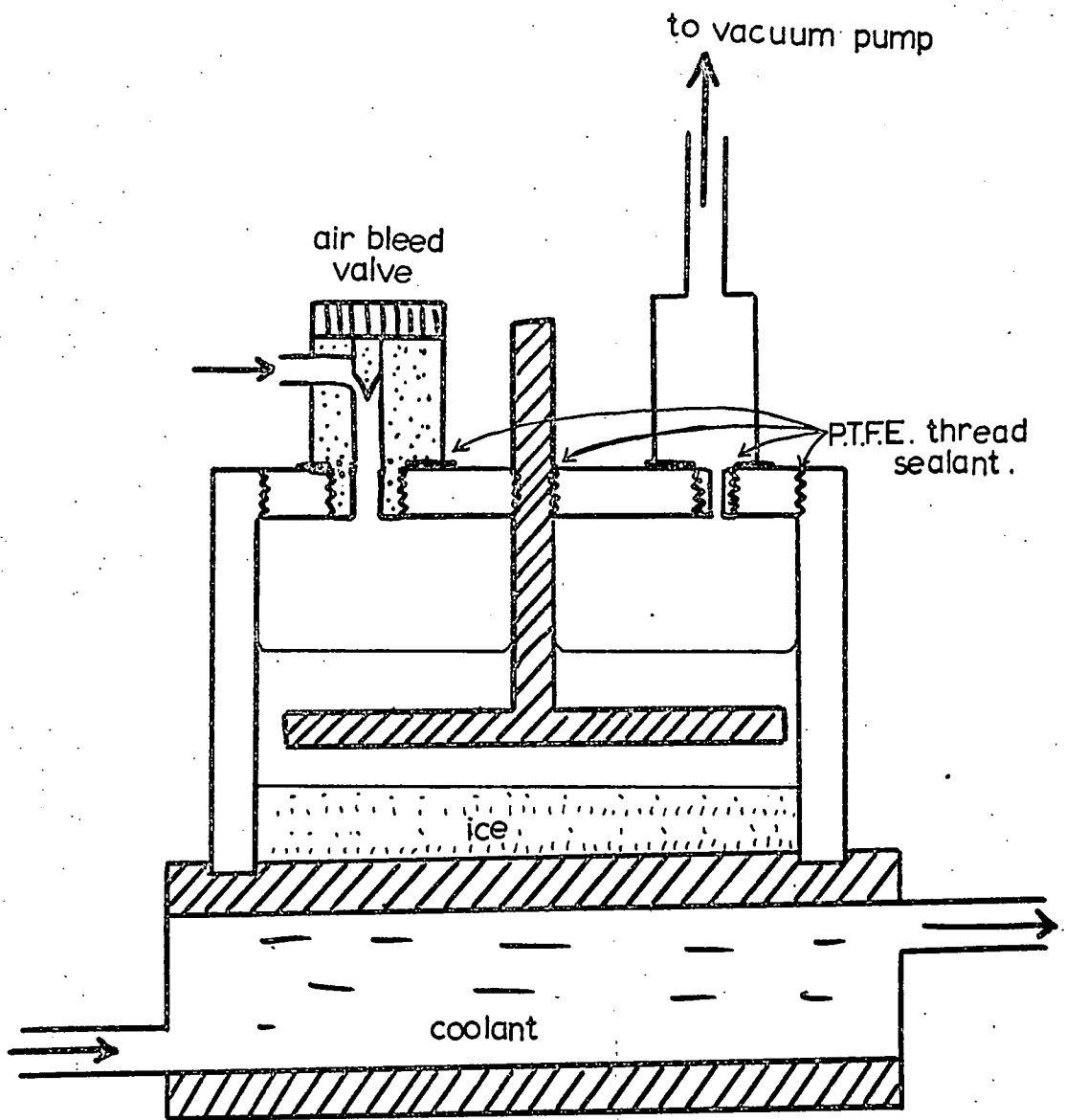


Fig. V. 3. APPARATUS TO DETERMINE THE EFFECT OF AIR BUBBLES ON FREEZING POTENTIALS.

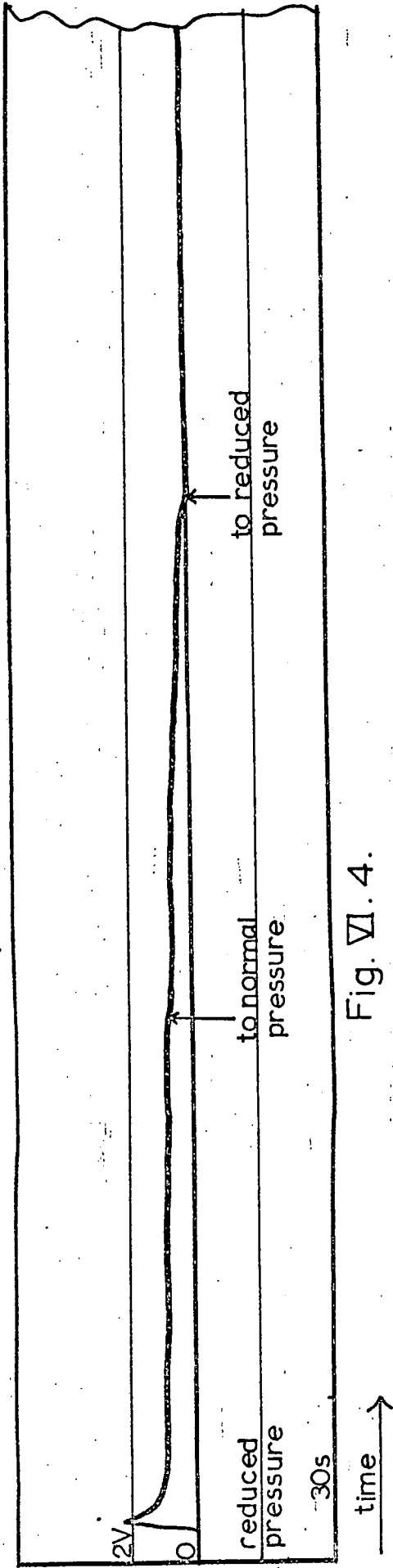


Fig. VI.4.

THE EFFECT ON THE FREEZING POTENTIAL OF CHANGING AIR PRESSURE.

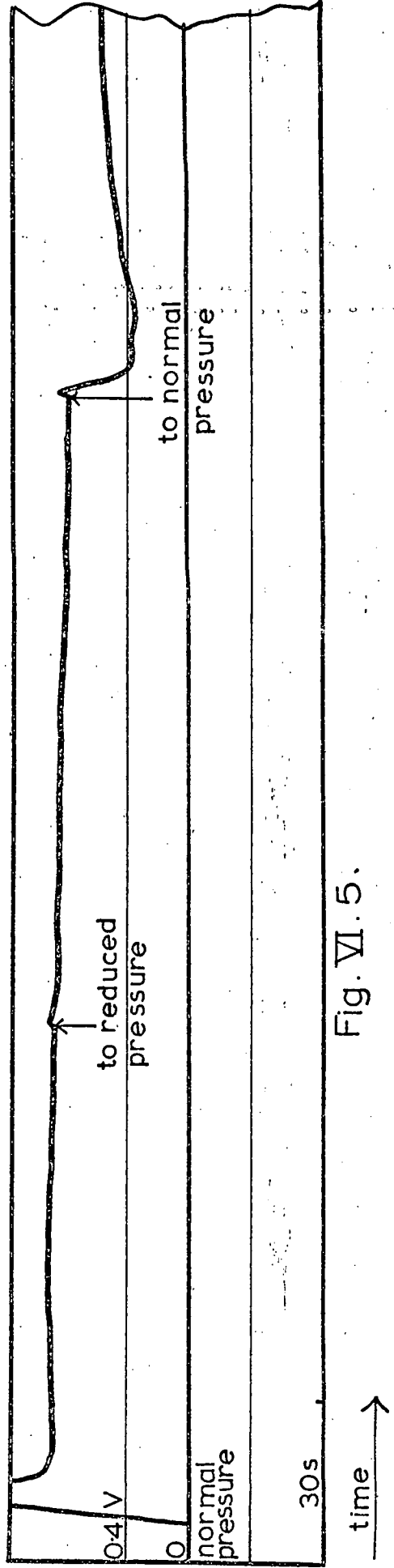


Fig. VI.5.

freezing potentials and not statistically significant. When the air pressure over the water was allowed to return to normal, during the course of a run, a rapid fall of 100 mV was noted in the voltage. Similarly, when the vacuum pump was switched on again, a fall of 200 mV was recorded.

Case 2. If some of the water was first frozen under normal air pressure, and then the vacuum pump was switched on, very little change was noted. However, when the air pressure was allowed to return to normal, a sharp fall of up to 400 mV was noted. (See Fig.VI.5.)

These apparently conflicting results may, perhaps, be explicable in terms of the volume occupied by the air bubbles within the interface. The ice produced by changing the air pressure repeatedly had bands of varying opacity, showing that either the number of bubbles or the volume occupied by them, had changed. Apart from this, no direct evidence has been obtained to support the explanation put forward below.

Let us consider a single bubble in the interface. (See Fig.VI.6.) If the air pressure above the liquid is reduced, the bubble will increase in volume. If the bubble breaks away from the surface, the interfacial resistance will fall. This is more likely to occur for initially large bubbles than for smaller ones and, therefore, it is more likely to happen in Case (1). When the interfacial resistance falls, the potential difference also falls. However, if the enlarged bubble remains at the interface and the

ice begins to advance around it, the interfacial resistance will slowly increase. Since the rate of freezing will be falling, the effect of this increase in resistance on the freezing potential will be offset, to some extent. If the air pressure is now allowed to return to normal, the bubble will shrink, and may retract into the ice completely. Water could then take the place of air in the interface, lowering the interfacial resistance, which in turn, causes the potential difference to fall. This should occur in both Case (1) and Case (2); and, indeed, both potential differences did fall when the vacuum pump was switched off.

In the light of some of the results on the effect of the temperature gradient across the ice, (see Section VI.4(b),) it is, perhaps, significant that if the drop in voltage resulted in a negative potential difference between water and ice, only small, negative potential differences were recorded and these were hardly affected by changes in air pressure.

VI.4. The Effect of the Freezing Rate on the Freezing Potential.

Workman and Reynolds (1950) stated that the freezing potentials were independent of the rate of freezing over a wide range of freezing rates. Gill (1953) showed that the freezing current was constant for various external resistances in the range 50 to 500 M Ω . By assuming a model with a constant freezing rate, he derived an expression for the freezing potential in terms of the maximum volume of charge density in the interface and the resistance of the interface. Gross (1965) investigated the effect of the

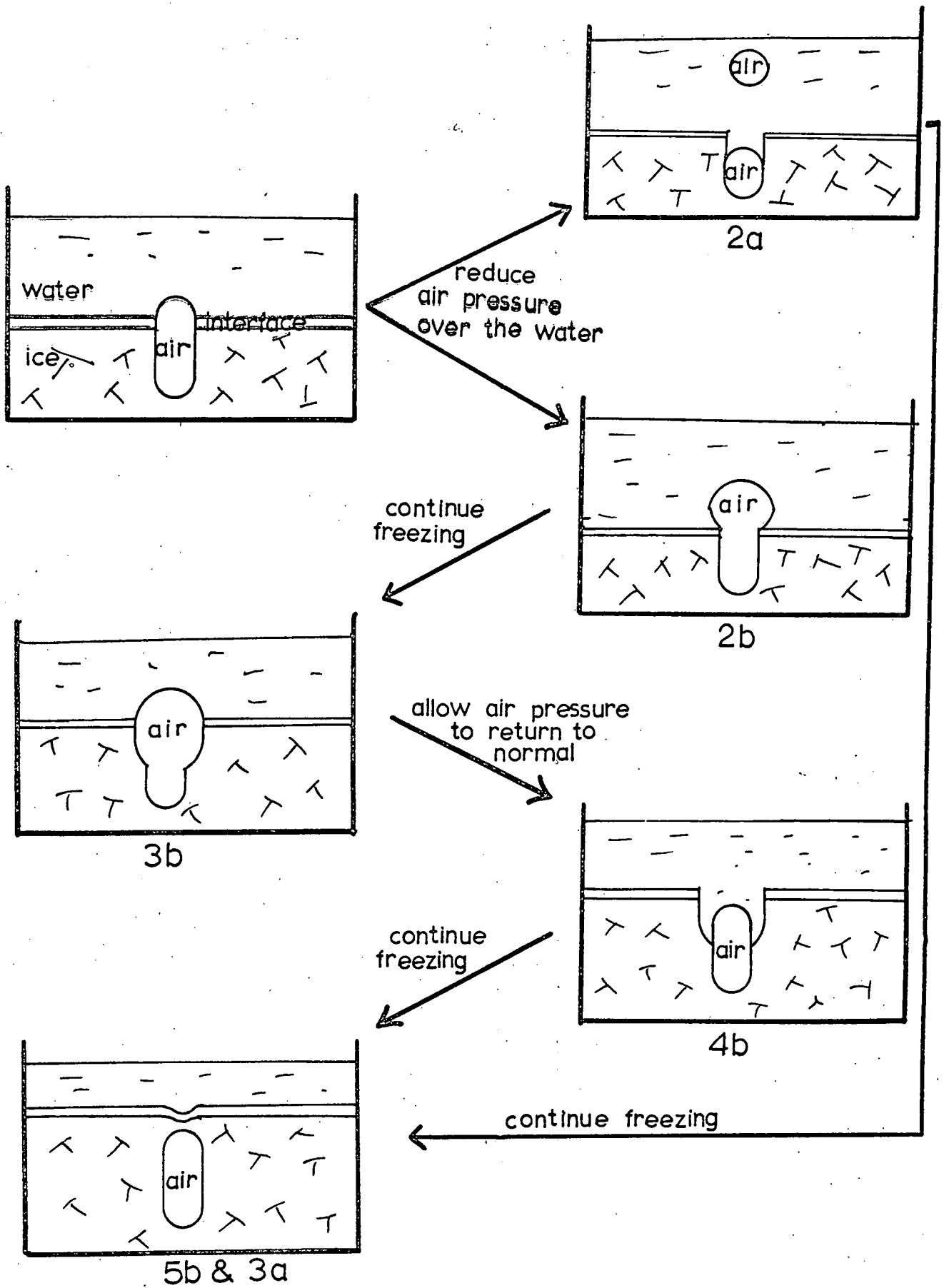


Fig. VI. 6. THE SUPPOSED EFFECT OF CHANGING THE AIR PRESSURE DURING A FREEZING RUN.

freezing rate on the rate of incorporation of impurity and hydrogen ions. He ascribed differences in the freezing potentials to differences between the rate of separation of ions and the rate of neutralisation across the interface.

The freezing potentials already measured appeared to depend on the freezing rate and experiments were undertaken to see if quantitative results could be obtained.

VI. 4(a) The effect of the supercooling on the freezing potentials.

Two basic types of voltage-against-time records had been obtained in the early experiments. (See Fig.VI.2.). Careful observation showed that type (A) was obtained when the face of the lower electrode became covered evenly and quickly in less than 1 s, whereas type (B) was obtained when only a portion of the electrode became covered in this manner and then the ice spread slowly over the remainder. The inference was that the water was supercooled in the solutions which gave type (A) graphs, but that the supercooling was less in the solutions giving the type (B) graphs.

These speculations were confirmed by attaching a small copper-constantan thermocouple to the lower electrode. The thermocouple leads were insulated with P.V.C. sleeving and were passed through a 5 mm hole drilled in the upper electrode. In order to increase the probability of supercooling, the freezing cell was transferred to a cold room maintained at about 0 °C. The thermocouple and electrometer leads were run through the cold room walls without being joined, to prevent contact potentials from giving spurious results. The results obtained are shown in Table

VI. 1.

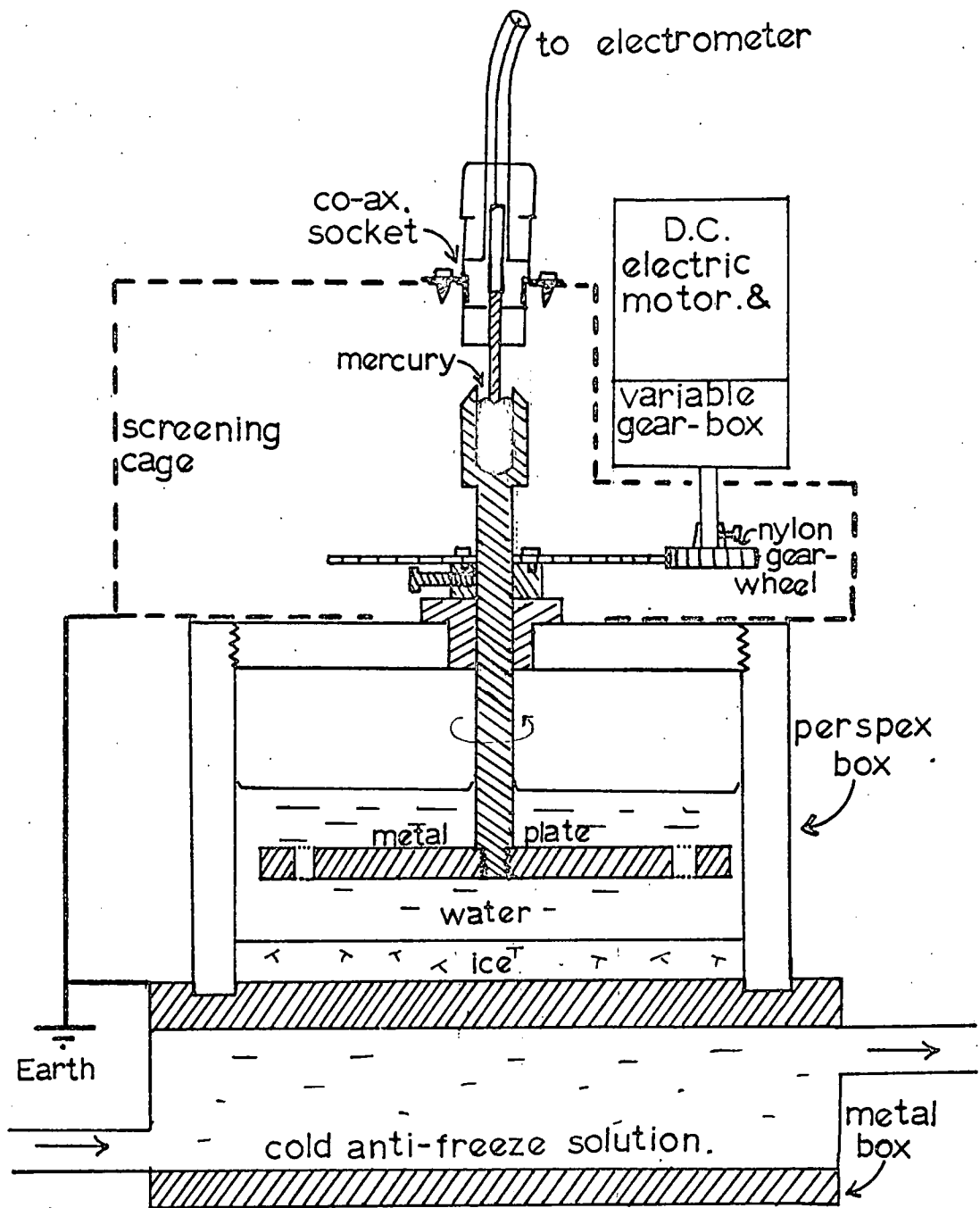
Table VI.1.

Temperature of the freezing face at the onset of freezing.	Type of freezing potential-against-time graphs.
($^{\circ}$ C)	(A or B)
+ 2.0	B
+ 1.0	B
+ 0.5	B
0	B
0	A
- 0.3	B
- 0.5	B
- 0.5	A
- 0.8	B
- 1.0	A
- 1.3	A
- 1.5	A
- 2.0	A
- 2.2	A
- 2.3	A
- 2.5	A
- 2.7	A
- 3.5	A
- 4.0	A
- 6.5	A

This table shows, that the greater the degree of supercooling the more chance there is of the voltage-against-time graph being of the type (A). In the cases where the thermocouple was registering temperatures above 0° C when freezing commenced, the thermocouple was not on the portion of the electrode initially covered by the ice. In those where the thermocouple temperatures were below 0° C the thermocouple was on the portion of the electrode which initially became covered with ice.

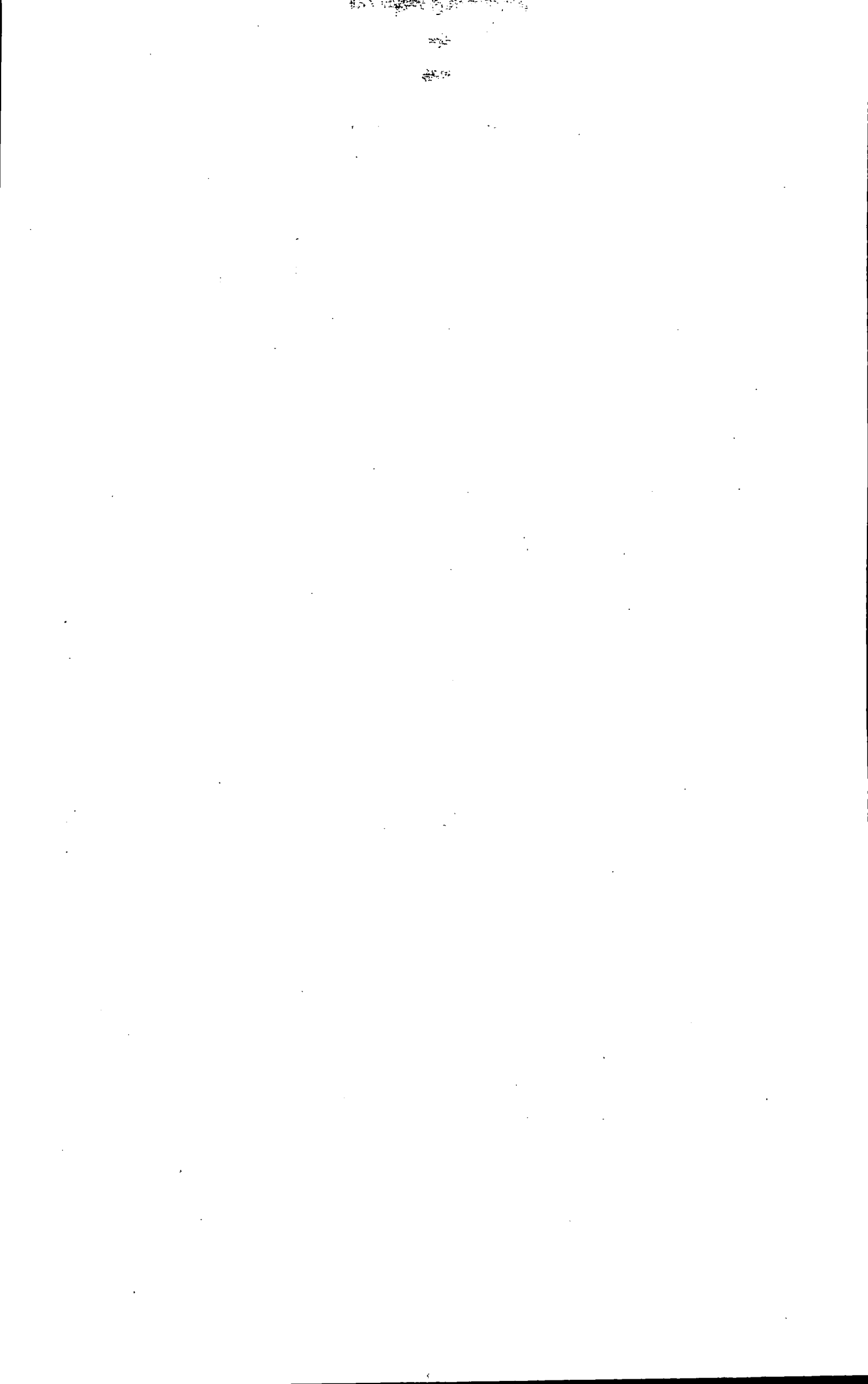
VI. 4(b) The instantaneous relationship between freezing potential and freezing rate.

It was suggested in Section VI. 2(b) that variations in



The freezing cell.

Fig. 7.7.



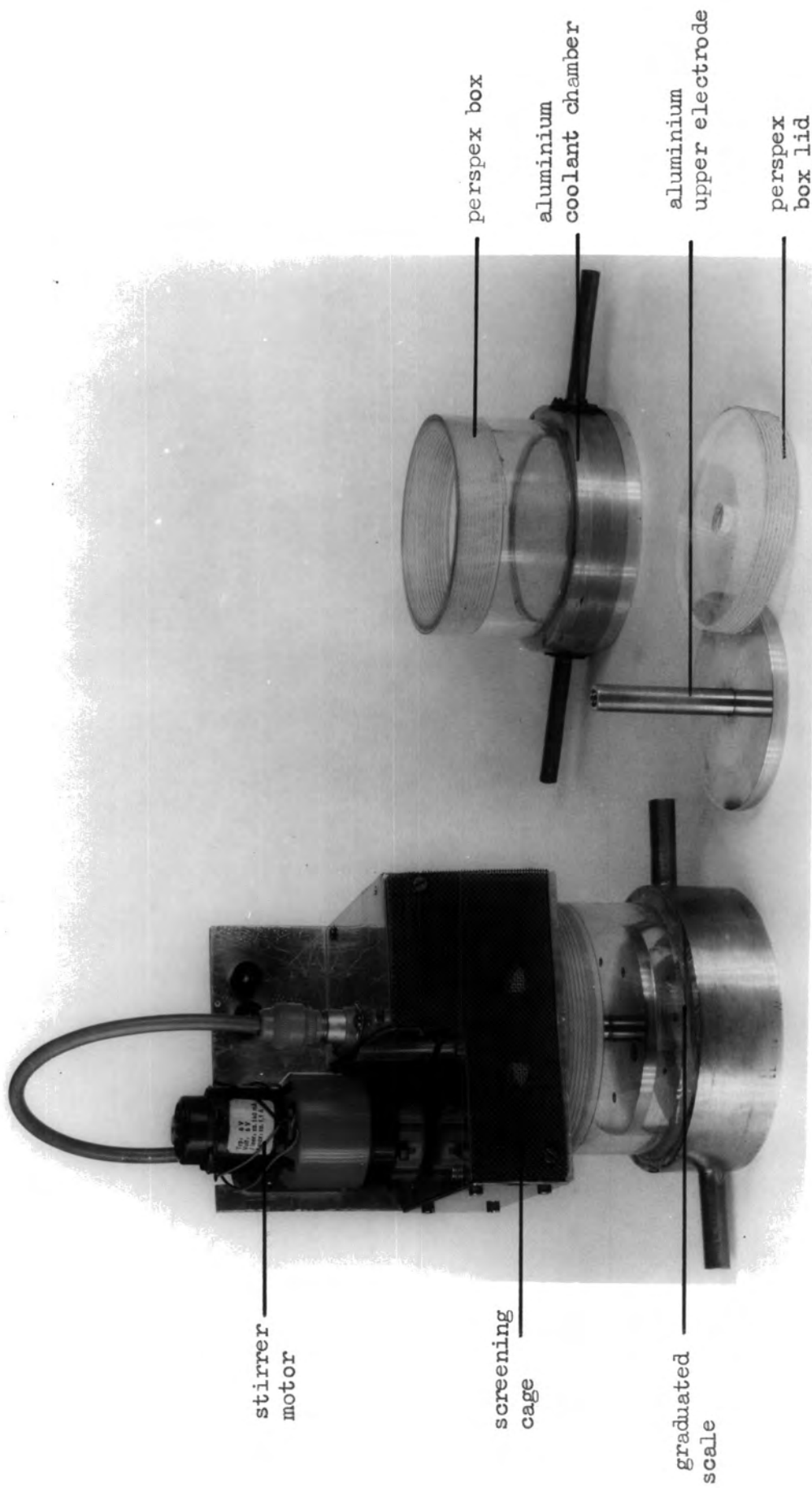


Fig. VI.3. The Freezing cell.

the freezing rate were responsible for the long term irreproducibility of the freezing potentials. It is possible that the variations within the individual voltage-time graphs might be related to short term variations in the freezing rate, and experiments were performed in the hope of obtaining a quantitative relationship between the potential difference across the interface and the freezing rate.

A freezing cell with brass electrodes was used. (See Fig.VI.7 and VI.8). The upper electrode could be rotated by means of a small, geared, electric motor and a scale with gradations approximately 0.25 mm apart, was engraved onto the bottom 10 mm of the perspex cylinder. The advance of the ice face past these gradations could be observed using a travelling microscope, but since freezing rates of up to $50 \mu\text{m s}^{-1}$ were being studied, the scale was calibrated beforehand with the microscope. Then, during freezing runs, microscope observations were recorded verbally onto a tape-recorder, and from the tape, the times for the ice face to pass between consecutive gradations were obtained at a later stage. Connection from the upper electrode to the electrometer was made through a mercury pool, and electrometer deflections were recorded on the Watanabe recorder at a paper speed of 1 mm s^{-1} . The background noise level was less than 1 mV with the upper electrode still, and less than 3 mV with it rotating.

Tests showed that when 75 ml of solution were used in the experiments, with an electrode separation of 13 mm, rotation of the upper electrode stirred the solution. If the stirrer was used

before freezing commenced, the onset of freezing was delayed, because the whole of the solution was being cooled before freezing began. If ice was present in the cell before the solution was stirred, switching on the stirrer motor slowed down the rate of freezing by allowing warmer water to come into contact with the ice. If the rate of stirring was high enough, it was possible to cause melting of the ice surface. However, the temperature gradient across the ice specimen is hardly affected by the stirrer, and hence we have a very convenient method for measuring the contribution of the electrification due to temperature gradients, to the freezing potentials.

A complete set of results obtained for 21 separate freezings of the same sample of de-mineralised water, using this apparatus, is set out in Appendix 4. The freezing potential results are also shown in graphical form in Fig.VI.9 and Fig.VI.10 (1 to 21). Fig.VI.9 is a plot of all the individual values of freezing rate against voltage. It confirms the long term irreproducibility of the freezing potentials and shows they are not solely dependent on the freezing rate. If, however, the values of the freezing potentials and freezing rates during each particular run are examined, see Fig.VI.10, some facts begin to emerge. In general, the freezing potentials increased as the freezing rate increased, in the range 10 to 50 $\mu\text{m s}^{-1}$; but the freezing potential did not react to relatively rapid changes in freezing rate, and the response time of the freezing potential seems to increase with increasing thickness of ice. This is perhaps because the effective

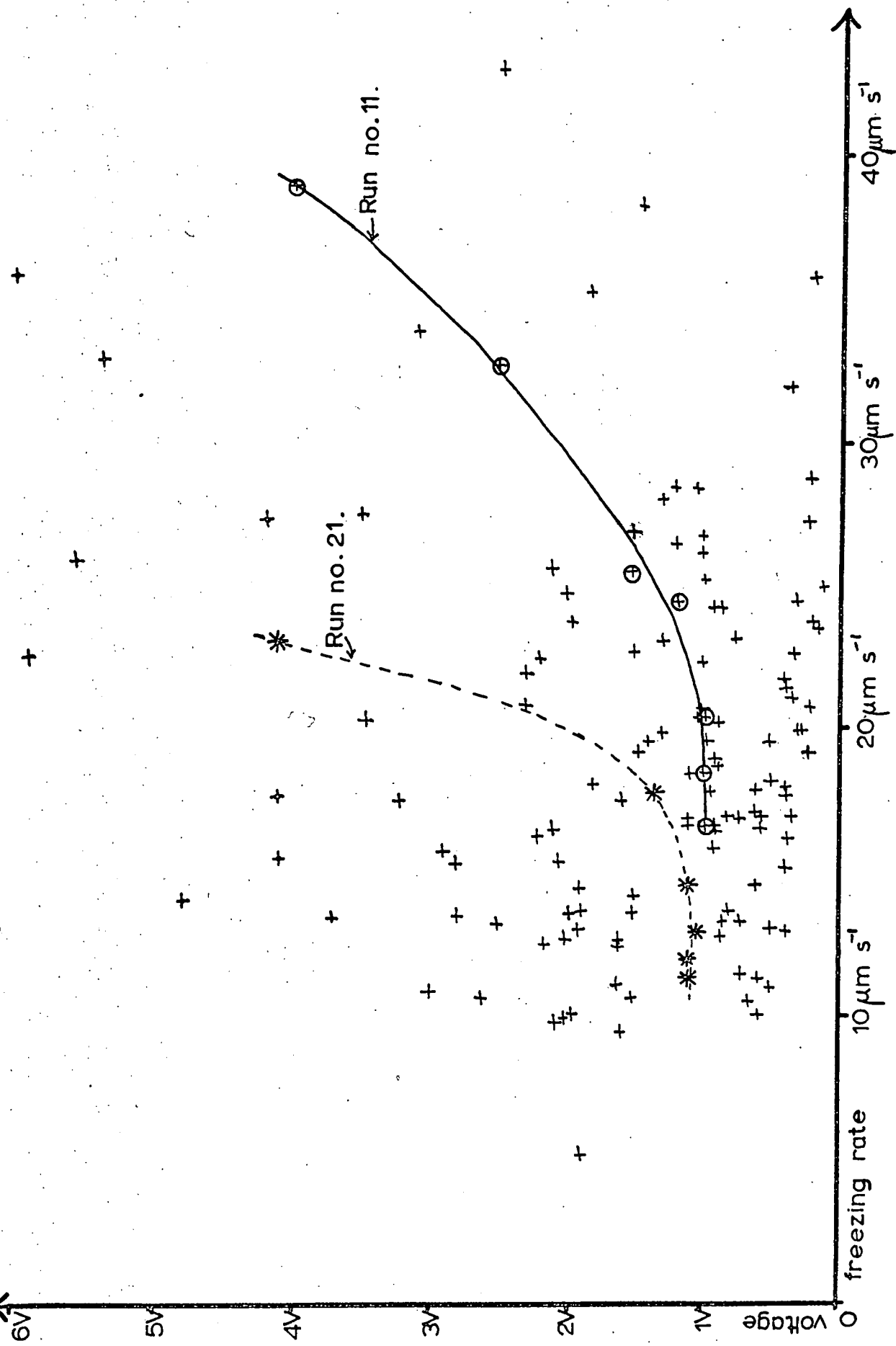


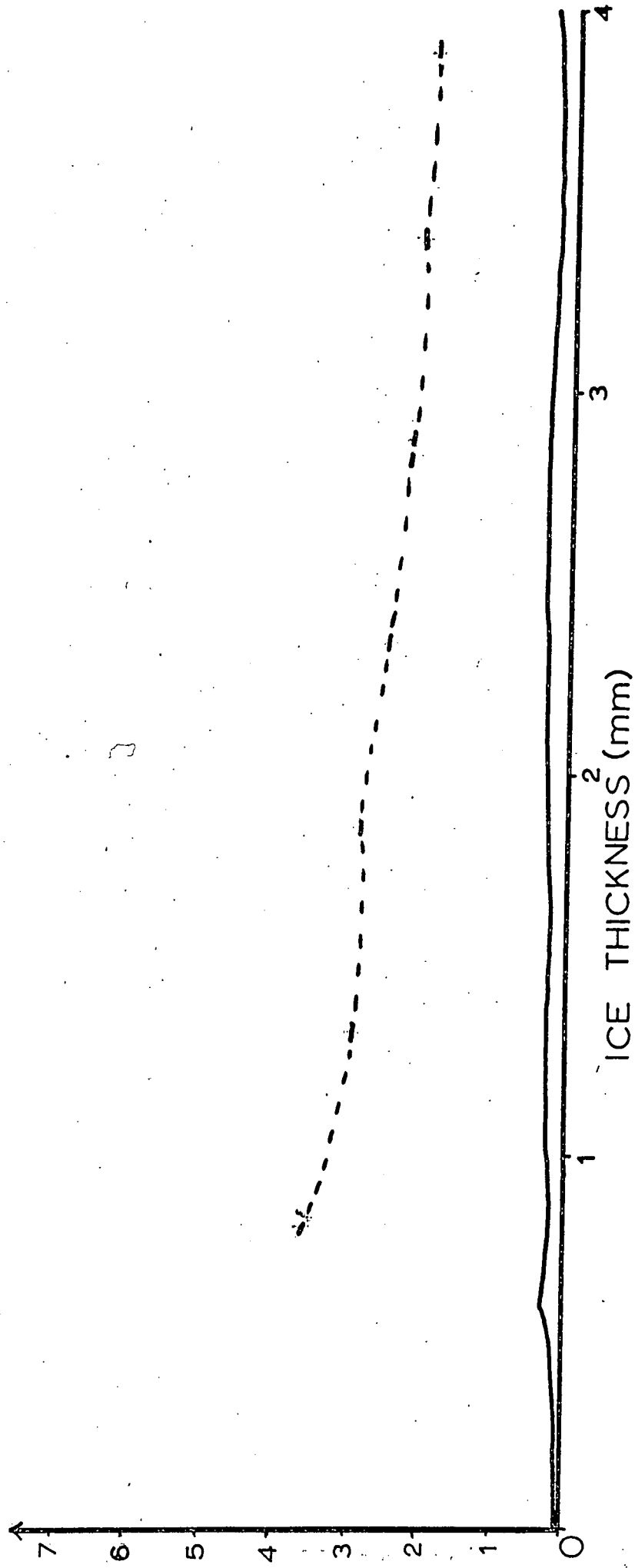
Fig. V. 9. THE VARIATION OF FREEZING POTENTIAL WITH FREEZING RATE.

THE
FREEZING
CELL
RESULTS.

Fig. VI .10.

VOLTAGE (V) &  & 
FREEZING RATE ($m s^{-1} \times 10^5$) 

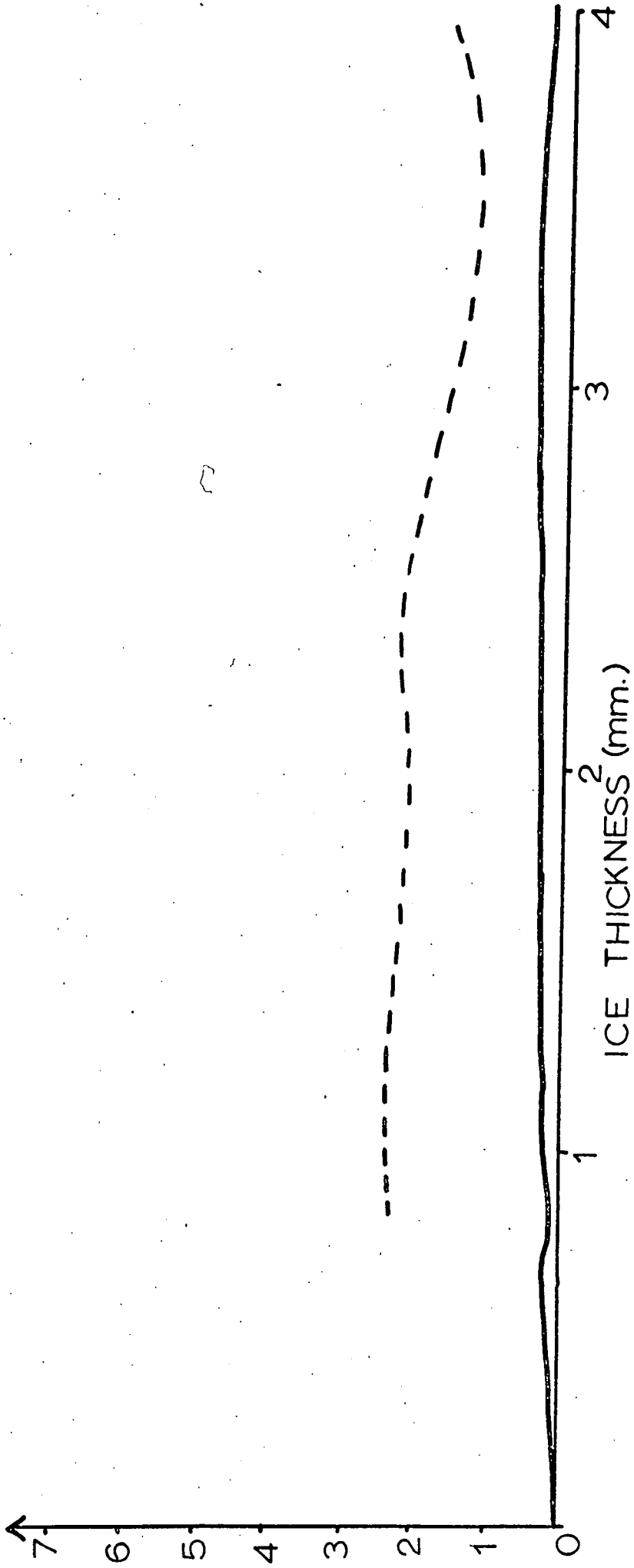
Fig. VI. 10.
Run no. 1.



VOLTAGE (V) —
& FREEZING RATE ($\text{m s}^{-1} \times 10^{-5}$) - - - -

Fig. VI.10.

Run no.2.



VOLTAGE (V) —
& FREEZING RATE ($m s^{-1} \times 10^{-5}$) - - - - -

Fig. VI.10.
Run no.3.

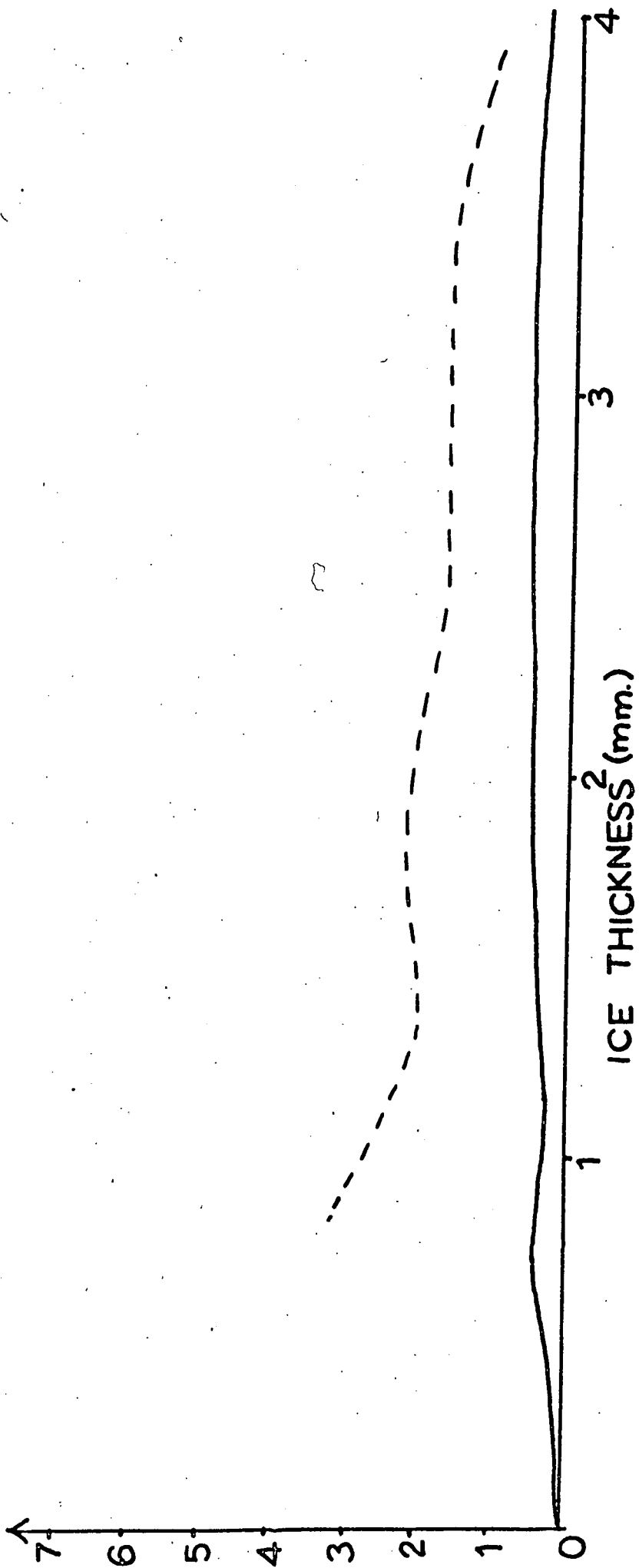
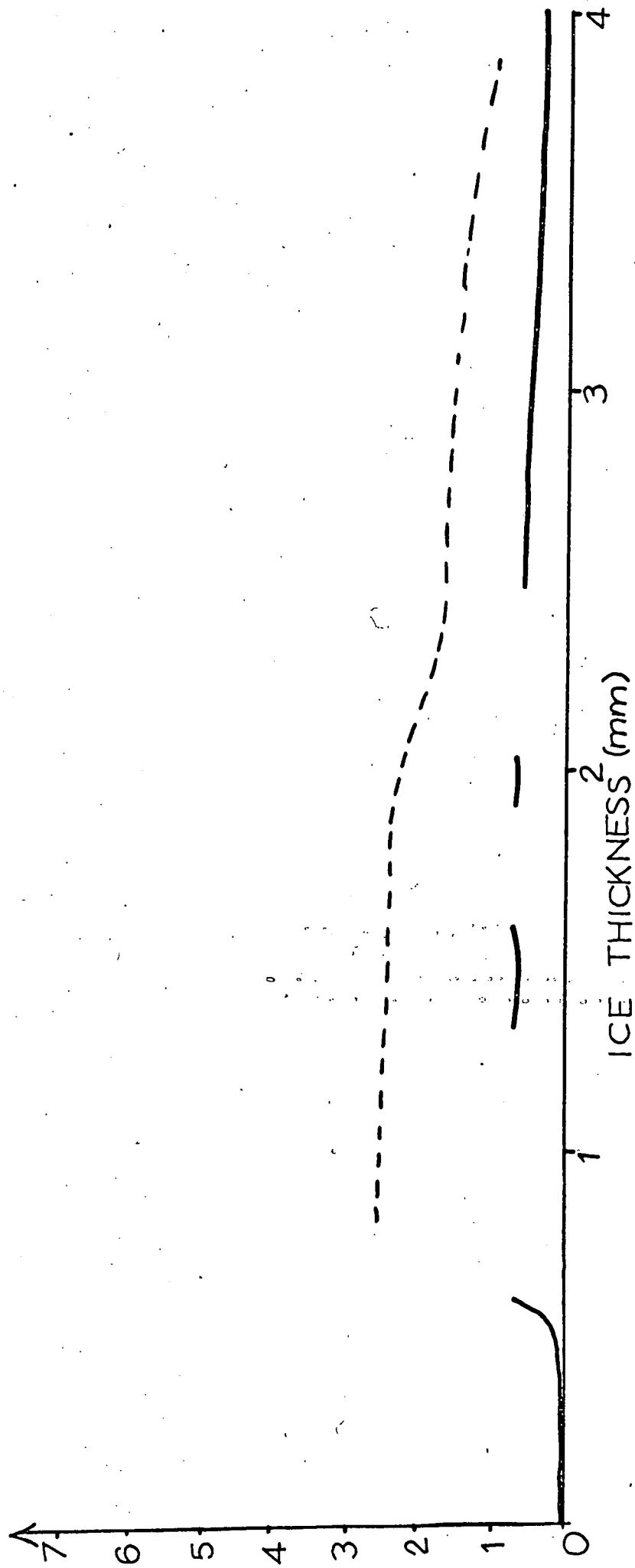


Fig. VI.10.

Run no.4.

VOLTAGE (V) —
& FREEZING RATE ($\text{m s}^{-1} \times 10^{-5}$) - - - -



VOLTAGE (V) —
& FREEZING RATE ($m s^{-1} \times 10^{-5}$) - - - -

Fig. VI.10.
Run no.5.

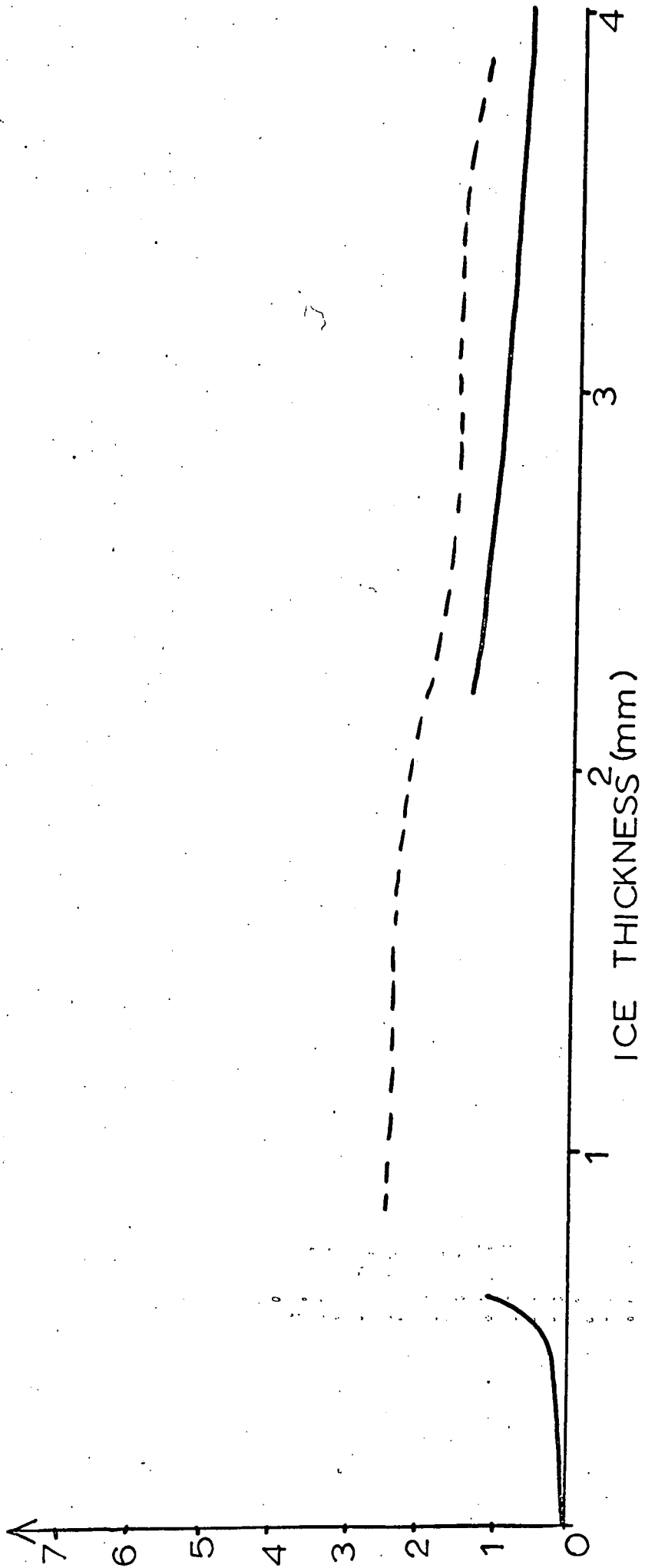
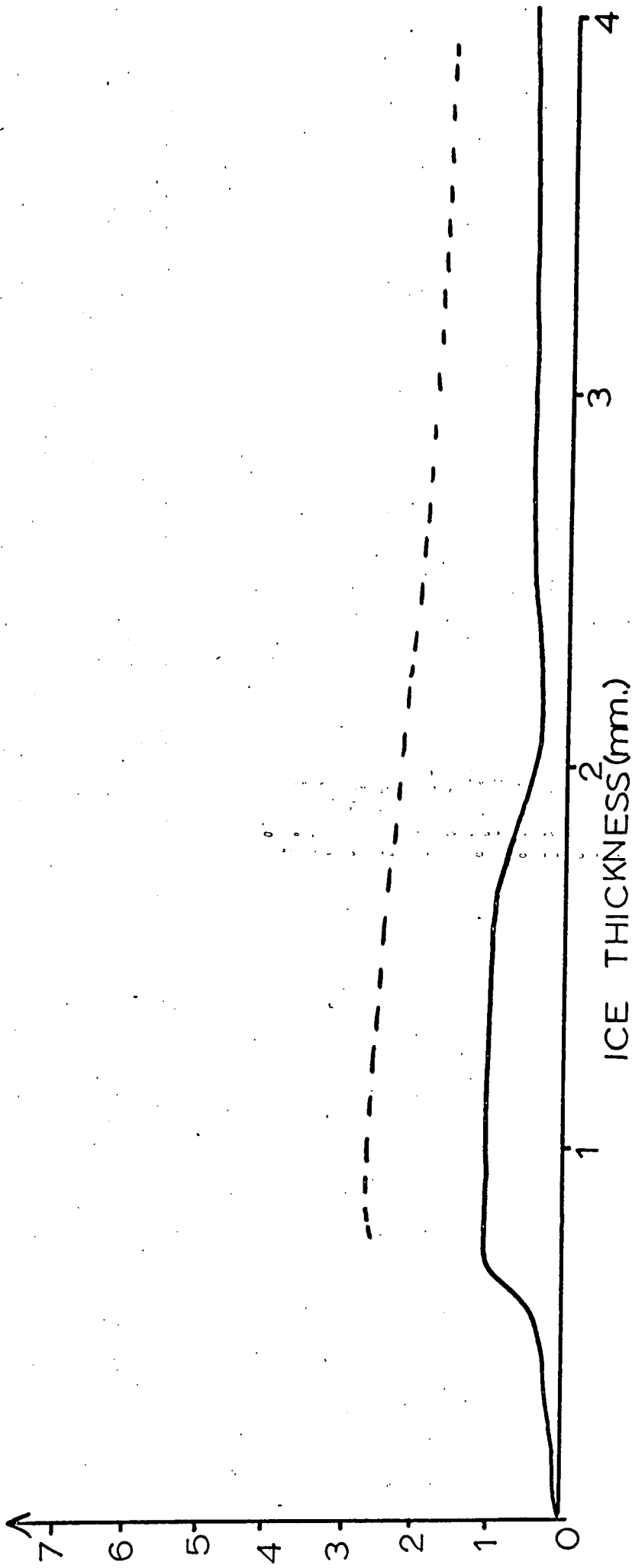


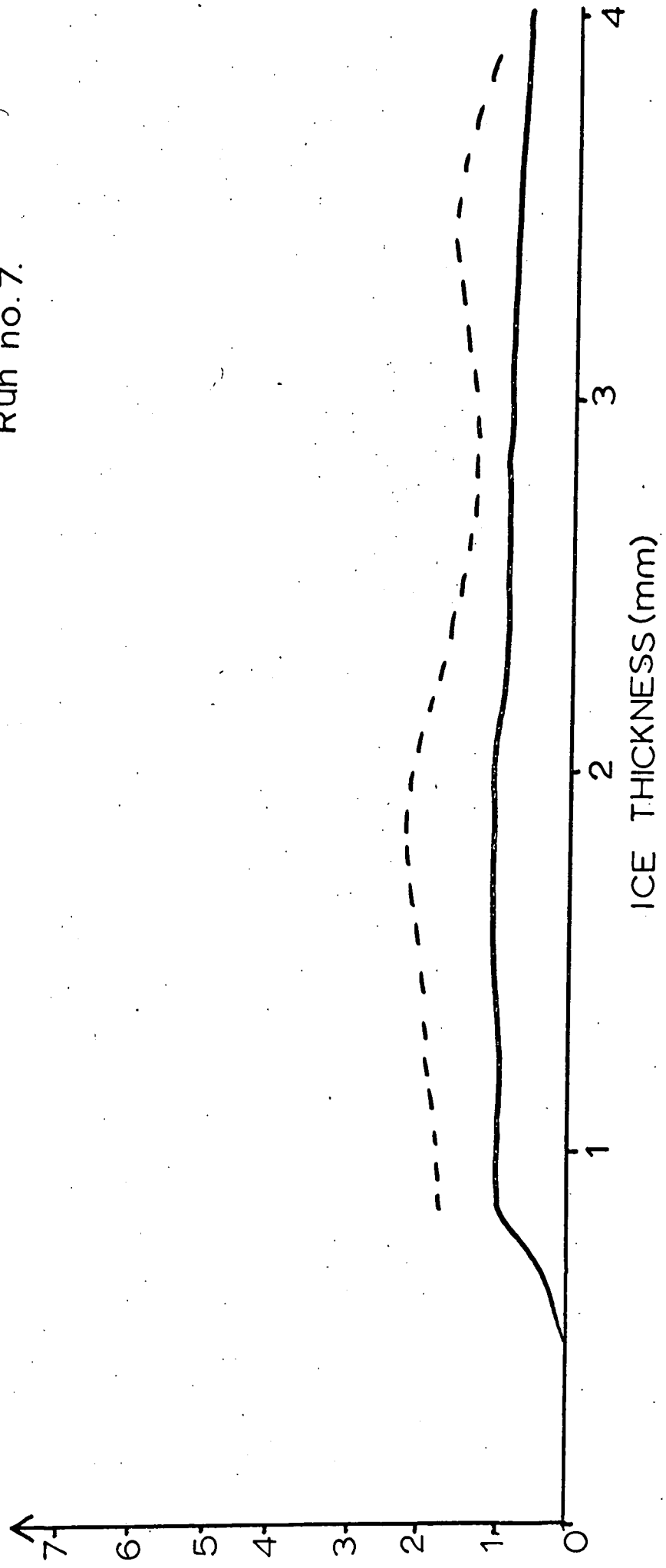
Fig. VI.10.
Run no.6.

VOLTAGE (V) —
& FREEZING RATE ($m s^{-1} \times 10^{-5}$) - - - -



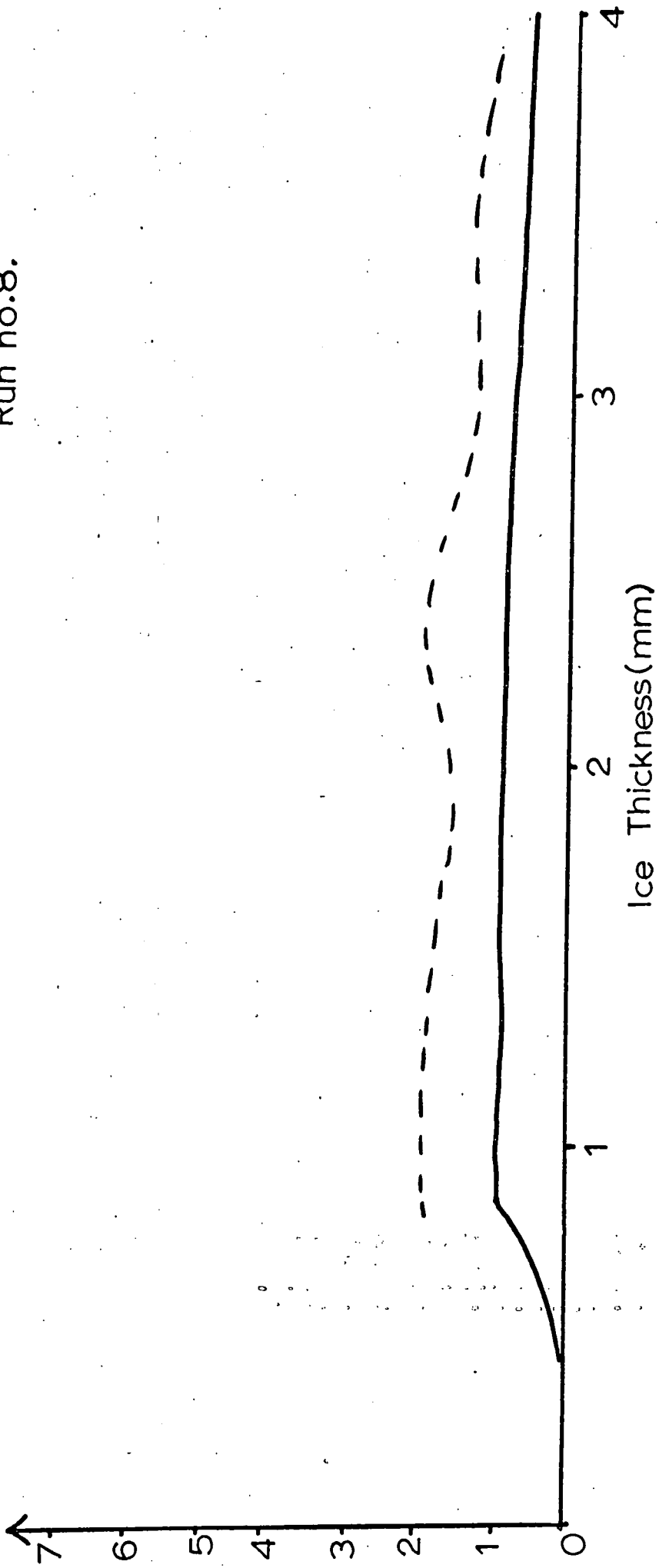
VOLTAGE (V) —
& FREEZING RATE ($m.s^{-1} \times 10^5$) - - -

Fig. VI.10.
Run no.7.



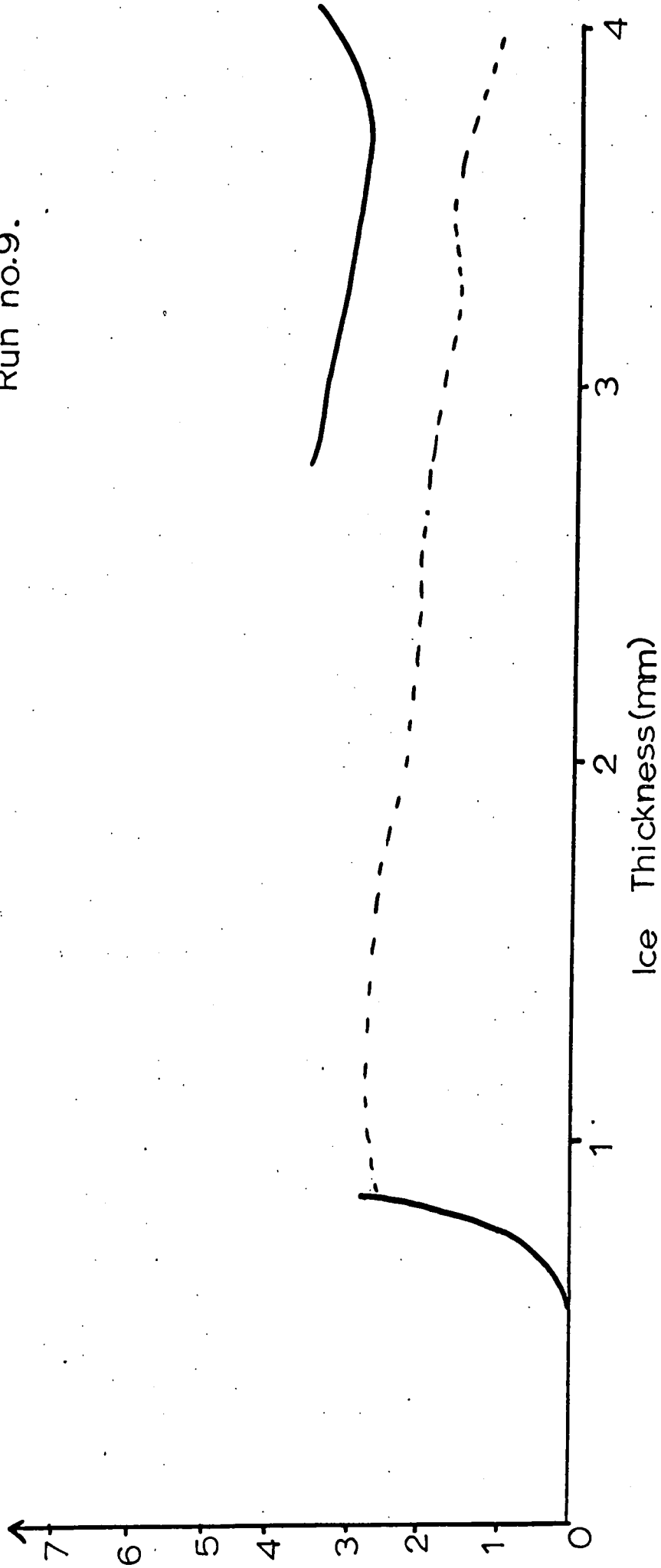
Voltage (V) —
& Freezing rate ($m s^{-1} \times 10^5$) ····

Fig. VI.10.
Run no.8.



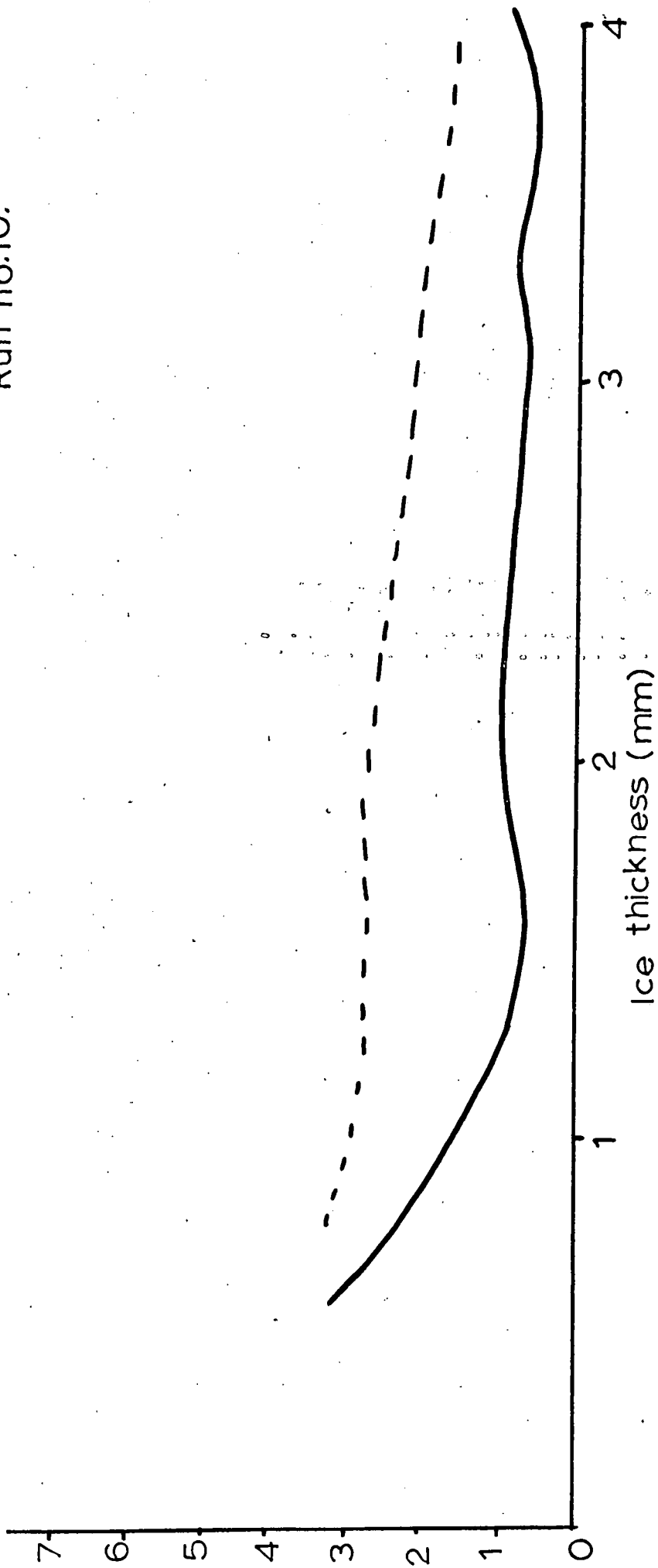
Voltage (V) —
& Freezing rate ($m s^{-1} \times 10^5$) - - -

Fig. VI.10.
Run no.9.



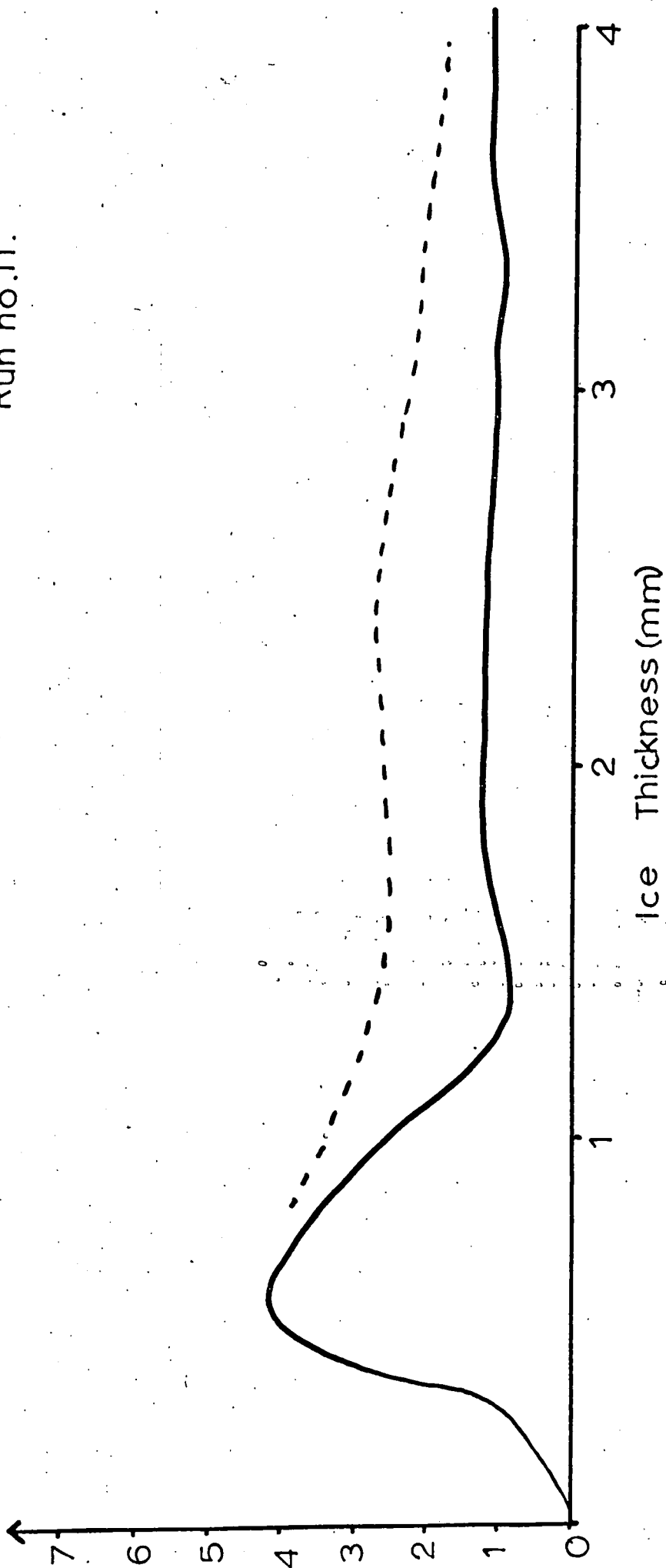
Voltage (V) —
& Freezing rate ($m^{-1} \times 10^{-5}$) ---

Fig. VI. 10.
Run no.10.



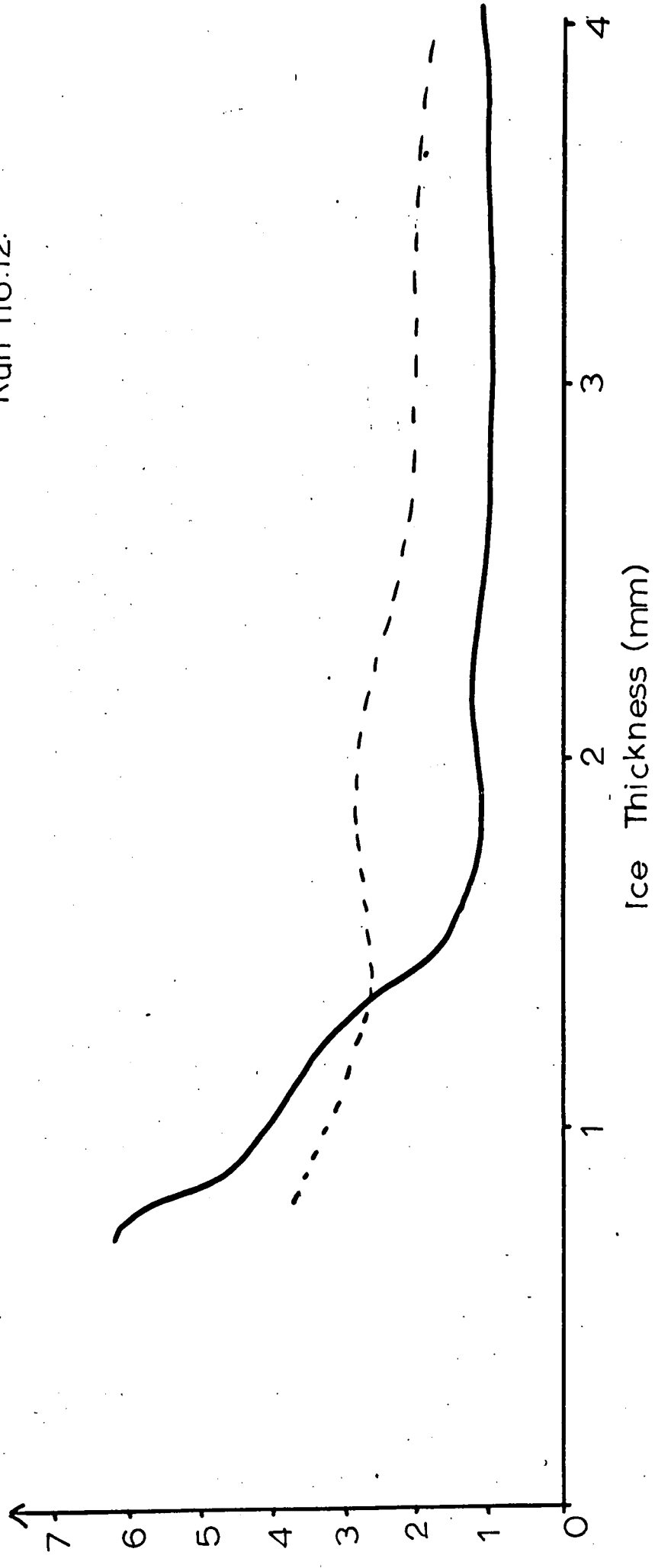
Voltage (V) —
& Freezing rate ($m s^{-1} \times 10^{-5}$) - - -

Fig. VI.10.
Run no.11.



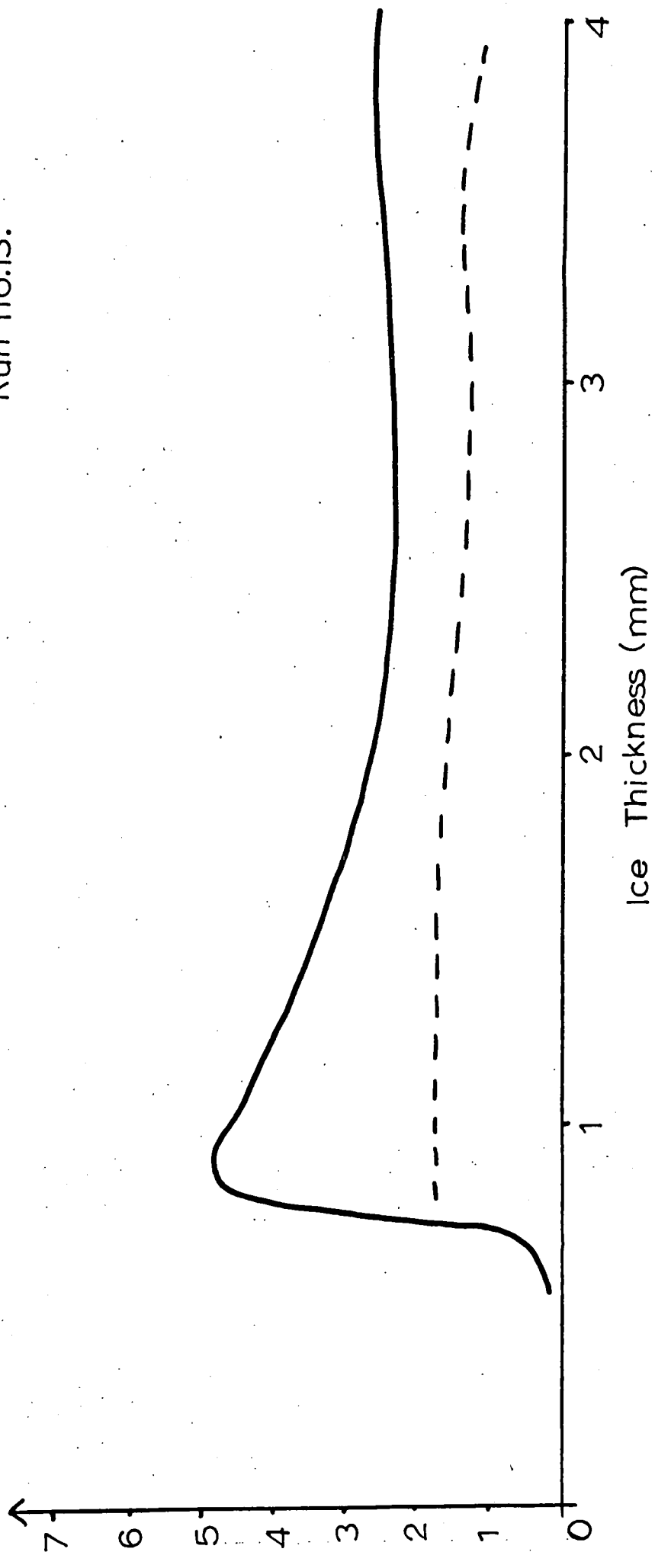
Voltage (V) —
& Freezing rate ($m s^{-1} \times 10^{-5}$) - - -

Fig. VI.10.
Run no.12.



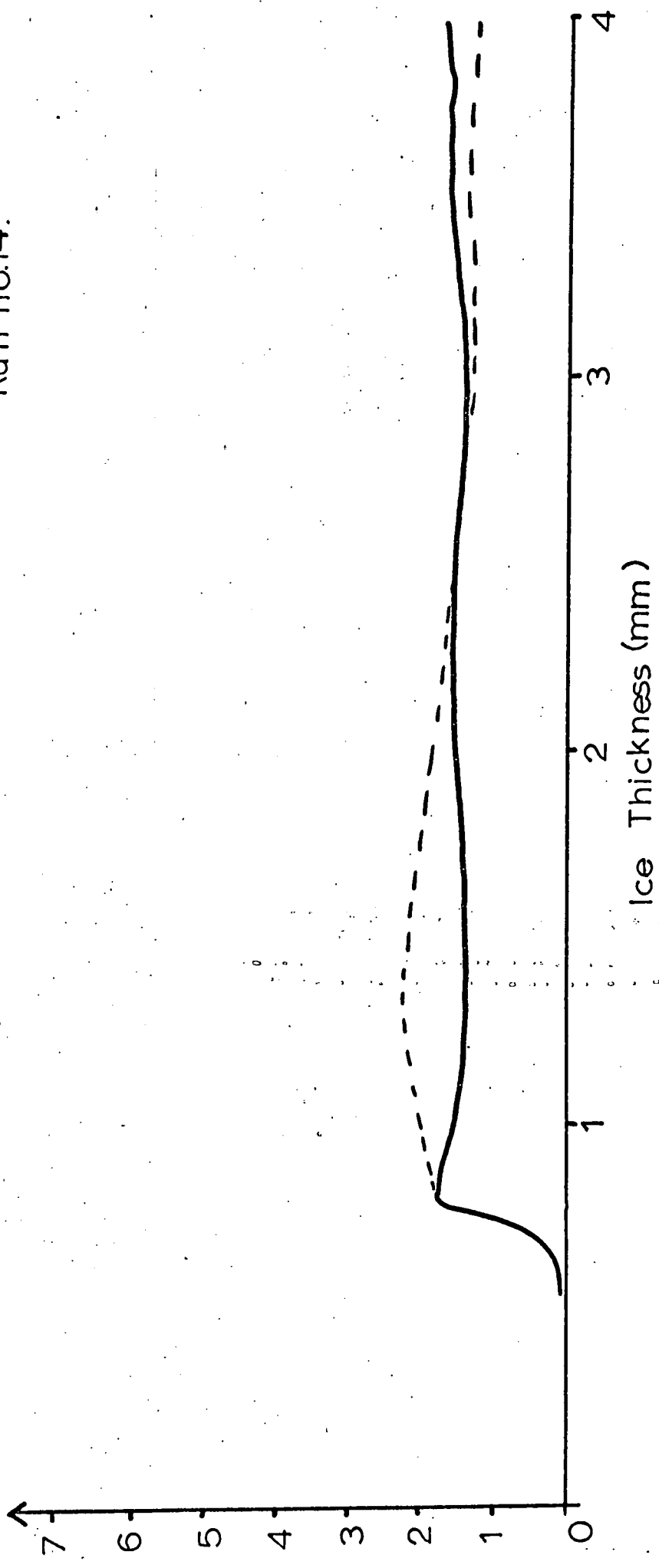
Voltage (V) —
& Freezing rate ($m s^{-1} 10^{-5}$) - - - -

Fig. VI .10.
Run no.13.



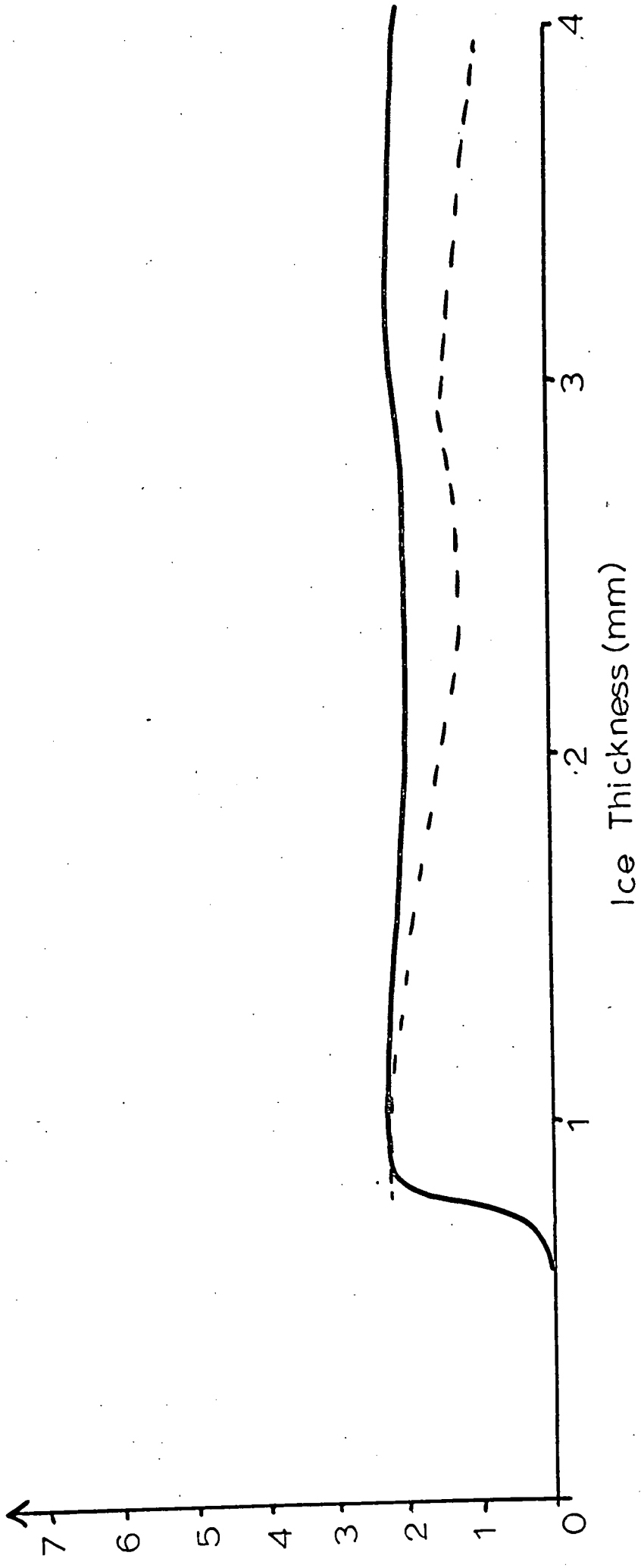
Voltage (V) —
& Freezing rate ($m s^{-1} \times 10^{-5}$) - - - -

Fig. VI.10.
Run no.14.



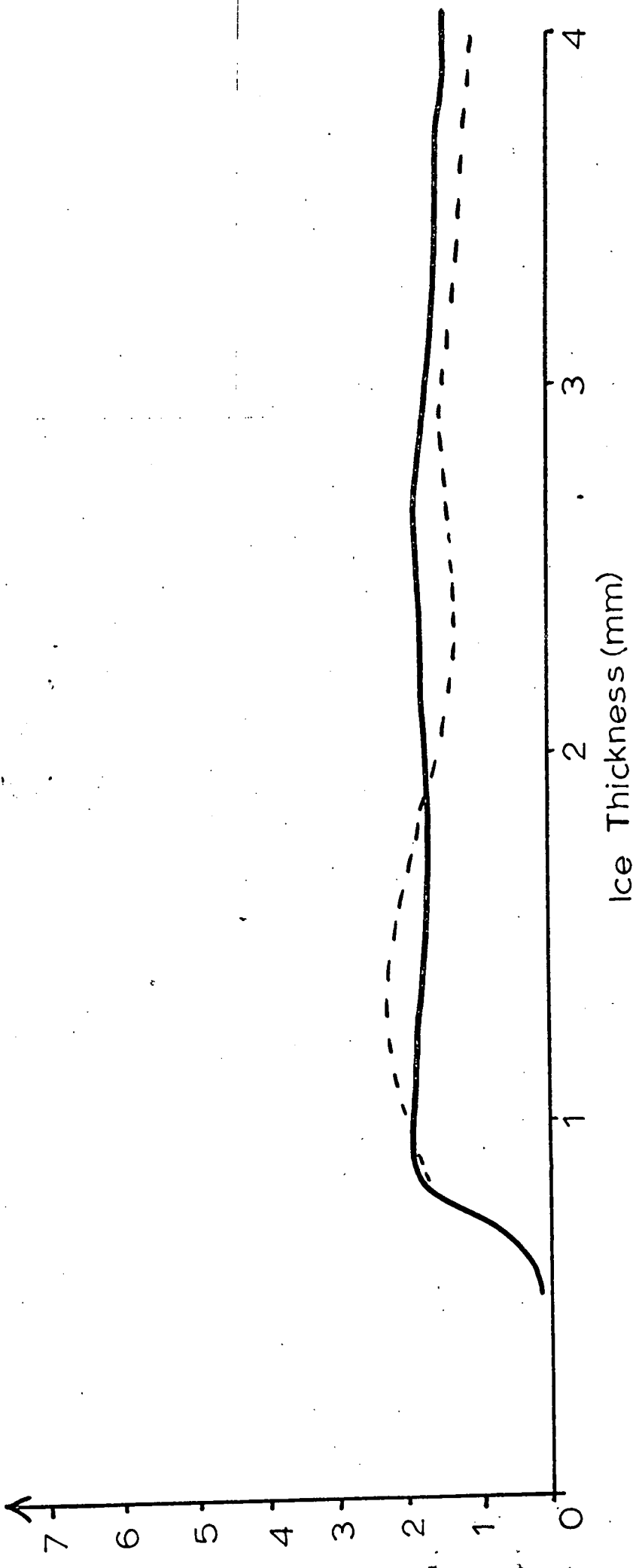
Voltage (V) ———
& Freezing rate ($\text{m s}^{-1} \times 10^{-5}$) - - - - -

Fig. VI.10.
Run no.15.



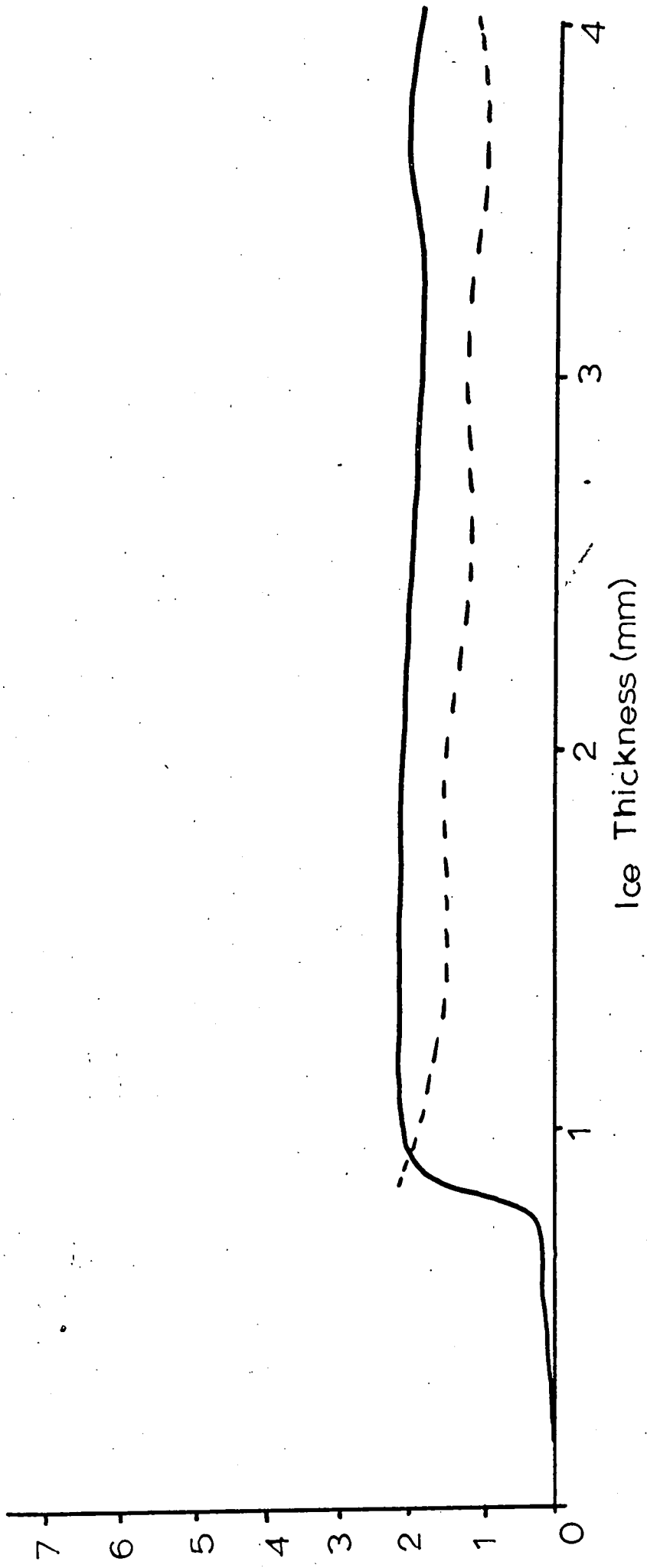
Voltage (V) —
& Freezing rate ($m s^{-1} \times 10^{-5}$) - - - - -

Fig. VI.10.
Run no.16.



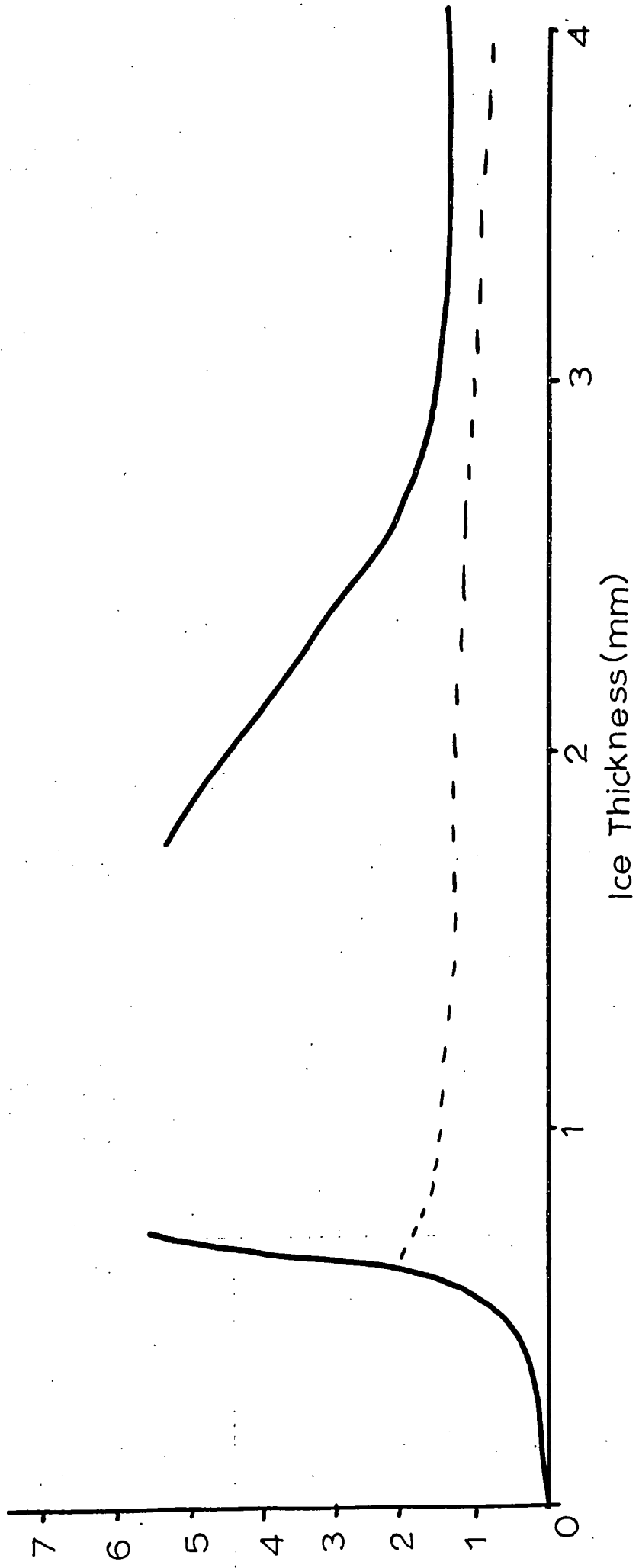
Voltage (V) ———
& Freezing rate ($m s^{-1} \times 10^5$) - - - - -

Fig. V.10.
Run no.17.



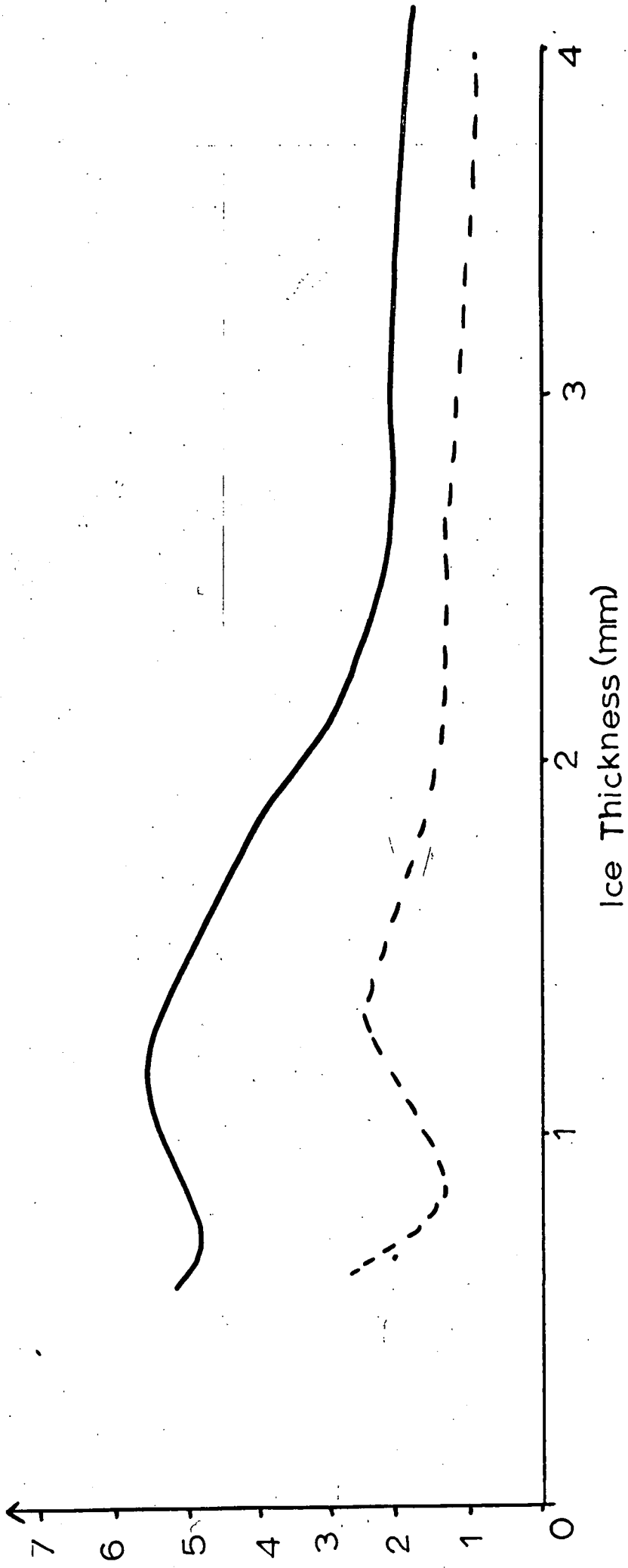
Voltage (V) ———
& Freezing rate ($m s^{-1} \times 10^{-5}$) - - - -

Fig. VI.10.
Run no.18.



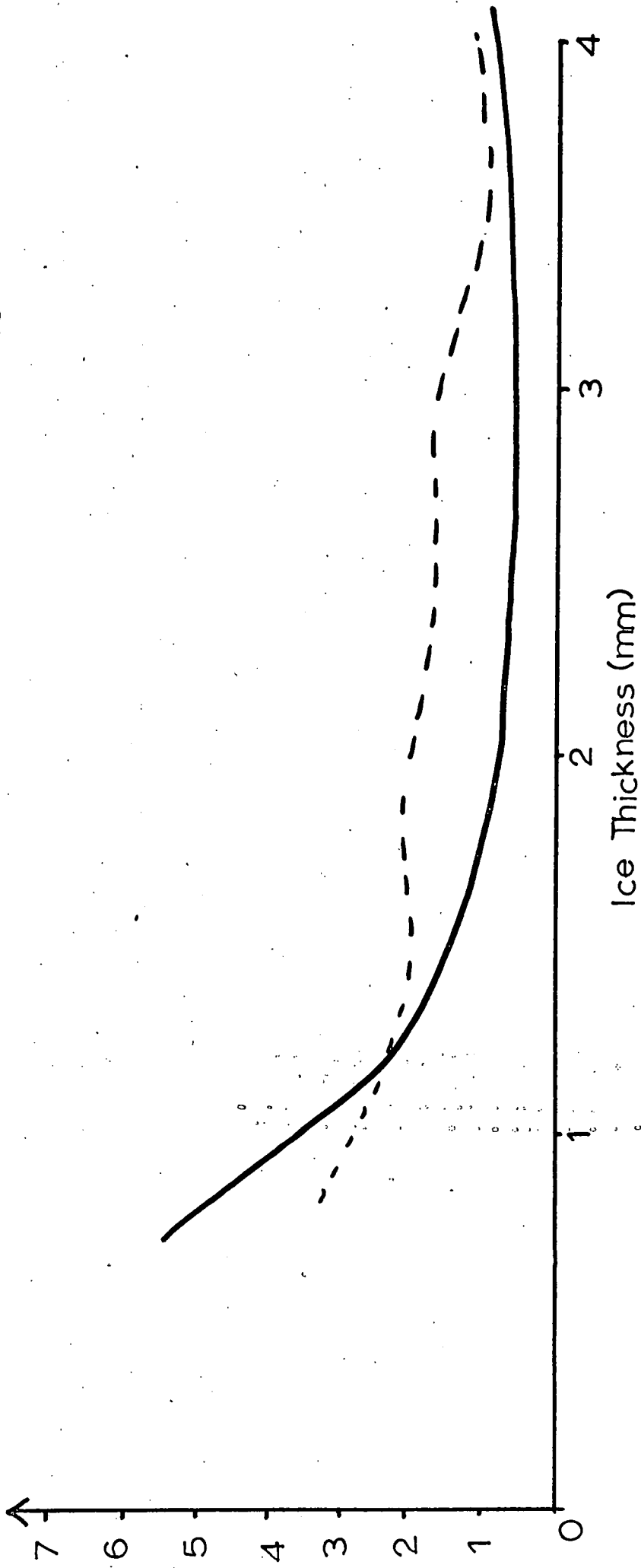
Voltage (V) ———
& Freezing rate ($\text{m s}^{-1} \times 10^{-5}$) - - - -

Fig. 7.10.
Run no.19.



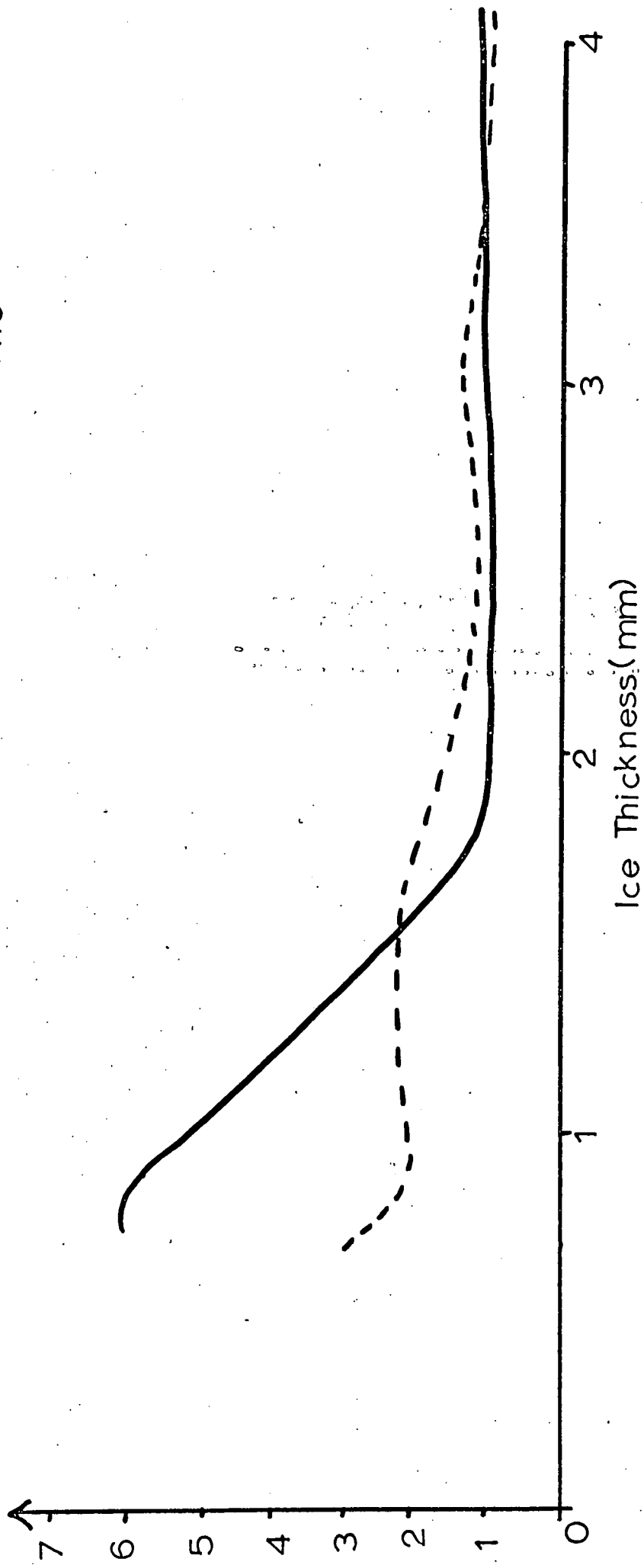
Voltage (V) —
& Freezing rate ($m s^{-1} \times 10^{-5}$) - - - -

Fig. 10.
Run no. 20.



Voltage (V) ———
& Freezing rate ($m s^{-1} \times 10^5$) - - - -

Fig. VI.10.
Run no.21.



thickness of the interface within the ice increases due to the presence of a frozen-in space-charge in the bulk of the ice sample, but more work would be required to prove this. The potential difference-against-freezing rate graphs have been prepared by averaging the time taken for the ice surface to pass between two gradations on the scale, to obtain a better fit. No results have been plotted in the cases where the lower electrode was not completely covered with ice as the freezing potentials cannot be regarded as representative, since the interface is being shunted by a very low resistance.

One fact stands out in these results, and that is that the thicker some portions of the ice became before the lower electrode was completely covered with ice, the higher were the potential differences at low freezing rates. At the present time, no explanation for this can be offered, but in general this happened more frequently at higher anti-freeze solution temperatures. It may, in fact, be due to a difference in the frozen-in space-charge, through having the interface shunted for a long period, or some effect from the initial low rates of freezing at the brass/water interface, but there is little evidence to support such speculations.

VI. 4(c) The effect on the freezing potentials of stirring the solutions.

In the previous section, ~~the previous section,~~ the effect of stirring on the freezing rate of the solution was mentioned. In view of the dependence of the freezing potential

on the freezing rate shown in the graphs in Fig.VI.10, it might be expected that changing the freezing rate during the course of a run would cause a sharp discontinuity in the voltage against time graph. This is, in fact, the case. (See Fig.VI.11) However, if a solution which gave first a positive freezing potential (i.e. the water positive with respect to the ice) and then a negative potential was stirred, only the positive potentials were affected by stirring, and further, if the positive potentials were made to go negative by stirring, the resulting negative potential was of the same order as the negative potential obtained without stirring.

The negative potential differences were attributed to the temperature gradient across the ice specimen, and this conclusion is supported by their insensitivity to changes in interfacial conditions, their variation with coolant temperature and their magnitude. (See Appendix 4). Since we know that the temperature of the upper ice face is 0°C and that of the lower ice face is the same as the anti-freeze temperature we can plot the temperature gradient against voltage. (See Fig.VI.12.) The graph shows that the negative potential difference increases with increasing temperature. The vertical and horizontal lines on the graph represent the accuracy of reading each voltage and temperature difference measurement. In view of the differences between the conditions in this experiment and those under which the quantitative relationship between temperature difference and voltage was originally worked out, this probably represents excellent

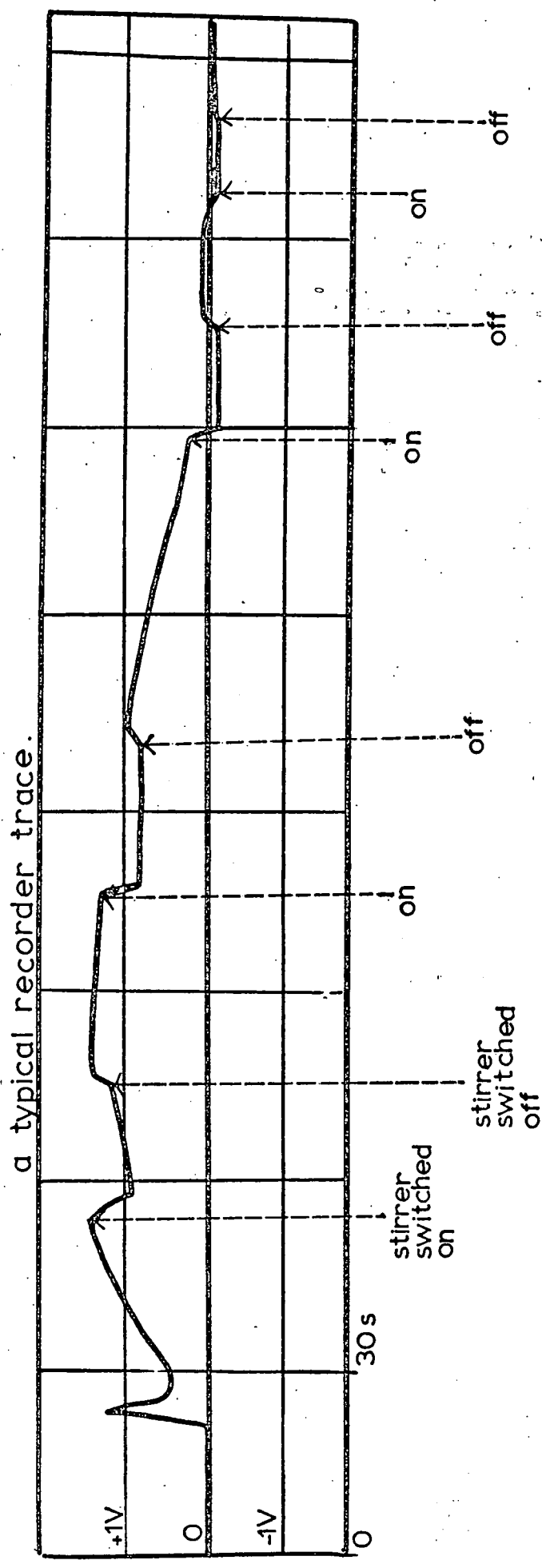


Fig. VI.11. THE EFFECT OF STIRRING THE WATER DURING A FREEZING RUN.

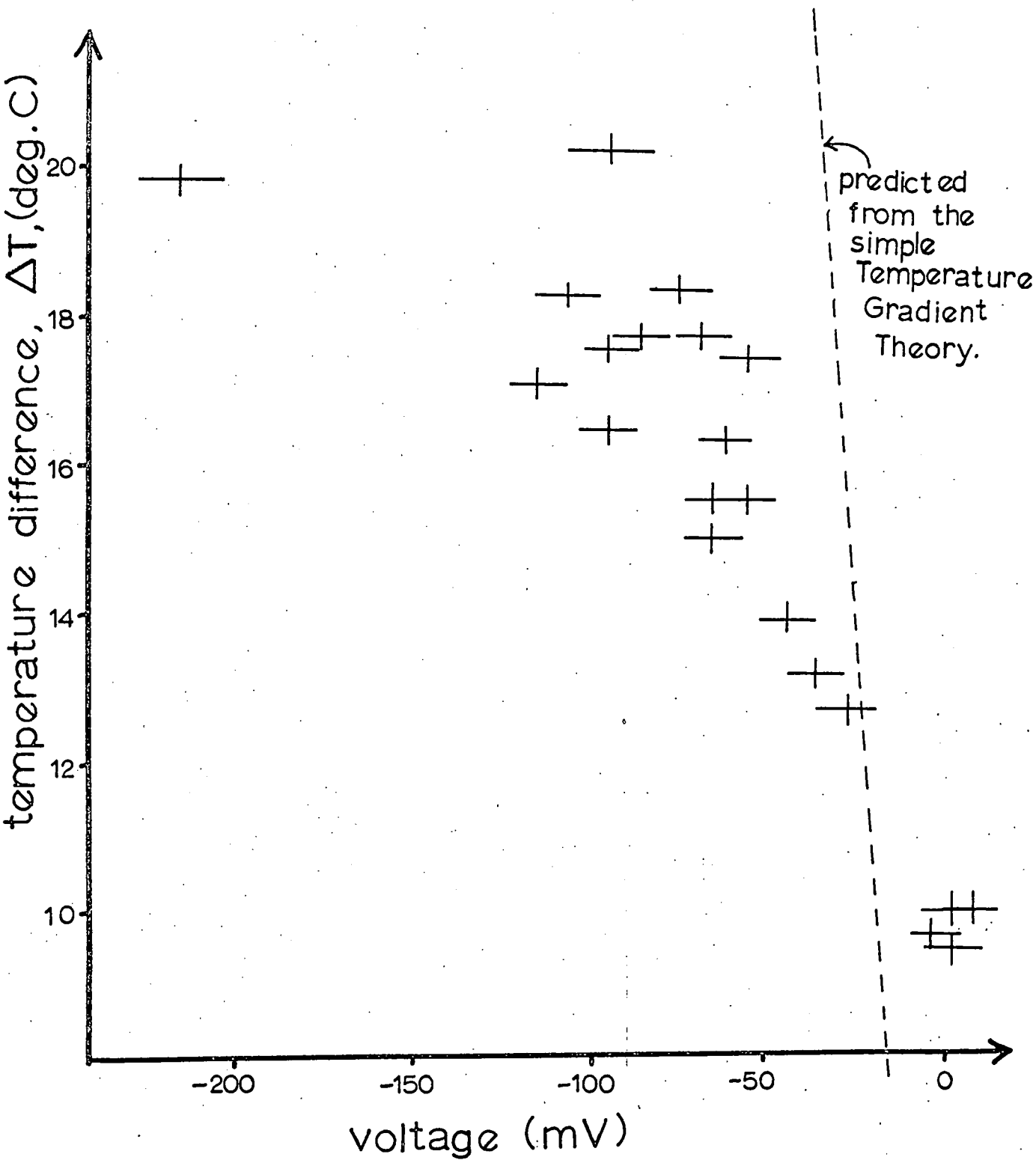


Fig. VI.12. GRAPH OF VOLTAGE AGAINST TEMPERATURE DIFFERENCE BETWEEN OPPOSITE FACES OF THE ICE IN THE FREEZING CELL. THE LIQUID PHASE WAS BEING STIRRED.

agreement with the simple theory. The deviations are probably attributable to having a large amount of the ice sample at temperatures above -7°C , where the simple Temperature Gradient Theory does not apply. Other factors which might affect the quantitative agreement with the theory are that there might be contributions to the potential differences from freezing effects or melting effects, and that the ice specimens had had widely differing histories and contained different amounts of air bubbles.

The results displayed in Fig.VI.12 were obtained on the ice samples produced by the freezing runs tabled in Appendix 4. Therefore, the reproducibility of the temperature gradient effect on the voltage shown in Fig.VI.12 may be directly contrasted to the irreproducibility of the freezing potential against time graphs shown in Fig.VI.9, and Fig.VI.10.

All results were obtained with a sample of water which had first been distilled and then passed through both a cationic and an anionic exchange resin until no reduction in conductivity resulted. The water had a specific conductivity of $1.54 \times 10^{-4} \Omega^{-1} \text{m}^{-1}$ in air by the time it had been transferred to the freezing cell. (This could be reduced to $1.98 \times 10^{-5} \Omega^{-1} \text{m}^{-1}$ by agitating under an atmosphere of nitrogen for ten days, showing that a large proportion of this apparently high conductivity was due to the presence of dissolved gases, e.g. carbon dioxide.) If such a sample of water, which, in theory, should exhibit no freezing potentials, should still give

freezing potentials greater than the potential differences due to the temperature gradients, at freezing rates of greater than $10 \mu\text{m s}^{-1}$, it seems reasonable to assume that most dilute solutions with conductivities less than $10^{-2} \Omega^{-1} \text{m}^{-1}$ will behave in the same way. Indeed, the potentials recorded by Workman and Reynolds (1950) Gill (1953), Gross (1965), Lodge et al. (1956) and others, confirm this, as they cannot be explained in terms of a Temperature Gradient Effect.

VI.4 (d) A possible explanation for the shape of the voltage against time graphs.

It is now possible to explain, qualitatively, the voltage against time graphs produced by the Watanabe Recorder during freezing runs. (See Fig.VI.2.)

Firstly, let us consider Case (A) where the ice forms rapidly due to supercooling and covers the ice face almost instantaneously. Since the freezing rate is rapid, we would expect a large freezing potential. However, it may not be very large, since the crystal orientation will be somewhat disordered and, according to Workman and Reynolds (1950), this reduces the freezing potential. Therefore, the first voltage peak is a compromise between freezing rate, ion incorporation rate and charge neutralisation rate. When the supercooled layer of water above the electrode freezes it releases latent heat, and its temperature rises to 0°C . This was proved by watching the effect of freezing on the temperature when a thermocouple was attached to the freezing face. (See Section VI. 4(a).) Before any more freez-

ing can take place, it is necessary to establish a temperature gradient across the ice and, therefore, the voltage falls. Once a temperature gradient is established, and this happens very quickly (sometimes more rapidly than the response time of the electrometer), the freezing proceeds and the voltage rises. A second maximum value is reached which is governed by the rate of cooling, the ice thickness, the rate of neutralisation, the temperature gradient and so on. Thereafter, the voltage falls as the freezing rate drops and eventually, if the freezing rate is low enough, the Temperature Gradient Effect within the ice predominates.

Secondly, let us consider Case (B) where the lower electrode became covered with ice slowly. The explanation is similar, but only very small freezing potentials are recorded until the lower electrode becomes completely covered with ice. The quicker this happens, the sooner the potential follows the line taken in graph A. In general, however, it will follow a line slightly higher than that in graph A, but the reason for this is not clear. (See Section VI.4 (b).)

Recently, Pruppacher, Steinberger and Wang (1968) reported the electrical effects accompanying the spontaneous growth of ice in supercooled solutions. They carefully cooled the solutions in polythene tubes in a low temperature, high-resistivity silicone oil bath. The ends of the tubes were sealed with chromium plated electrodes. When the liquids had become supercooled to the desired amounts, freezing was initiated by cooling one electrode with a

piece of solid carbon dioxide. The freezing potentials they recorded, on an electrometer connected between the electrodes, bear a striking resemblance in size, sign, overall appearance and time scale to those obtained in my freezing cells at freezing rates which were very much lower than those of Pruppacher et al. (See Fig. VI.13.) It is possible that the fall with time of the voltages recorded by Pruppacher et al. might be due to a fall in the rate of growth of ice crystals, rather than the enmeshment of ions of opposite sign as suggested by these workers. Nevertheless, the results of these workers show that the results obtained in the experiments described above are qualitatively applicable over a much wider range of freezing rates than was actually examined and add weight to the conclusion that freezing potentials usually predominate over temperature gradient potentials.

VI.5. The Effect of Impurities on the Freezing Potentials.

VI.5(a) Changes in pH.

Since de-mineralised water gave substantial freezing potentials, an attempt was made to see if these potentials could be explained in terms of the variation in pH of the sample on freezing.

The method used by Workman and Reynolds was to freeze a portion of a sodium chloride solution whose pH was known. The water was decanted and its pH was measured. The ice was washed with de-mineralised water and melted and its pH was measured. All the measurements were carried out at the same temperature.

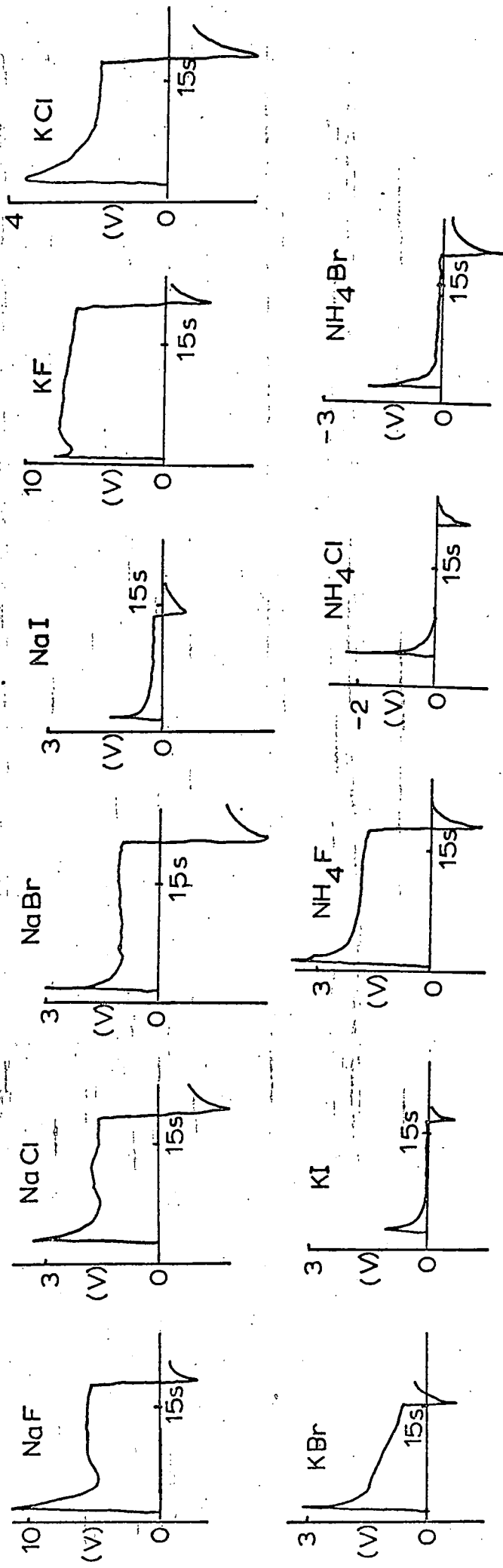


Fig. VI. 13. THE VARIATION OF FREEZING POTENTIAL WITH TIME IN 10^{-4} MOLAR SOLUTIONS (after Pruppacher, Steinberger & Wang, 1968).

However the pH of de-mineralised water is extremely sensitive to the presence of small quantities of ionic contaminants. When the pH of a small sample was measured in the freezing cell it was found to be 6.8; when it was poured into a carefully cleaned and dried pyrex beaker and the pH was again measured, it had changed to 6.4. This change in pH, if it had occurred on freezing, would represent a considerable charge transfer. Therefore, results obtained in this manner would be highly suspect. More reliance could, perhaps, be placed on the measurements if they were performed in situ, and so a brass freezing cell was modified to enable simultaneous measurements of freezing potential and pH be made. Holes were drilled in the upper brass electrode, to allow free passage of water around the bulb of the glass electrode of an Analytical Instruments Pocket pH Meter, which was mounted just above the upper brass electrode. A small thermocouple was positioned next to the bulb so that corrections could be made to the reading for changes in temperature during freezing. About 80 ml of water were poured into the cell and freezing was started. Readings of pH, temperature of the water and freezing potential were taken every 15 s.

Although the thermocouple showed that convection was occurring in the water, no significant change in the temperature-compensated value of pH was noted throughout the experiment. The pH meter showed rapid, high speed fluctuations of ± 0.1 pH units but no definite trend. Perhaps significant changes in pH would have been recorded if the bulb of the pH meter had been nearer

the interface, or if the solution had been stirred. However, neither of these proposals was tried since the probe unit was too large to be positioned nearer to the interface, and because it had been necessary to remove the stirrer drive-motor and gear-wheels in order to allow access for the probe of the pH meter in the first place. Experiments of this type were discontinued as time did not permit the major modifications of the apparatus necessary.

The main ionic impurity present in the de-mineralised water was probably sodium chloride which had been used to re-generate the de-ionising resins.

VI. 5(b). Changes in Conductivity.

Measurements of the conductivity of the solutions in the freezing cells were carried out either in special conductivity cells or in the freezing cells themselves, using an Electronic Switchgear A.C. bridge. Each freezing cell was calibrated using liquids of known conductivity and its "cell constant" determined. (The cell constant is the number by which measured conductivity must be multiplied to give the specific conductivity.) The conductivity could then be determined at any time without removing solution from the cell. Unfortunately, when the solution had been frozen and melted, the air bubbles which had been released were collected by, and remained underneath, the upper electrode, changing the cell constant and invalidating the measurements. Therefore, conductivity was measured only before a solution was frozen for the first time and again, this time in a special cell, before it was discarded.

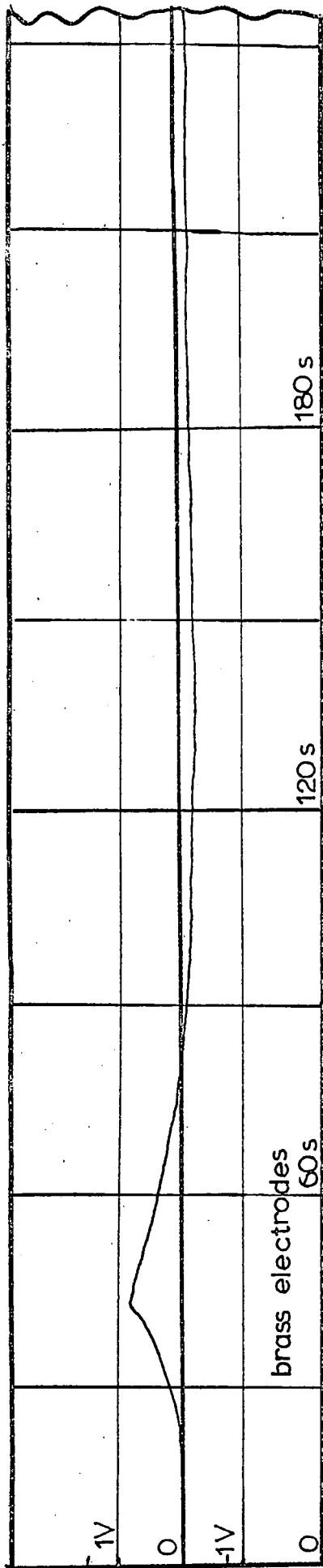
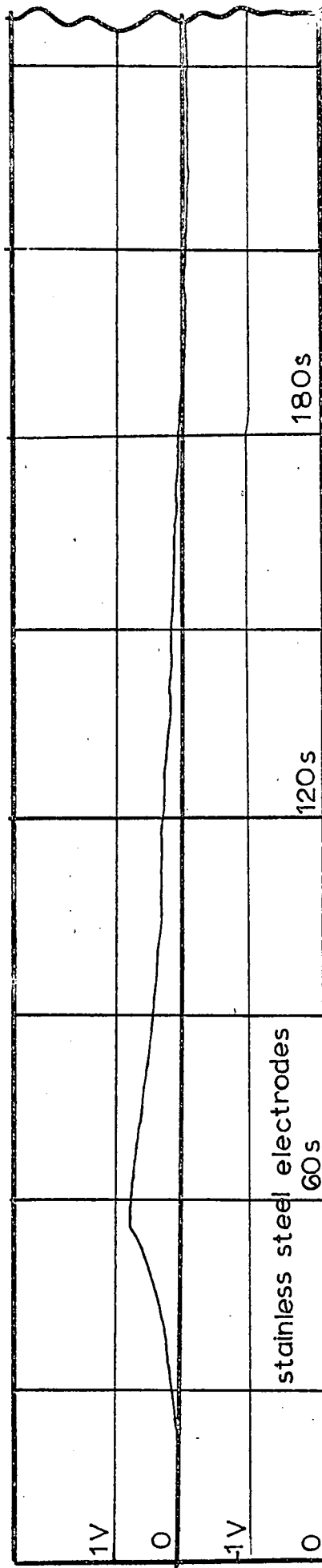
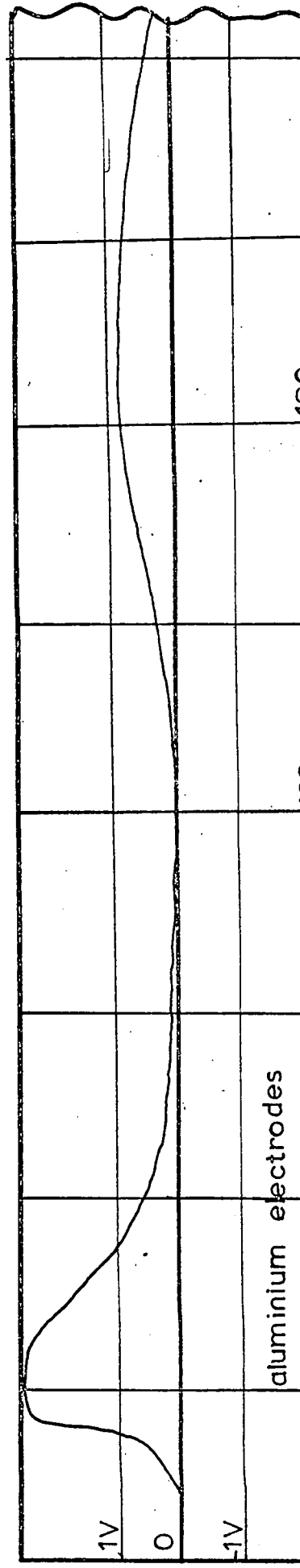


Fig. VI.14.



THE EFFECT OF DIFFERENT ELECTRODE MATERIALS ON FREEZING POTENTIALS.



All the samples of de-mineralised water increased in conductivity on being in the freezing cell for any length of time, whether or not the solutions were frozen, and even when the gold-plated cell was used. Hardly any difference in behaviour was noticed between the brass, the aluminium or the gold cells, but in the stainless steel cell, the conductivity changed more markedly and rust appeared on the electrodes after two days. The brass and aluminium cells showed some oxidation of the electrodes after a period of about a week, but the conductivity differed little from samples of water stored in the gold cell or the carbon-electrode conductivity cells. It was concluded that such changes in conductivity could be attributed to increases in the amounts of volatile impurities, and samples were rarely allowed to stand in the freezing cells for periods of more than three days.

VI. 5(c) Changing the electrode material.

When the same solution was frozen in the brass electrode cells, the aluminium cell and the stainless steel cell, or when different portions of the same solution were frozen in each cell, no significant differences were noted in the potential-time graphs which could be directly attributed to anything other than differences in freezing rate, or in the degree of supercooling before freezing. Typical recorder traces are shown in Fig.VI.14. The brass and stainless steel cells have comparable heat capacities and give similar potential-time graphs. The aluminium cell has a much smaller heat capacity and the degree of supercooling before freezing

tends to be greater. However, since the aluminium cell was more fragile and the stainless steel cell was inclined to rust, the brass cells were almost invariably used in the other experiments.

VI.6. Other Experiments with the Freezing Cells.

In order to check if the freezing potentials depended on whether the ice was formed at a vertical surface, downward from a horizontal surface or upward from a horizontal surface, the lid of a freezing cell was made leak-proof by sealing the screw threads with P.T.F.E. ribbon. It was then filled completely with de-mineralised water and "runs" were made in each of the orientations described above. The voltage against time graphs obtained are reproduced in Fig. VI.15. If anything, the differences between these graphs are less than the normal variation between consecutive runs on the same solution in a fixed orientation. This result suggests that the previous conclusions will be valid for all freezing orientations.

The possible application of these results to cloud phenomena is discussed in Chapter VIII.

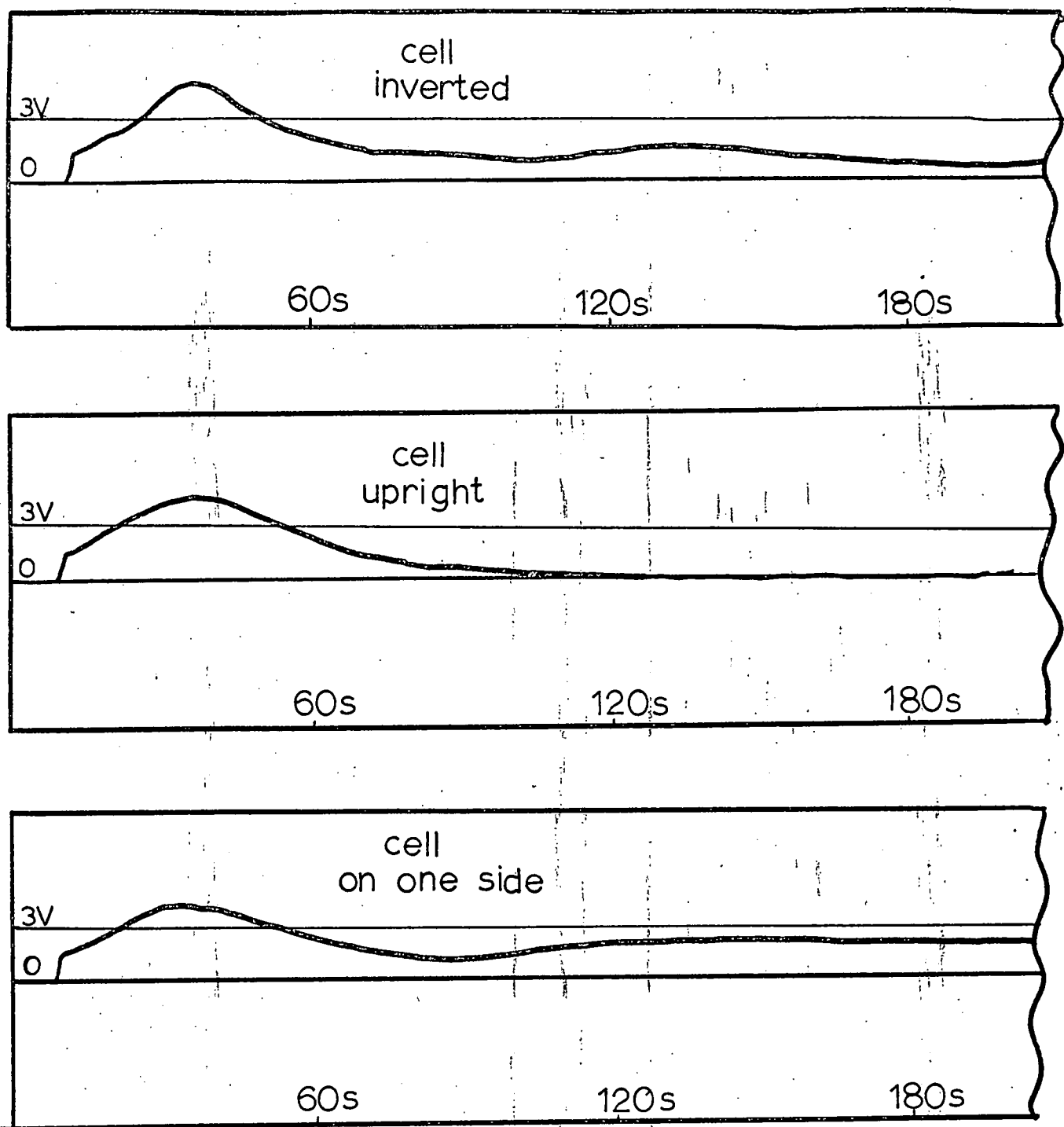


Fig VII. 15. THE EFFECT ON THE FREEZING POTENTIALS OF CHANGING THE ORIENTATION OF THE FREEZING FACE.

CHAPTER VII.

THE ELECTRIFICATION OF WATER FLOWING THROUGH AN ICE TUBE SUPPORTED IN A GLASS COOLING-JACKET.

The previous attempts to measure the electrification of water flowing through ice tubes, described in Chapter V, suffered from two big disadvantages. Firstly, it was not possible to see what was happening to the ice when electrification was being detected and secondly, it was not possible to control the temperature long enough to maintain stable conditions for more than a few seconds. If the first of these disadvantages could be overcome, the second would be much less of a problem.

An attempt had been made (see Section V. 3(b).) to allow visual observations by using a perspex support tube. But this tube showed appreciable charging when cold, dilute anti-freeze solution was pumped around it and it was, therefore, encased in an earthed brass tube. Some of the properties of pyrex glass suggested that it could be used instead of perspex. It has a lower resistivity than perspex, but still appreciably higher than that of ice over the temperature range obtainable with a dilute anti-freeze solution. Therefore, extraneous static charges on a glass support tube will leak away more rapidly than on perspex and would not be registered by the electrodes inside the tube, but the magnitude of static charges between ice and water would hardly be affected.

Glass is considerably more brittle than perspex and it might be expected that the expansion of water on freezing would shatter the tube. Tests showed that most of the expansion was

taken up in the liquid and the glass tubes did not break, provided that the water was kept flowing through the tube.

VII. 1. The Design of the Apparatus.

VII. 1(a). The basic apparatus.

The basic requirements were that the tube should be transparent, that it should be cooled as symmetrically as possible, using a transparent cooling-jacket, that electrodes be attached at both ends and that no water should leak from around the seal between the electrodes and the glass tube, and that, so far as is possible, there should be laminar flow of the liquid in the tube. Other, perhaps less obvious, requirements were that there should be some means of preventing air bubbles, produced on freezing, from being trapped in the tube, where they might interfere with the symmetrical formation of the ice tube. And it is essential that the electrodes should not become blocked with ice.

The apparatus resembled a liebig condenser and consisted of a double-walled, pyrex glass tube with a length of 0.30 m and an inside diameter of 20 mm.. At one end of the inner tube was a male "Quickfit", ground-glass, B 19 tapered cone and at the other was a female cone. These Quickfit cones are all made with a standard 1 in 10 taper. The tube was mounted vertically, with the female cone uppermost, and brass electrodes were fitted into the cones. (See Fig.VII. 1. and Fig. VII. 2.) These electrodes were turned out of adjacent portions of a 25.4 mm diameter brass bar, and had a 1 in 10 taper cut into them. To ensure that they

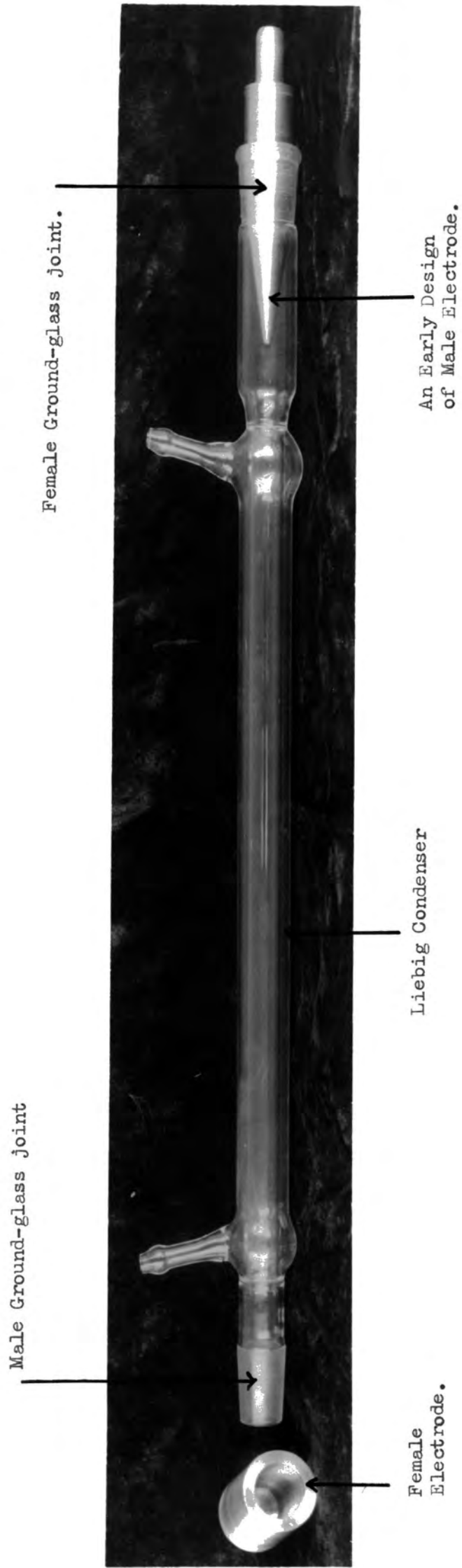
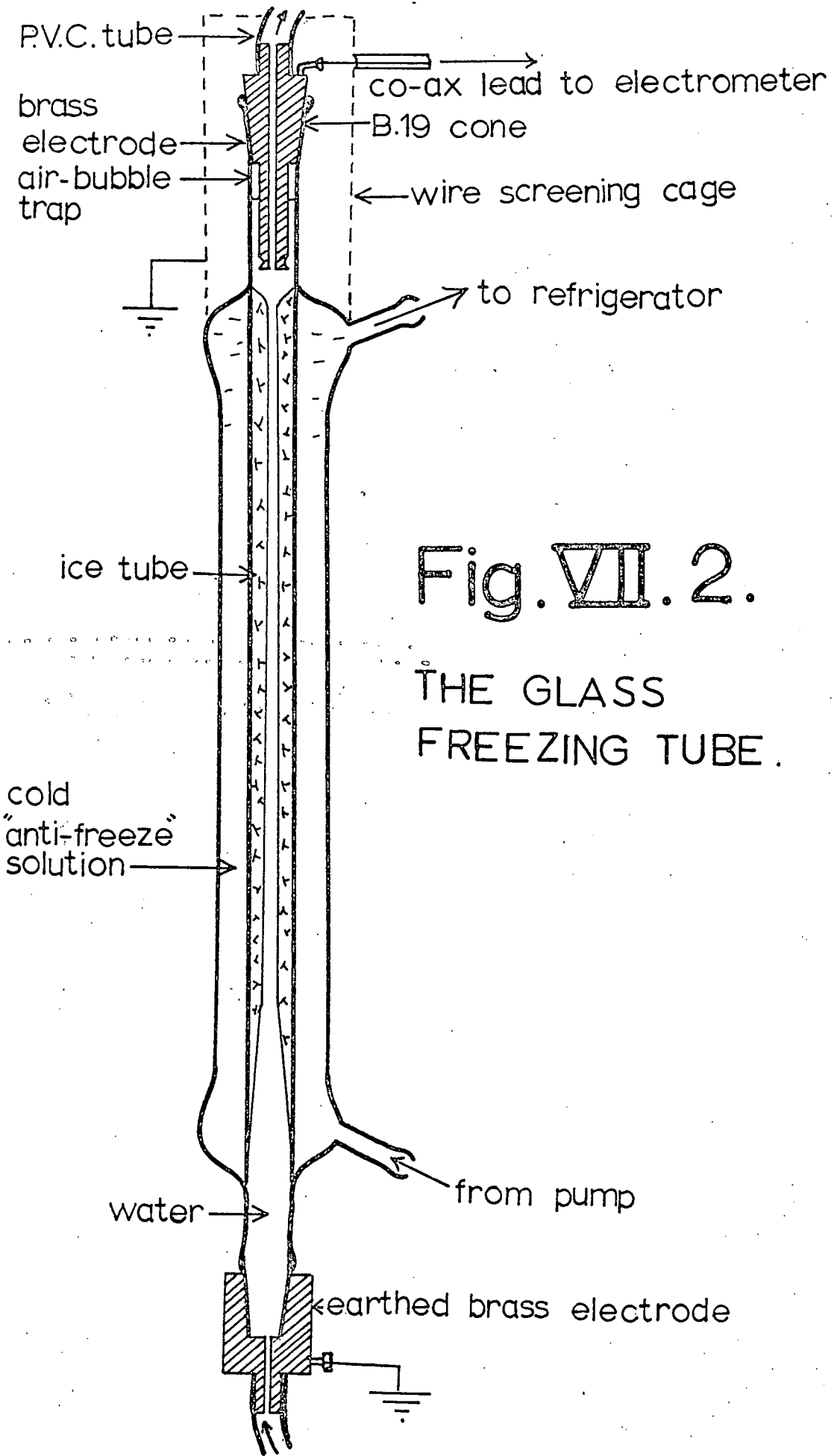


Fig.VII.1. The Prototype Glass Freezing Tube.



fitted the glass cones perfectly, they were ground into them, using an abrasive paste. The electrodes had small holes drilled through them with a no. 60 drill. Water entered through the hole in the lower electrode, passed through the tube and out through the hole in the upper electrode. This electrode was shaped so as to present a plane face towards the lower electrode, and yet allow air bubbles to collect in a bubble trap around its sides (see Fig. VII. 2.) so that they did not build up and intermittently isolate the electrode from the liquid.

The following precautions were taken to ensure that the flow of liquid through the tube was not unduly turbulent. Ideally, the tube should expand to its maximum diameter of 20 mm by approximately a 1 in 7 taper to maintain laminar flow in the water. In this case a 1 in 10 taper was used, as dictated by the commercially produced ground-glass joints. The face of the electrode through which the water enters was plane and perpendicular to the direction of flow, as this also reduces turbulence. So that water could be made to flow in either direction through the tube without introducing unnecessary differences in the conditions of flow, the upper electrode was also given a plane face.

Cooling of the water was achieved by pumping cold anti-freeze solution through the cooling-jacket. The maximum rate of flow of coolant was about 4 litres per minute.

VII. 1(b). Experimental method and the early results.

The tube was cleaned with a chromic acid solution and washed thoroughly with de-mineralised water. The brass electrodes were scrubbed in a liquid detergent and rinsed thoroughly in de-mineralised water. (Metal polish was not used in cleaning these electrodes as it would be very difficult to ensure that all traces of it had been removed from the fine holes.)

The female electrode was clamped with its open end uppermost and the glass tube was fitted into this. In order to ensure a perfectly water-tight joint, a trace of silicone grease was smeared on the glass cone before assembly. The cone on the other electrode was also smeared with a trace of grease and placed in the upper cone of the tube. Both joints were rotated slightly, to ensure that they were properly seated and then 0.5 m lengths of 10 mm diameter P.V.C. tubing were fastened onto the electrodes by means of hose clips. Brand-new P.V.C. tubing was always used for these water lines; before use it was carefully cleaned by washing with a soap-solution, and any solid particles, from the packing material in which it was delivered, were washed out by forcing a tight-fitting plug of poly-urethane foam through the tube, using water pressure. Finally, the tubing was rinsed thoroughly with de-mineralised water.

Separating funnels were clamped into the other ends of the tubing (See Fig. V.4.), and the one attached to the lower electrode was filled with water. Both funnels were raised up

above the level of the glass tube and the taps were opened. The tube filled up with water and air bubbles in the P.V.C. tubing were dislodged by shaking. Finally, when all the other air-locks had been removed, the upper electrode was loosened for a few seconds to allow most of the air trapped around it to escape, thus ensuring a good contact between the electrode and the water. (See Fig.VII. 2.) The water could be made to flow through the tube by raising or lowering one or other of the separating funnels.

To measure the electrification, the lower electrode was earthed and the upper electrode was connected to the vibrating-reed electrometer which was on the voltage measuring range with an input impedance of $10^{12} \Omega$. The 100 mV full-scale range was used and with the upper electrode unshielded there was a certain amount of pick-up of extraneous fields. However, most of these were attributable to the operator and, provided that unnecessary movement was avoided, these deflections gave a background noise level of less than ± 3 mV.

Before any electrical measurements were made, the degree of turbulence in the flow of the water in the tube was checked. The tube was set up as described and water was caused to flow through the tube by raising one of the separating funnels. About 10 ml of a slightly acidified, concentrated potassium permanganate solution was added to the water in this separating funnel and its progress through the tube was observed. The coloured water

entered through the electrode and rose in a narrow stream through about a third of the tube. Then it became unsteady and started to mix with the surrounding water, but a thin, pale, purple line did reach up to the hole in the top electrode. When the experiment was repeated with the flow reversed, the permanganate solution got about half-way down the tube before becoming diffuse. Inverting the tube gave similar results. The male electrode was slightly worse at maintaining the laminar flow than the female electrode in both cases, but both electrodes performed better when they were uppermost. From these results, it was concluded that, despite the rather qualitative approach to streamlining taken during the designing of the equipment, the turbulence was not excessive and that the difference in the behaviour of the permanganate solution, depending on whether it was rising or falling in the tube, was probably due to the difference in density between water and the solution. In any event, even if the tube had been hydrodynamically designed, the profile would be changed when there was ice in the tube and all that could be said to justify a certain amount of streamlining is that it might help to produce a more symmetrical ice tube in the first place. In this respect, the tube was quite good and a typical ice tube profile is shown in Fig. VII. 2.

The early electrical measurements were, however, less satisfactory. Despite the precautions taken to eliminate chemical electrode potentials, standing potentials often existed

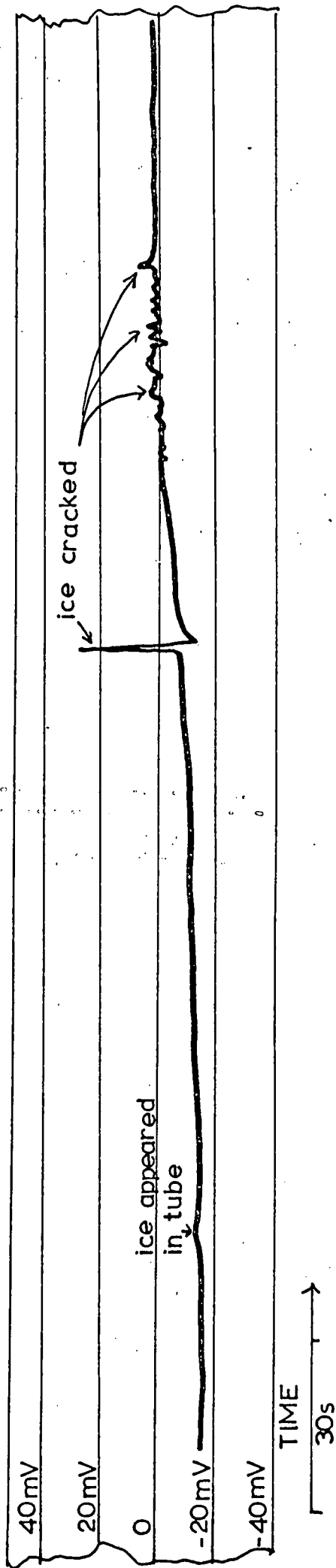


Fig.VII.3. A TYPICAL RECORDER TRACE FROM EARLY EXPERIMENTS WITH THE GLASS FREEZING TUBE.

between the upper and lower electrodes. These could be of either sign, but were usually negative (the lower electrode is earthed). Sometimes they were reduced by allowing the water to flow through the tube, but often they persisted almost unchanged. They varied in value but might be as high as ± 50 mV. They were very slightly temperature dependent, but this effect was small in going from room temperature. Usually, if the equipment was left undisturbed for a few hours, they disappeared of their own accord. No satisfactory explanation of this effect can be put forward for the appearance of these potential differences and, where possible, electrification measurements were avoided when it was present.

Water was made to flow through the tube by lowering the separating funnel connected to the upper electrode and then cold anti-freeze solution was pumped into the cooling-jacket from the bottom.

Eventually, about three-quarters of the surface of the inner tube became covered in a thin layer of dendritic ice crystals which began to be formed at some point near the top of the cooling-jacket and spiralled down the tube for about 1 s. The rapid way in which they had appeared suggested that the liquid layer next to the tube wall had become supercooled and that freezing had been initiated in the coolest portion of the tube. Usually the appearance of ice in the tube was accompanied by a small, positive deflection of up to 5 mV on the electrometer. (See Fig. VII.3.)

At about this time, visual observation of the ice in the inner tube was rendered impossible by the formation of hoar frost on the outer surface of the cooling-jacket. A temporary solution to this problem was to wipe the outer surface of the tube with a rag soaked in methylated spirit; however, within two or three minutes, heavy condensation of water vapour diluted the methylated spirit to such an extent that the tube iced over again and it became essential to find a more permanent solution to the problem. (See Section VII. 1(c).)

Often the water in the tube became highly supercooled before the onset of freezing and when freezing did occur, a mass of dendritic ice crystals extended out of the top of the jacketed tube and initiated freezing of the water in the upper electrode. Unless prompt action was taken to drain out the coolant from the cooling-jacket before the flow of water through the tube ceased completely, all the water in the tube became rapidly frozen and shattered the inner glass tube. The only practical solution to this problem was to shorten the upper electrode so that it stood about 10 mm above the top of the cooling-jacket and never came into contact with the ice at all. Surprisingly enough, this appeared in no way to affect the measurements made in the tube in the cases where this high degree of supercooling did not occur, so far as could be judged without taking a statistical sample of measurements which the tube mortality rate precluded.

During the next 10 s of a run, the ice sheath became thinner and its appearance changed to a clear, transparent shell

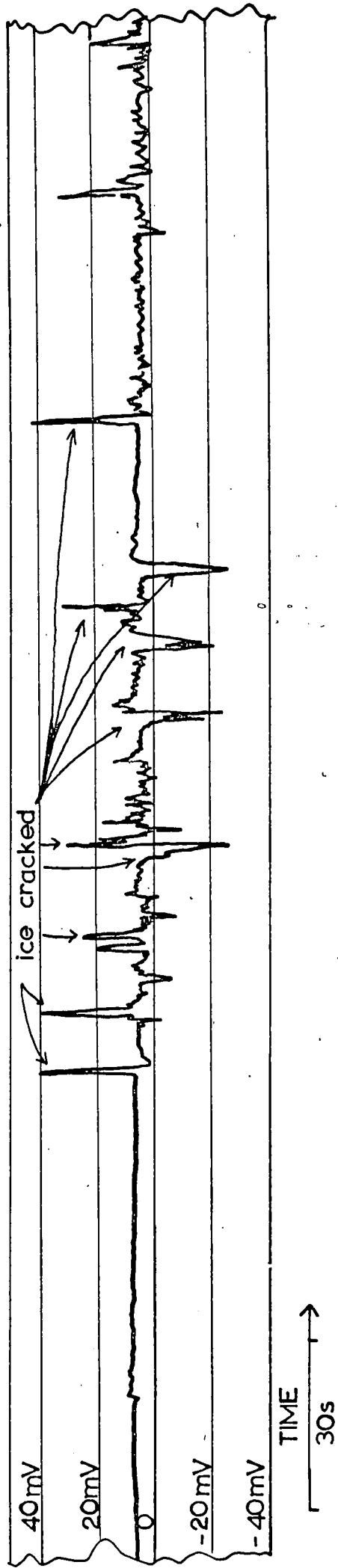


Fig.VII.4. A TYPICAL RECORDER TRACE FROM EARLY EXPERIMENTS WITH THE FREEZING TUBE :

containing a few air bubbles. Meanwhile, the electrometer deflection died away to zero. However, as cooling continued, the clear ice shell became steadily thicker and the electrometer again registered a positive potential which increased with increasing ice thickness. The ice was always thicker near the top of the tube (See Fig. VII.2.) and when the hole remaining at the narrowest point had diminished to a size comparable with the holes in the electrodes, the ice, but not the glass, tube fractured. Each crack observed to appear in the ice tube corresponded to a sharp peak on the electrometer trace. (See Fig. VII.3. and Fig. VII.4.) Ultimately, the tube became completely blocked and the flow of water through the tube ceased, but often the electrometer still registered a constant deflection of about + 20 to + 30 mV. When the flow of coolant was stopped and the tube was allowed to warm up to room temperature, the ice melted and this constant potential difference fell away to zero.

In only half of the experimental runs made with the glass tube was electrification detected of the type described above. In the other half no electrification was detected until fissures appeared in the ice tube. Then electrometer deflections of both signs with no significant general trend were produced. (See Fig. VII.4., and contrast it with Fig. VII.3.. These recorder traces were obtained with the same solution on the same day within 1 hour of each other.)

It appeared that the initial peak on the electrometer trace could perhaps be attributed to the charge separated between

ice and water at an interface, but that the general trend was probably due to temperature differences along or across the ice tubes. Therefore, it was decided to see if any of the potential differences could be correlated directly with the Workman and Reynolds type experiments and the measurements of temperature gradients reported in Chapter VI. A controlled-environment glove box was constructed to facilitate these measurements.

VII.2. The Controlled Environment Box.

Observations on the glass tube had been hampered by the formation of hoar frost on the outer surface of the cooling-jacket. Although the deposit could be cleared for a short period by rubbing it with a methylated-spirit-soaked rag, heavy condensation had continued and occasionally liquid on the outside of the tube had appeared to be short-circuiting the electrodes. The condensation of water vapour on the cooling-jacket would be reduced if the air surrounding the tube was dried. A glove-box would enable the air around the tube to be kept dry.

Also, since we have already seen in Chapter VI that the values of freezing potentials were not reproducible, and this appeared to be the case with the early measurements on the glass tube, it was decided to try to provide a completely self-contained system for the freezing tube measurements in order to ensure reproducible conditions as far as possible. It was also hoped to be able to compare the results obtained with measurements in the freezing cells with

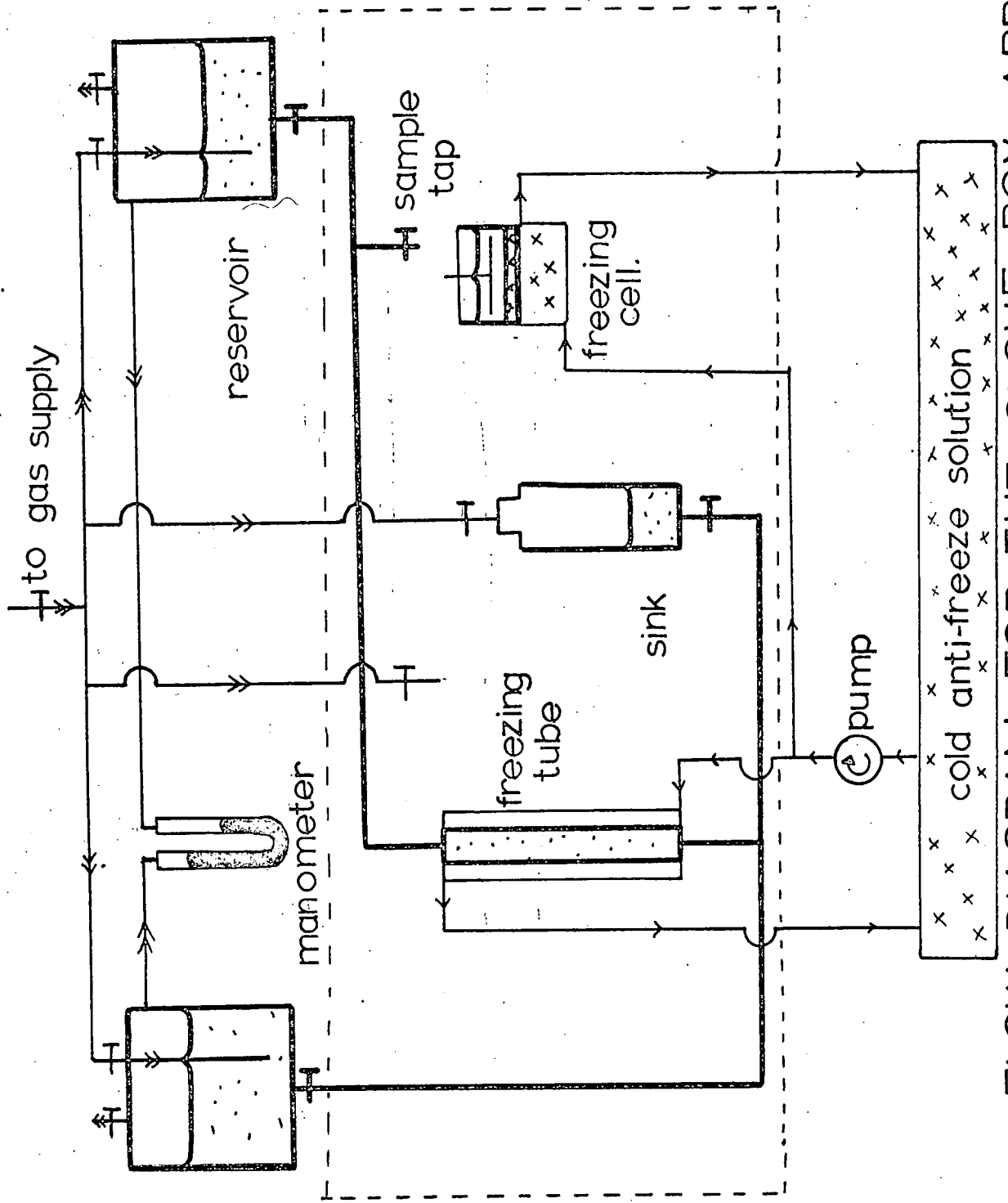


Fig.VII.5. FLOW DIAGRAM FOR THE GLOVE BOX APPARATUS.



Fig.VII.6. The Apparatus within the Glove-box.

the same sample of water.

A controlled-environment glove-box was constructed on a wooden frame measuring 0.92 m x 0.76 m x 6.4 mm thick. Two circular holes were cut into the perspex sheet and glove-ports, complete with neoprene gloves, were bolted onto the front of the box. (See Fig. VII.6.) The aluminium sheets were all connected to earth and the joints between sheets were sealed with adhesive P.T.F.E. tape. Access to the box could be gained either by removing one of the gloves or by removing the perspex panel which was bolted to the wooden frame and fitted with rubber gaskets so that a good seal could be maintained. The box was not completely gas-tight, but by maintaining a slight overpressure of gas inside the box, laboratory air could be excluded quite satisfactorily. The apparatus was arranged in the box according to the diagram shown in Fig. VII.6. All the gas, water, anti-freeze and electrical supplies to the box enter through the left hand panel of the box, as shown in Fig. VII.7.

(i) The gas supply.

The gas, either air, from a Broom and Wade "Handyair" compressor, or nitrogen, from gas cylinders, was metered through a Rotameter flow-meter to a series of glass cold-traps, immersed in the anti-freeze in a refrigerated tank, and thence to the glove-box. Water vapour and oil from the compressor were condensed out of the gas in the cold-traps but the gaseous components were unaffected. The gas line diverged so that a supply of gas was delivered to the

two water reservoirs, which consist of 10 litre pyrex aspirators, and to the box itself. The flow of gas to each reservoir and to the box was controlled by screw clips on the rubber tubing. (See Fig. VII.7.) Gas entered the water reservoirs through pyrex glass tubes immersed in the water and the reservoirs could be vented from the top. It was envisaged that water could be purified to a certain extent by bubbling nitrogen through the water to remove volatile constituents, and by closing one or other of the vents water could be forced from one reservoir to the other. The gas pressure difference between the reservoirs was indicated by the mercury manometer and the pressure differences due to the head of water could be read off from the scale on the side of the reservoirs.

The gas entered the box through a length of copper pipe bolted through the side panel of the box and fitted with an 'O' ring to ensure a gas-tight joint. This gas lead ended in a ground-glass B 19 cone which could be left free to pressurise the box or could be inserted into the top of the "sink" to force water, which had been sampled, back into the water system for recirculation.

In practice a gas flow rate of about 5 litres per minute was required to pressurise the box alone so that the gloves remained taut, and a flow rate of 10 litres per minute was sufficient to permit gas to be bubbled steadily through both reservoirs and still maintain pressure within the box.

(ii) The water system.

About 10 litres of water were stored in the two reservoirs

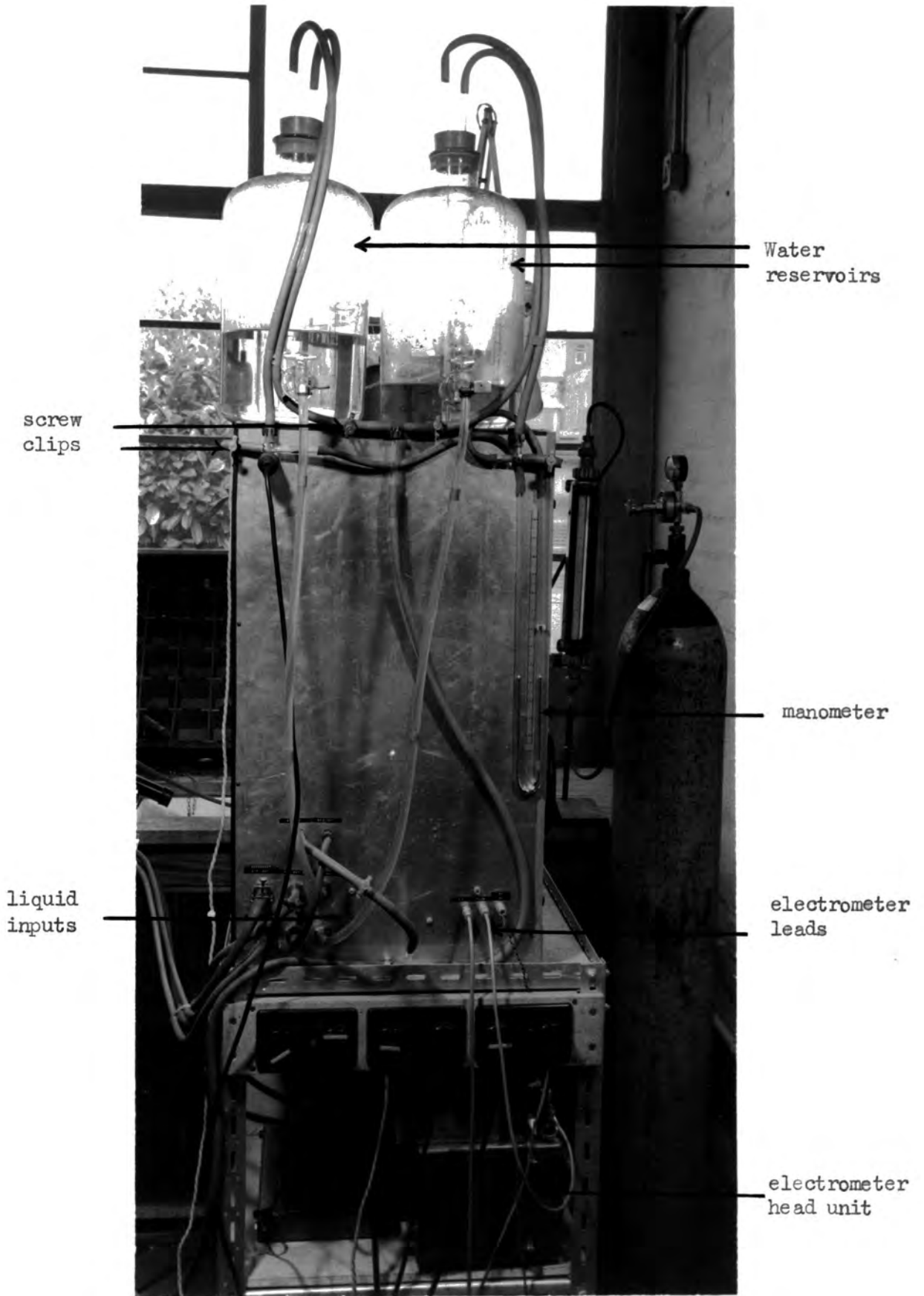


Fig.VII.7. Detail of Glove-box fittings and Controls.

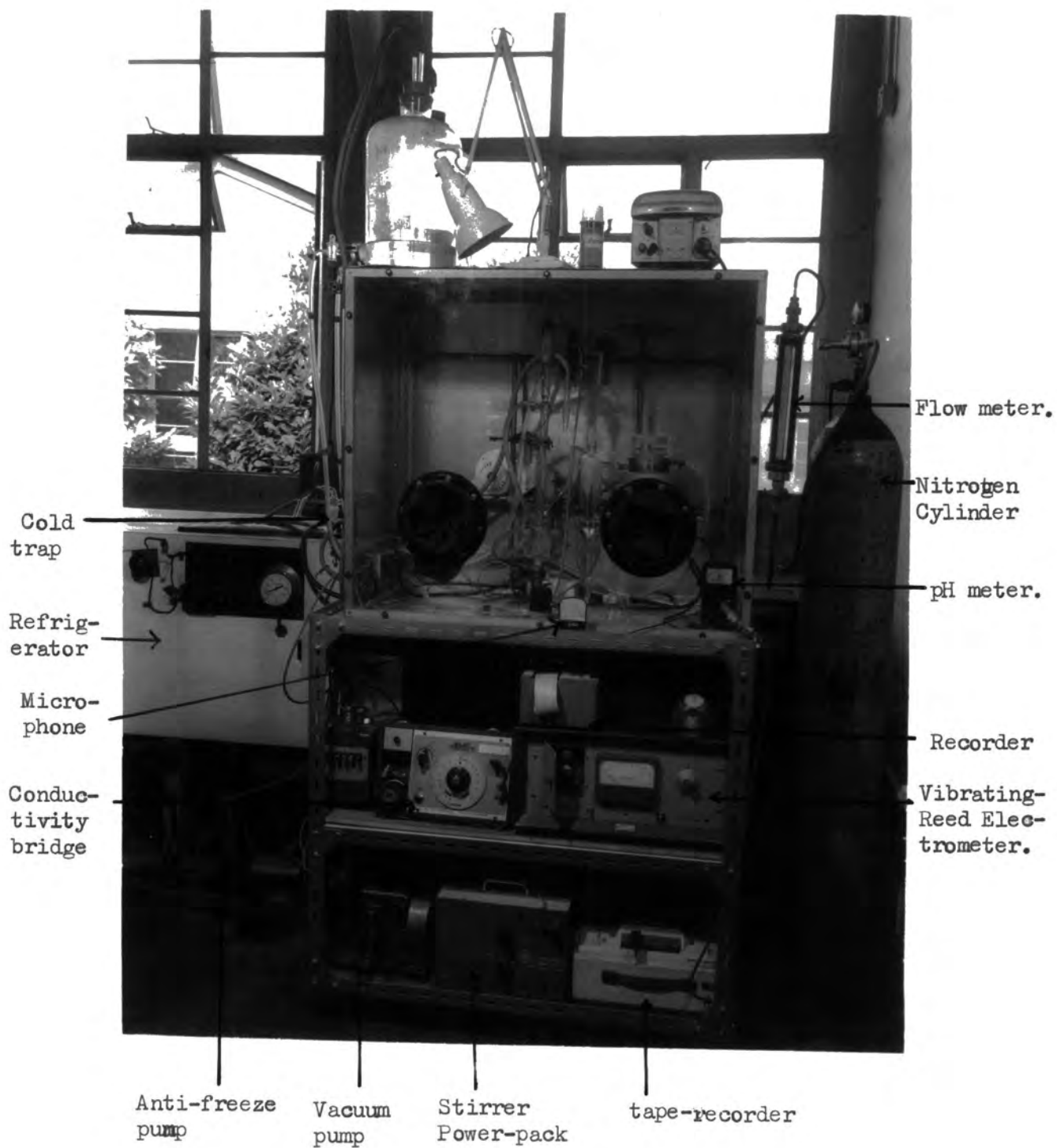


Fig.VII.8. A General View of the Apparatus.

mounted on the roof of the box. (See Fig. VII.8.) The reservoirs were connected together with new P.V.C. tubing via the freezing tube, a length of glass tubing fitted with a 'T' joint and tap from which water samples could be withdrawn, so that freezing potential, conductivity and pH measurements could be performed, and a similar 'T' joint connected to a pressurised sink through which the samples could be returned.

The water passed through the wall of the box through two earthed brass nozzles. Pyrex glassware was used throughout to minimise contamination of the water from sodium ions as it is much less soluble than soda glass.

(iii) The cooling system.

Cooling was achieved by pumping cold, dilute anti-freeze solution from the 80 litre capacity refrigerated tank in which the cold-traps were mounted. The input tube was split into two and fed both the cooling tube and a freezing cell. They had separate return tubes to the refrigerated tank and the cooling rate in each piece of apparatus could be altered by restricting the appropriate outlet tube.

(iv) Electrical systems.

250 V A.C. mains and 0 to 30 V D.C. for the freezing cell stirrer were supplied to the box through air-tight plugs. The electrometer leads were connected through the box using B.N.C. co-axial sockets and co-axial leads were used inside the box to reduce pick-up. A vibrating-reed electrometer and recorder could be connected to each piece of apparatus in turn.

(v) Other facilities.

In addition to the freezing tube and freezing cell, the glove box also contained a pH meter and a conductivity cell. An electric hair-dryer was placed in the box to ensure rapid thawing of the freezing tube after a run and the freezing cell was mounted on a small, electric hot-plate for the same purpose. For convenience, the glove-box and the ancillary equipment were mounted on a trolley. (See Fig. VII.8.)

VII. 2(a) The purity of the water.

A study was made of the electrification of a sample of de-mineralised, distilled water. The water had been distilled in a commercial, glass-lined still and then passed through a Permutit Mk. 8 de-ionising unit, consisting of anionic and cationic exchange resins in separate columns, until no change in conductivity was detectable. The resulting water initially had a conductivity of $1.00 \times 10^{-4} \Omega^{-1} \text{ m}^{-1}$ when measured under air in the glove-box.

Both the resins used in the de-ionising unit are particularly effective for removing strongly acidic and strongly basic ions, e.g. Cl^- , SO_4^{2-} , Na^+ , Ca^{2+} etc. However, weak acids and bases, such as ammonia and carbon dioxide are less efficiently removed from solution.

Some idea of the contribution to the conductivity of such volatile weak acids and bases is shown in Fig. VII.10. A 10 litre sample of the water was placed in one of the aspirators on top of the glove-box. Nitrogen was bubbled through this dilute solution

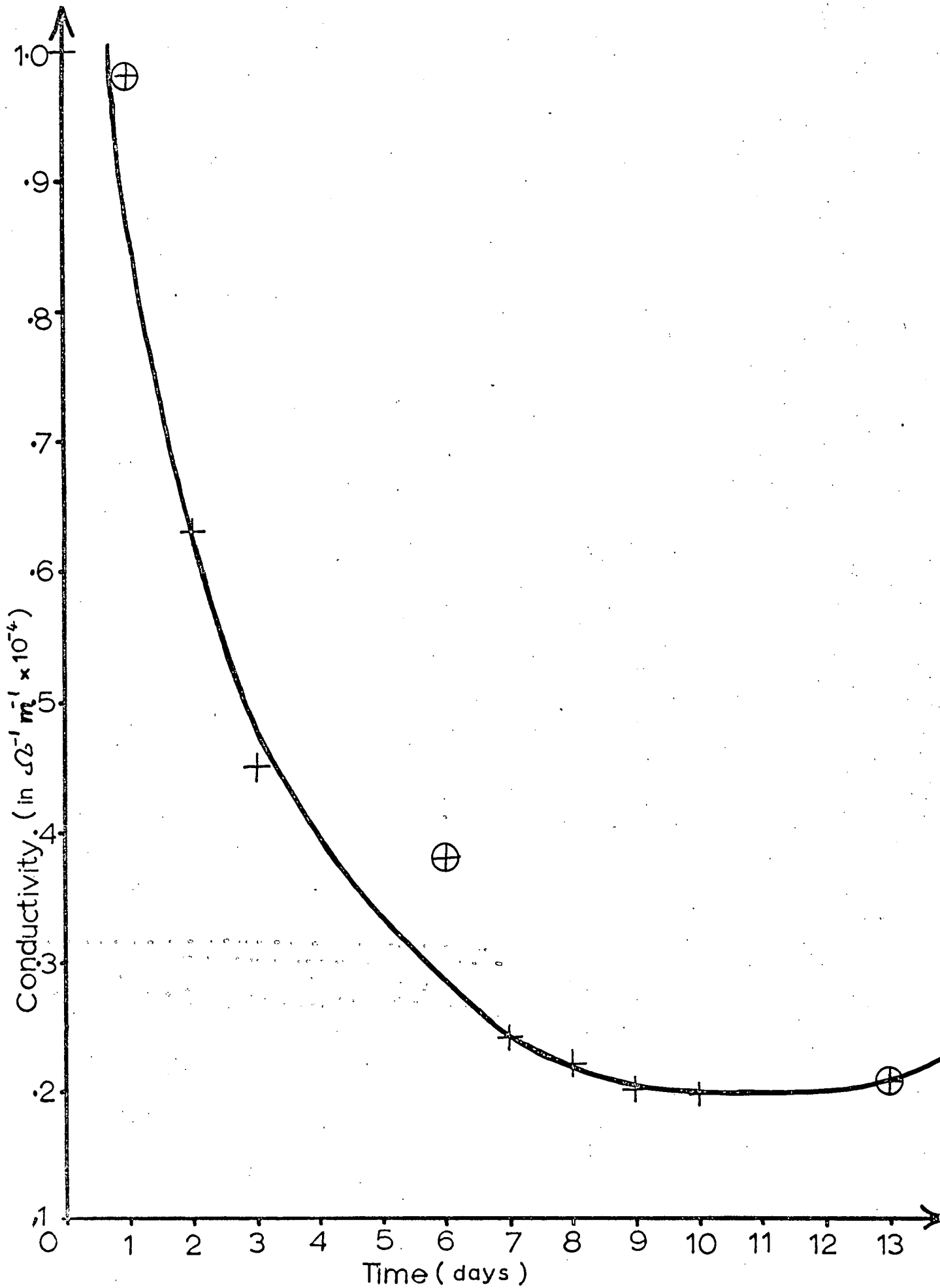
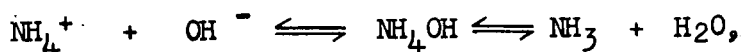
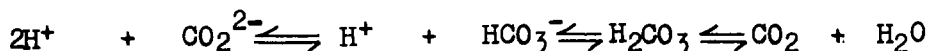


Fig. VII.10. THE VARIATION OF CONDUCTIVITY OF WATER WITH TIME OF BUBBLING NITROGEN THROUGH IT

at a rate of about 1 litre per minute. The conductivity of the water was measured daily and plotted against time of bubbling to give the graph reproduced in Fig. VII.10. This shows that the conductivity decreased with time to less than $0.2 \times 10^{-4} \Omega^{-1} \text{ m}^{-1}$ after 10 days. The deviations from a smooth curve can probably be attributed to variations in the rate of nitrogen flow, because although the flow was set to about 1 litre per minute when a new nitrogen cylinder was opened, the flow rate changed as the pressure inside the cylinder fell. The ringed points on the graph represent the values of conductivity on the days when the nitrogen pressure had dropped overnight to about 1 bubble per minute. The principle behind this method of purification is as follows. The nitrogen sweeps all the air out of the aspirator and, therefore, reduces the partial pressure of carbon dioxide, ammonia and any other dissolved gases, above the solution. Since the volatile impurities in the solution are in equilibrium with the vapours above the liquid, some of the impurity comes out of solution in an effort to restore equilibrium. This vapour is in turn swept away by the nitrogen and, ultimately, all the impurity will be removed. The equilibrium reactions which are involved can be represented by the following equations:



and



As the gases are removed, so the equilibrium is displaced toward the right.



When this purified sample had had air blown through it for 2 days, the conductivity had increased to $1.54 \times 10^{-4} \Omega^{-1} \text{ m}^{-1}$, and it remained constant at about this value for several weeks. This increase over the original value indicates that the nitrogen may also have been responsible for adding some impurities, which were non-volatile as they were not removed from the solution by bubbling air through it. Perhaps these impurities were from the nitrogen cylinders themselves, e.g. rust particles, or from the reducing valve, but their nature is uncertain. The other trace impurity which would be expected to be present in the water is sodium chloride from the solutions used to regenerate the column. The pH of this solution was 5.8 and it was used to obtain both the freezing potential results shown in Appendix 4 and the freezing tube results shown in Appendix 5.

VII. 2(b) Experimental details.

The glove-box had facilities for controlling the rates of flow of anti-freeze solution, water and gas. All were found to be satisfactory with the exception of control of the stability of the gas supply. This was not critical for the air supply because the compressor unit was fitted with a pressure switch, but the nitrogen cylinders could not be left on overnight for fear of damaging the box or of water sucking back from the aspirators into the gas lines and thence syphoning into the glove-box itself. As a result, no experiments have been conducted in which the water was in

equilibrium with pure nitrogen. In practice, dry air had to be passed through the glove-box overnight to ensure that the humidity was low enough to eliminate condensation on the freezing tube.

The individual experimental procedures adopted were the same as those described in Chapter VI and Chapter VII.1. However, charging of the perspex front of the glove-box was picked up on the freezing tube electrodes, and it was necessary to screen the upper electrode with an earthed, brass-mesh tube (see Fig. VII.6.) to reduce the noise level. Manipulating the neoprene gloves was avoided during freezing runs for the same reason.

It was not necessary to raise or lower the water reservoirs to cause the water to flow through the freezing tube; the desired head of water was set up by blowing water from one reservoir to the other, using air pressure, before the start of a run.

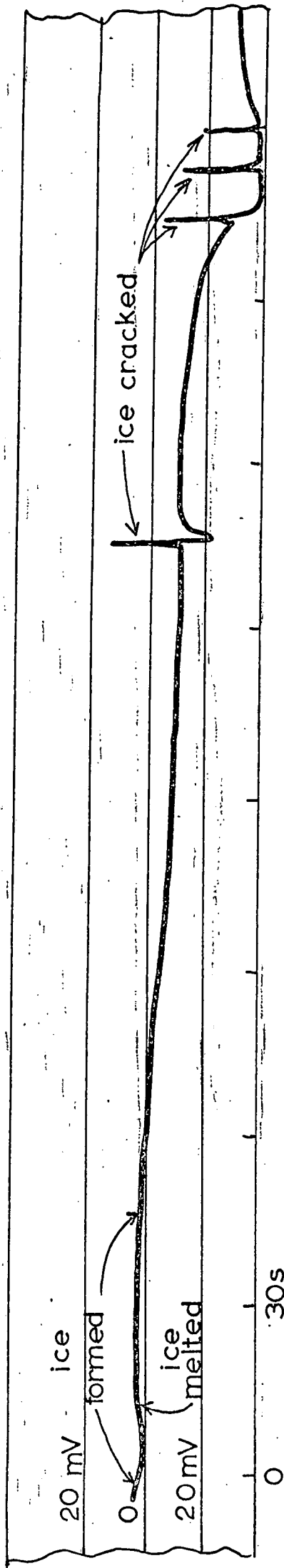
Standing potential differences in the freezing tube were reduced by causing the water to flow through earthed brass nozzles, situated between the reservoirs and the tube. However, sufficient length of 10 mm diameter P.V.C. tubing was left between the nozzle and the floating electrode to ensure that the freezing tube was being shunted by a resistance through the water of more than $1.5 \times 10^8 \Omega$. In theory this resistance should permit the measurement of freezing potential, temperature gradient effects and flow electrification. In fact, electrometer traces of the same general shape as those obtained earlier were produced, although the voltage peaks caused by the fracturing of the ice tube were reduced. The same could also be said of the large, broad peak

which was detected when the hole in the ice column was very narrow. (Compare Fig. VII.3. with Fig. VII.9.)

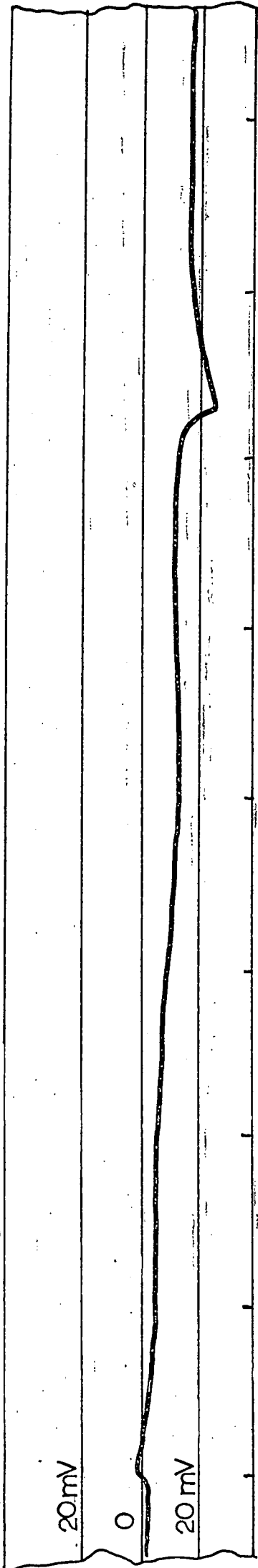
Unfortunately, the number of runs made using the freezing tube in the glove-box under reproducible conditions has been limited to the 13 runs listed in Appendix 5 and shown graphically in Fig. VII.9. This is because, to ensure reproducibility, it is essential that the runs are made as soon after one another as possible, so that the amounts of dissolved air, impurities, flow rates and temperatures are constant. Unfortunately, no ice could be formed in the tube, even at relatively low water, and high anti-freeze solution, flow rates if the anti-freeze tank temperature was above -14°C . The lowest anti-freeze solution temperature obtainable in the tank was -26°C which represented a drop of about 32°C . on the room temperature at that time. During the summer months the laboratory temperature was often over 15°C and under these conditions the anti-freeze temperature rose to -17°C and above. As each freezing run produced a temperature rise of about 2°C , it proved impossible to perform the experiment with any degree of regularity or success, except on the occasions when the ambient temperature had been below 15°C for at least 2 days. The apparatus was not completed until March 1969 so that the opportunity for freezing runs was severely limited, particularly as the cold room was not operational for much of the period between February and June.

THE VOLTAGE AGAINST TIME GRAPHS
FOR
THE GLASS FREEZING TUBE.

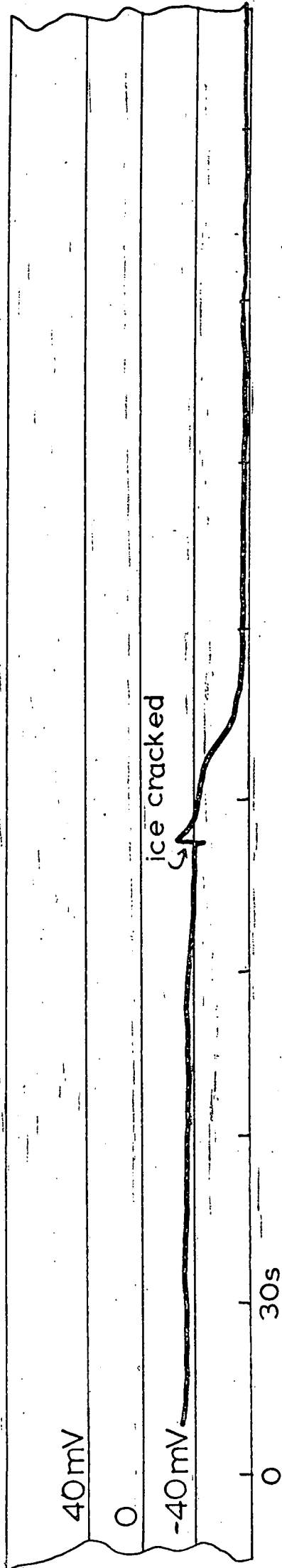
Fig. VII.9.



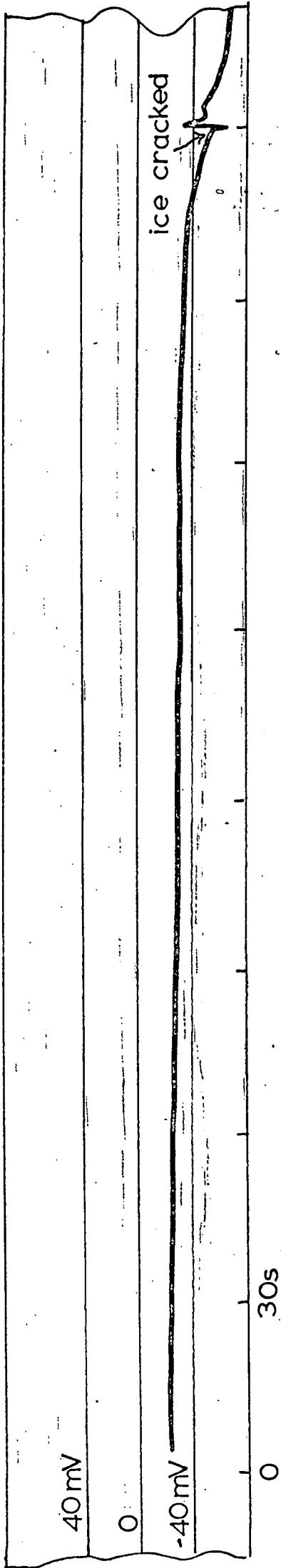
Run no.1.



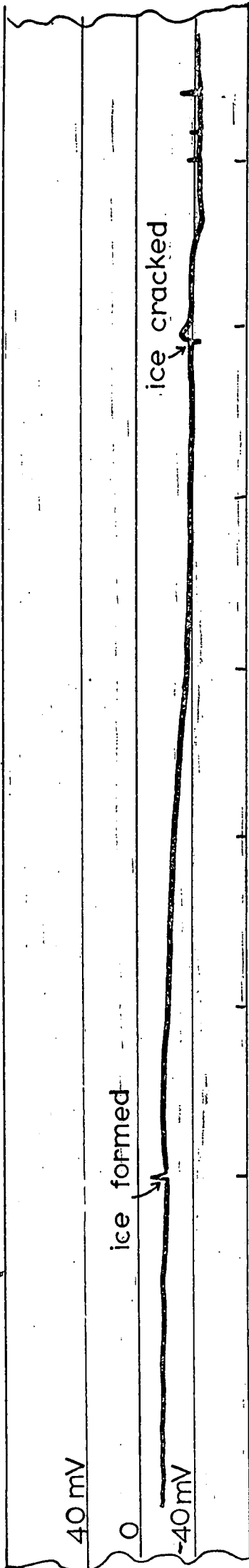
Run no.2.



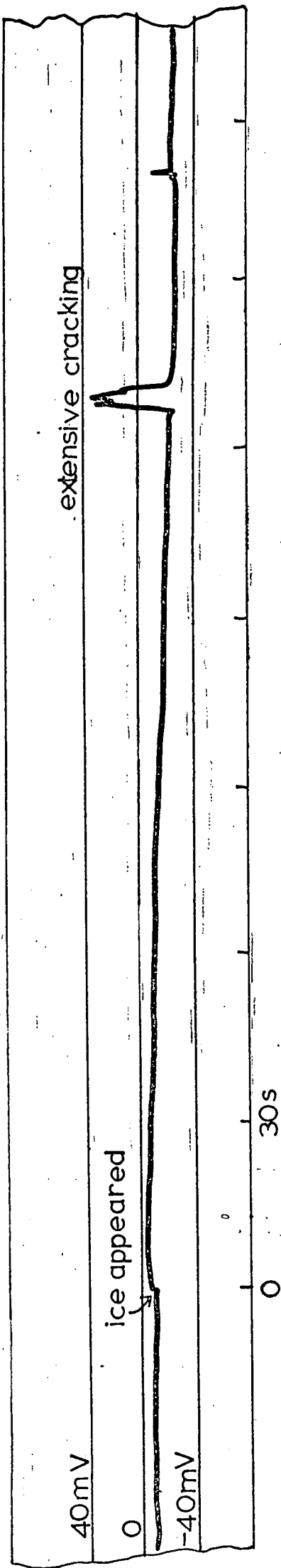
Run no.3.



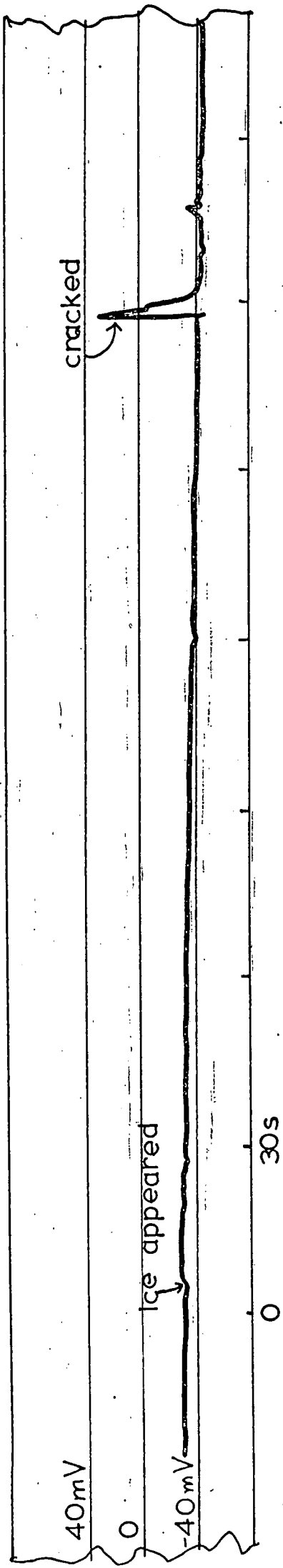
Run no.4.



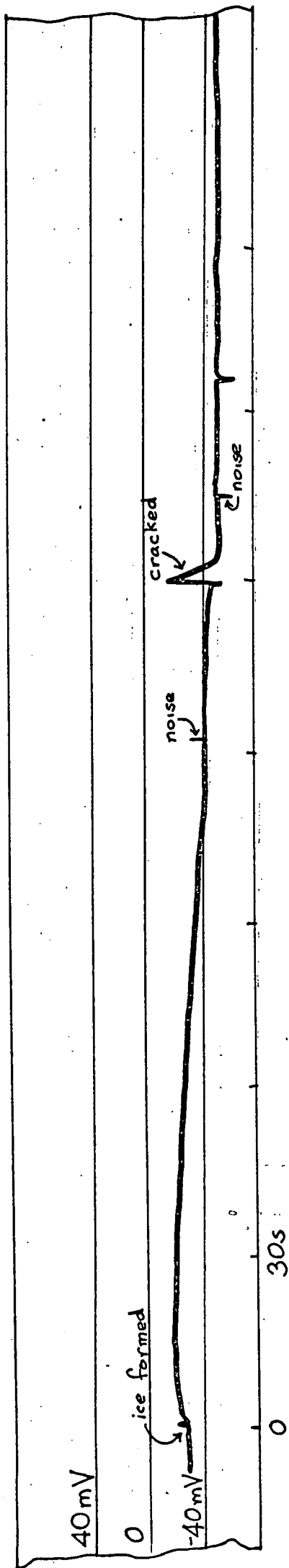
Run no.5.



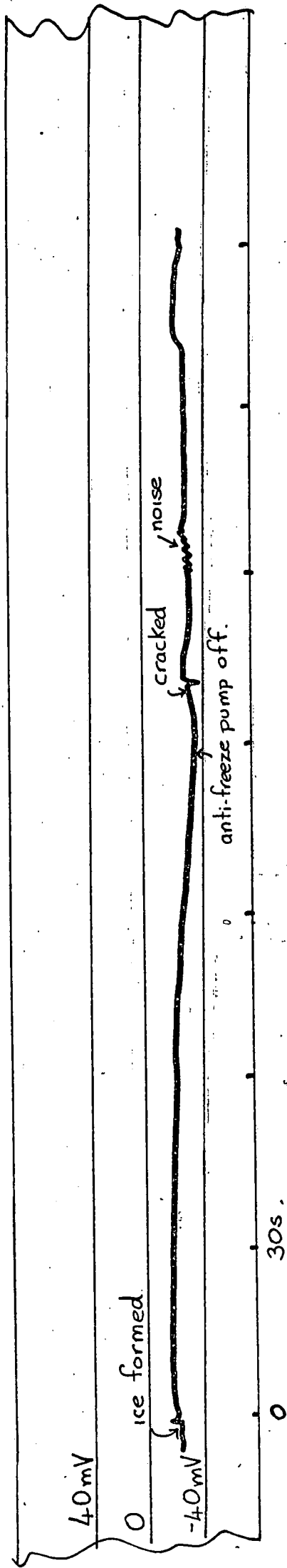
Run no. 6.



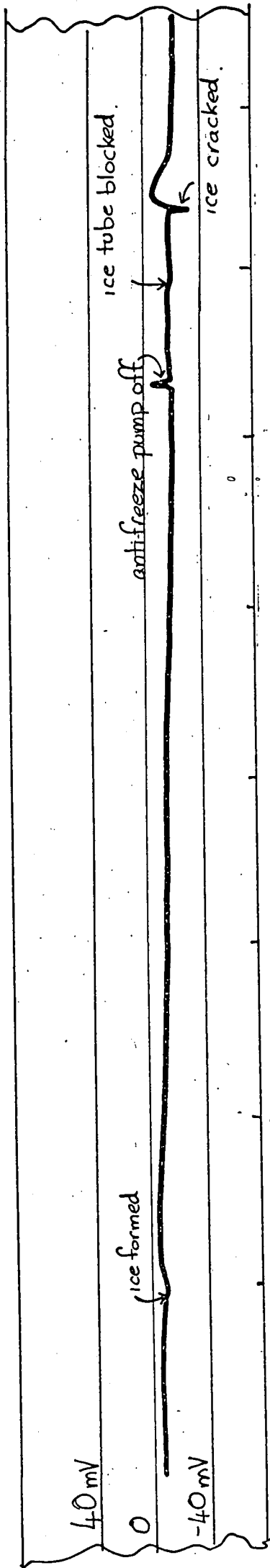
Run no.7.



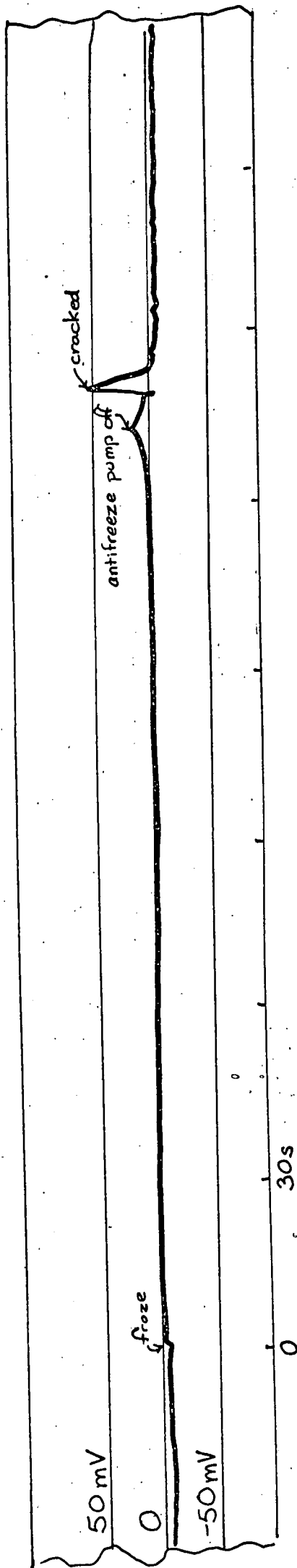
Run no.8.



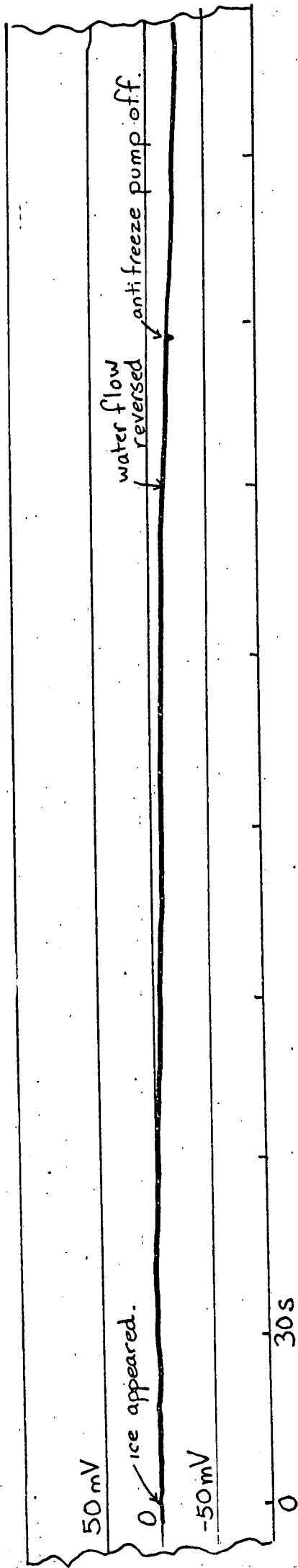
Run no. 9.



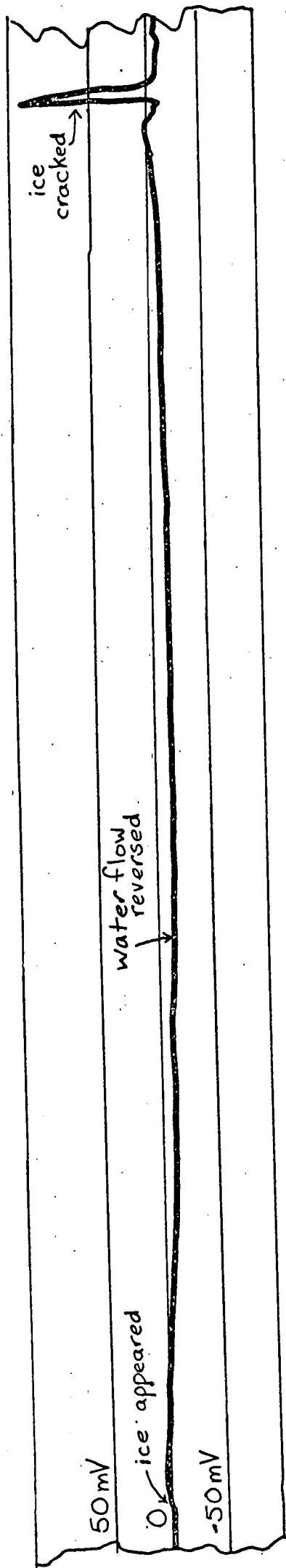
Run no.10.



Run no.11.



Run no.12.



Run no .13.

Nevertheless, sufficient results have been obtained to show definite trends, even if they cannot give statistical proof, and it appears to be unlikely that much more information could have been obtained from additional runs.

VII. 2(c) The graphs of voltage against time for the freezing tube. (See Fig. VII.9.)

The initial, small peak, which coincides with the appearance of ice in the tube, shows all the characteristics exhibited by the typical freezing potential graphs. With one exception, in Fig. VII .9 (1), the upper electrode always registered a positive potential, regardless of the direction of flow of the water through the tube. However, Run (1) was notable in that the ice shell, which formed initially from supercooled water near the walls of the tube, melted completely before re-appearing again. These voltage peaks were measured without having electrodes touching the ice directly and the water between the ice and the electrodes must have been behaving as a conductor. In view of the sign of the electrification, it appears as though, initially, the ice may be considered to be mainly connected to the lower, earthed electrode. It might be expected that this effect would be particularly marked in the cases where the warm water entered through the upper electrode, as in Runs (11 to 13) and Fig. VII.9(11 to 13), and in which the freezing took place nearer the lower electrode, but this does not seem to be the case. However, failure to observe such a difference in only three readings is hardly significant when one bears in mind the irreproducibility of freezing potentials.

It can also be seen that the sign of the initial potential was always opposite to that of the standing potential present before the start of a run; but as the standing potentials were nearly always negative and the freezing potentials were usually positive, both in the measurements taken with the glove box and outside, this may be a coincidence. On the rare occasions that standing potentials were present in the freezing cells they did not affect the sign of the charge separation produced by freezing.

The characteristic increase in potential when the hole through the ice tube becomes very narrow does appear to depend on the direction of flow of the water. However, since these potentials usually persist after the hole becomes completely blocked with ice, they must be due to a charge separation process not involving the movement of water through an ice tube. It is possible to explain these potentials in terms of both the Temperature Gradient Theory and the charge separated on freezing. All that can be said with certainty, is that the electrode nearer the end of the tube towards which the water had been flowing registered a negative potential.

The differences between the electrification produced by cracks appearing in the ice tube when it was shunted with a $10^8 \Omega$ resistor and when it was not shunted suggested that the electrification was a consequence of physically separating the ice surfaces while a charge separation mechanism was operating. It is perhaps significant that in Fig. VII.4, where there is no general trend in

the potential difference, the cracks produced electrification of either sign, showing that perhaps two opposing charge separating mechanisms had been operating.

It is possible that this explanation might also apply to the production and release of air bubbles in the perspex tube experiments. (See Chapter V). If the air bubbles were responsible for removing a leakage path across an interface when they were produced, this would allow a build-up of voltage. When the air bubble broke away from the surface, the leakage path would be restored and the voltage would return to its previous value. The sign of these voltage peaks would be determined by the charge separating process which was operating in the tube and hence the change in the sign of the peaks on removing the coolant from around the tube. Since no details are known of the freezing rates in this apparatus it is not possible to say with certainty which charge separating mechanism was operating at any one time.

VII. 3. Conclusions.

It appears that the results obtainable with the freezing tube are no more reproducible than were the results obtained with the freezing cell and their interpretation is considerably more difficult. An insufficient number of runs has been carried out to draw any statistical conclusions, but a subjective examination of the recorder traces leads to the conclusions that the Workman and Reynolds effect is definitely observable at the start of a run and

that freezing potentials can be transmitted through water over quite large distances.

In the later stages of a freezing run the freezing potentials as measured by the electrodes in the water may change sign, particularly as the ice becomes very thick and increases the resistance between the electrodes *asymmetrically* so that what may have become a low resistance path from the interface to an electrode becomes a high resistance path. It is certain that there are temperature gradients both along and *across* the ice tubes and some of ~~the~~ electrical effects may be explicable in terms of these, particularly in view of the freezing rates involved. (See section VI.4(c).)

While it was not possible to measure freezing rates directly owing to the apparent magnification of the ice tube when viewed through an anti-freeze solution, they were certainly lower than those in the unstirred Workman and Reynolds type experiments described in Chapter VI.

No electrification which could be solely and directly attributed to the movement of water over ice has been detected. A possible explanation for the lack of an electrokinetic effect is put forward below.

The Workman and Reynolds Effect is explained by the selective incorporation of ions into the ice. It might be expected that when freezing was stopped the frozen-in space-charge of ions would maintain the potential difference between ice and water, but protons flow across the interface to neutralise the space-charge

and the double layer of ions at the interface disperses. However, we have already seen in Chapter III that electrokinetic effects depend upon the existence of an electric double layer at the interface; but since the double layer will only be present while freezing is progressing, electrokinetic effects will only be detectable when water is freezing. Under these conditions, it will be almost impossible to separate the electrokinetic potential from the freezing potential but, from the point of view of the electrification of clouds, the separation of these processes is unlikely to be of importance.

The existence of an electric double layer not involving the presence of impurity ions but simply arising out of absorption of water molecules at the ice/water interface is also unlikely. In order that molecules can be absorbed, they must become orientated to enable them to be electrostatically bound to the ice phase, but once they have become orientated in this way, they will be indistinguishable from the other molecules in the bulk of the ice phase. In this respect they will be different from water molecules absorbed onto a glass surface.

The conclusions from the freezing tube experiments, together with those from the freezing cell experiments, are summarised in Chapter VIII and possible applications of the results to cloud phenomena are discussed.

CHAPTER VIII

CONCLUSIONS AND POSSIBLE APPLICATIONS TO CLOUD PHENOMENA.

VIII.1. Conclusions which can be drawn from the Freezing Experiments.

The conclusions which can be drawn from the experiments with the freezing cells and freezing tubes may be summarised as follows.

- (i) Freezing potentials are greater than the corresponding temperature gradient potentials for freezing rates in the range 10^{-5} to $4 \times 10^{-5} \text{ m s}^{-1}$, for de-mineralised water with a conductivity of $1.5 \times 10^{-4} \Omega^{-1} \text{ m}^{-1}$.
- (ii) Changing the amount of air bubbles in the ice/water interface can change the freezing potentials by altering the interfacial resistance. The temperature gradient potentials will be less affected by the amount of air in the sample.
- (iii) The freezing potentials are somewhat dependent on the freezing rate. But since the freezing potential is, at any one time, a function of the charge separation rate, of the charge neutralisation rate and of the temperature gradient, it is not directly proportional to the freezing rate.

- (iv) Freezing potentials measured in very dilute solutions are not exactly reproducible.
- (v) Freezing potentials have been observed when both electrodes are in contact only with water.
- (vii) On freezing, de-mineralised water always becomes positively charged with respect to ice, provided that the Workman and Reynolds Effect predominates over the Temperature Gradient Effect.
- (viii) There is no direct evidence to suggest that charge can be separated by water flowing over ice, in the absence of any other form of charge separation.

In the light of these findings, certain other suggestions and explanations may be put forward.

Although only a relatively small range of freezing rates was studied in the freezing cell measurements described in Chapter VI, the work of Gill (1953), Gross (1965) and Pruppacher et al. (1968) shows that Conclusion (i) is applicable over a wide range of freezing rate. However, it will only be valid if the ions present in the solution are such that the freezing potentials which would have been recorded are not very small; otherwise, they would be less than the temperature gradient potentials, which may be regarded as being independent of impurities.

Conclusion (iv) is that the freezing potentials are not exactly reproducible. While this is true, many of the factors involved have been qualitatively characterised and it seems likely

that more reproducible results could be obtained from runs made under vacuum, with very small quantities of water to reduce convection, and quite high, and exactly reproducible, freezing rates, e.g. spontaneous freezing of supercooled solutions, initiated at precisely controlled temperatures. Nevertheless, Fig. VI.10 demonstrates that they can be reproduced to within an order of magnitude to each other.

Conclusion (vii), that water always becomes positively charged with respect to ice when the Workman and Reynolds Effect predominates, only applies to the samples of water used in the experiments. It was generally true for all the samples of demineralised water obtainable on the Durham University Science Site and it was also true for similar samples of distilled water and for Durham tap-water; but in all cases a likely contaminant would be sodium chloride, or at any rate the chloride anion. Workman and Reynolds (1950) and subsequent workers report that water becomes positively charged on freezing when sodium chloride is present in association with most cations. This is not to say that the presence of additional and different ions would not change the sign of the charge separation but their effect was not investigated in these experiments since they have been fully characterised by other workers. On one occasion only was a drop of ammonia solution added to a sample of de-mineralised water in a brass freezing cell. The amount of ammonia added was sufficient to make the molarity of the solution about 10^{-2} , but the addition of this amount of ammonia

did not change the sign of the freezing potential. It may have been that all the ammonia was not in a form suitable for incorporation into the ice lattice, because the solution developed a slightly blue caste, which is characteristic of solutions of a suprammonium complex-ion.

VIII. 2. Possible Applications of the Results to Cloud Electrification Phenomena.

Great care must be exercised in applying the conclusions of experiments on bulk ice and water to conditions in clouds. It is, perhaps, more reasonable to expect the results to apply to the results of laboratory experiments designed to simulate such conditions and the reader of this thesis will be left to form his own judgement of how far individual laboratory simulations can be applied to clouds.

VIII.2(a) The electrification of simulated hailstones.

Let us first consider the case of a simulated hailstone moving at a speed equal to the free-fall value relative to the surrounding air. When the hailstone is accreting small supercooled water droplets to give a rimed ice surface, the droplets which collide with the hailstone will be freezing spontaneously. According to Pruppacher (1967), the rate at which ice crystals will grow in the impinging droplets is of the order of tens of millimetres per second. Therefore, from Conclusion (i), we should expect the Workman and Reynolds Effect to predominate. However, the hailstone will not acquire a net charge until some of the ice or water in the

freezing droplet becomes detached. Latham and Mason (1961B) report that ice splinters are likely to be ejected under such conditions. If the droplets were composed of de-mineralised water of the type available in Durham, we should expect the hailstone to become positively charged and that the splinters will carry away negative charge. Rogers (1967), in experiments with ice-spheres of 15 mm diameter, supported on an air jet, observed that the ice-spheres became positively charged on accreting droplets whose temperature was below -12°C . This agrees well with the predicted sign of charge separation. However, when these simulated hailstones were accreting droplets whose temperature was above -12°C , they became negatively charged. Rogers attributed the negative charging to the splashing off of small positively charged water droplets produced by the shattering of freezing droplets on the hailstone surface. Although no details of the accretion rates are given by Rogers to confirm this proposal, the work of Latham and Mason (1961B) suggests that splinter production continues at a constant rate until the droplet temperature rises to -6°C . Therefore, it might be more realistic to consider that this change in sign is attributable to a change in the mechanism of charge separation at higher temperatures. At higher temperatures, the Temperature Gradient Mechanism may predominate and under the influence of this effect we should expect the ice splinters to be positively charged, leaving the hailstone with a net negative charge, as found in practice at temperatures between -10 and -7°C .

Because the water droplets used by Rogers were those naturally present in the air stream and probably not of a high degree of purity, the agreement found between the predicted charge separation and the experimental results is probably fortuitous. However, it is likely that the results of workers using the same solutions as those used in the experiments described in Chapters VI and VII should be explicable in terms of the results obtained in these experiments. Church (1966), Stott and Hutchinson (1965), Evans and Hutchinson (1963) conducted their research in Durham and used water samples from the same sources as those used in the freezing tube and freezing cells. The water used by other workers may have contained different impurities and the sign of the freezing potentials, which would have been obtained in their samples, is uncertain.

Church (1966) investigated the charge acquired by an ice-coated rod when it was whirled through a stream of supercooled water droplets with diameters in the range 50 to 150 μm . The surface of the rod became rippled and glassy and small droplets were flung off. Under these conditions the rod became negatively charged when the droplets were below 0 $^{\circ}\text{C}$. (See Fig.IV.2.) He suggested that the Workman and Reynolds Effect was responsible for the observed charge separation and his results agree with the results which would have been predicted from the freezing cell experiments. He was unable to explain the reduction in negative charging at low temperatures, although the production of spongy ice or the ejec-

tion of ice splinters may be responsible. Church also noted that the net charge separated was a maximum at a temperature of -3°C and that the rod became positively charged when the droplets were at temperatures above $+2^{\circ}\text{C}$. It is possible that this last observation can be explained in terms of the Temperature Gradient Effect which was measured in Section VI. 4(c). When a warm droplet collides with the cold rod, it will freeze much more slowly than the supercooled droplets would have done, particularly since the warm water will be running over the ice surface in the way that warm water runs over the ice surface in the freezing cells when the stirrer is operated. Therefore, the Temperature Gradient Mechanism will predominate and, since the rod is below 0°C while its iced surface is at 0°C , the ice/water interface will be negatively charged with respect to the core of the rod. Some of this negative charge will be carried off by splashing droplets, leaving the rod with a positive charge.

The results of Evans and Hutchinson (1963) and Stott and Hutchinson (1965), who also used water from the Durham Science Site, can be explained qualitatively in terms of the Workman and Reynolds Effect. Their results indicated that the water in their single drop experiments became positively charged with respect to the ice, during freezing.

Kachurin and Bekryaev (1960) noted that ice became negatively charged with respect to water, whereas the results of Mason and Maybank (1960) suggested that the charge separation is,

perhaps, in the opposite direction. This conclusion is only valid if it is assumed that the major residues contain more water than ice and the minor residues consist mainly of ice. Workman and Reynolds(1953) dropped water onto a cold hailstone and, apparently, obtained charge separations in either direction, depending on the impurities present in the water.

Another experiment on the electrification of accreting hail pellets was performed by Latham and Mason (1961B). They were endeavouring to investigate the charging associated with the growth of soft hail pellets by measuring the electrification of an artificial hailstone which was collecting supercooled water droplets. Latham and Mason report that the freezing of droplets on the surface of the hailstone caused it to become negatively charged and was accompanied by the ejection of small ice splinters. The charge separated was proportional to the rate of splinter production, which is what one might expect if the charge is being separated by the Temperature Gradient Effect, but, equally, it is one would expect if it was being separated by the Workman and Reynolds Effect. The sign of the charge separation is opposite to what would be predicted from my freezing experiments with distilled water in Durham, but the same as that found by Workman and Reynolds for distilled water in New Mexico. Since the work of Latham and Mason and Mason and Maybank was carried out using samples of distilled water, probably from the same source, in the atmosphere of a large industrial city, it is likely to contain ammonia, and, therefore, it

would be expected to give a charge separation such that the water became negative with respect to the ice, on rapid freezing. Therefore, the sign of the charge separation alone is not diagnostic of a temperature-gradient-directed separation of charge. However, Latham and Mason heated the hailstone with radiation from a tungsten lamp and noted that the charge separation rate fell. Unfortunately, this too is not conclusive proof of a charge separation mechanism governed by temperature gradients as we have already seen that the Workman and Reynolds potentials are a function of the freezing rate, which must itself be governed to a certain extent by the temperature difference. In fact, the freezing rates in these experiments would be more likely to favour the Workman and Reynolds Effect, rather than the Temperature Gradient Effect, as the main charge separation process. Latham and Mason also noted that the artificial hailstone became positively charged for high air stream velocities past the hailstone. This they attributed to the throwing off of water droplets from drops which shattered on impact. This observation too is consistent with a charge separation mechanism operating on freezing. However, in this case it may be either the Workman and Reynolds Effect or the Temperature Gradient Effect, because the water is moving relative to the ice, which can reduce the freezing rate, as mentioned earlier.

Unfortunately, it is not possible to explain these results quantitatively in terms of the Workman and Reynolds Effect, because the freezing potentials which would have been produced in the freezing cell by their samples of water are not known. The charge which would

be separated on freezing a solution at a rate of 10^{-5} m s^{-1} , which produced a freezing potential of 1 V in the freezing cell described in Chapter VI corresponds to a charge separation of about $2 \times 10^{-8} \text{ C}$ per ml of solution frozen. This is more than adequate to explain the electrical effects described above, and, if anything, this represents an under-estimate of the charge separated in the freezing cell measurements. The charge which can be separated by water flowing over an ice surface in the freezing tube is three to four orders of magnitude less than this, which corresponds well with many of the measurements of the charge separated when water droplets are splashing off an ice surface. Clearly, it is essential that further measurements are made to compare directly the results obtained on the bulk freezing of ice and water, and the freezing of supercooled droplets on a simulated hailstone.

The charge separation processes involving the presence of both small ice particles and supercooled water droplets are much more difficult to interpret from measurements of bulk electrification of ice and water, and, until a detailed model of the processes occurring is produced, any explanations must be based on speculations without adequate scientific backing. Therefore, at the present time, it is unrealistic to attempt to explain the results of Reynolds, Brook and Gourley (1957) and Magono and Takahashi (1963) in terms of the results obtained in Chapters VI and VII.

VIII.2(b) The charge separated on melting.

In Section VI. 4(c), the effect of stirring the freezing

solutions was described. It was noted that Temperature Gradient Effects persisted when melting of the ice surface was occurring. This may be significant in the electrification of melting hail. If a large, cold hailstone falls into an area of a cloud below the 0°C isotherm, its outer surface will become warmed and begin to melt. If droplets are flung off its surface while the core of the hailstone is still below 0°C , they will carry away net negative charge leaving the hailstone with a positive charge. The relative efficiency of this proposed mechanism of charge separation compared with that of the Dinger and Gunn Effect will depend on the heat capacity of the hailstone and the melting rate. The charge separation noted by Rogers (1967) was opposite to this and it is possible that hailstones of the size used by Rogers were warmed completely to 0°C before droplets were flung off. Alternatively the Dinger and Gunn Effect, which charges the melt-water relative to the air, was predominating. Clearly, further laboratory work is required on the electrification of melting hail.

VII. 3. The Electrification of Melting Snow on the Ground.

In this case, both the Temperature Gradient Effect and the Dinger and Gunn Effect will be acting in the same direction and it is possible that both were contributing to the electrification over rapidly melting snow detected by Bent and Hutchinson (1965). In view of the unusual atmospheric conditions prevailing

at the time of their measurements, there is, perhaps, scope for a laboratory experiment to simulate the conditions to examine the relative contributions of the two effects.

These conclusions show the limits to which the results described in Chapter VI and Chapter VII may be applied. In order that more detailed predictions of the electrification processes in clouds may be made, further experiments will be necessary. Some suggestions for possible experiments are put forward in Chapter IX.

CHAPTER IX.

Suggestions for Further Work

The irreproducibility of the freezing potentials, described in Chapter VI, shows that conditions within the ice/water interface could be profitably investigated. The effect on the freezing potentials of various hydrogen bonding solutes, e.g. alcohols and amines, might allow further conclusions to be drawn on the charge separation mechanisms. Such work is more in the province of the physical chemistry of solvent systems and could probably be investigated more profitably in a physical chemistry laboratory. However, the results might allow quantitative prediction of the freezing potentials which might be obtained with a given solution.

Because no attempt has been made to simulate conditions which are known to exist in clouds, the results of the experiments described in Chapters V to VII should not be applied directly to cloud phenomena. Consequently, it would be of little use to propose experiments to investigate particular aspects of cloud electrification. However, the results cause some doubt on the validity of some of the explanations for electrification of ice and water in experiments designed specifically to simulate conditions in clouds, and so it is in the field of simulations that further experiments need to be done. The electrification of an ice-sphere, accreting water droplets whose temperatures

vary over a wide range, should be investigated in association with measurements of the freezing potentials of the bulk water sample from which the droplets are to be produced. It appears that the accretion rates, the freezing rates, the ice-sphere temperature and the configuration of the air-flow around the sphere may be of importance in determining the electrification of the sphere and, if possible, their effect on the net charge separated should be examined so that the relative contributions of the Workman and Reynolds Effect and the Temperature Gradient Effect to the electrification can be estimated.

A laboratory investigation of the contribution of temperature gradients to the electrification on melting of hail and the electrification of falling and lying snow might also lead to a fuller understanding of the problems posed by the discrepancies between the field and laboratory measurements of MacCready and Proudfit (1965), and to a quantitative explanation of the electrical effect over a rapidly melting snow surface which was observed by Bent and Hutchinson (1965).

Since any electrical charge separation directly attributable to the motion of water over an ice surface appears to be small compared to the charge separated by the Workman and Reynolds Effect and the Temperature Gradient Effect, it does not look as though this process will be of importance in separating electric charge in clouds. Therefore, there should be no need to investigate such an effect further in this context.

The results of the experiments into the electrification of ice and water show the need for water of a high degree of purity as a starting point for all electrification experiments with ice and water. It is recommended that the water should be distilled from a permanganate solution, that it should be de-ionised through new cationic and anionic ion-exchange resins and then passed through a "mixed-bed" resin before use. If necessary it should then be re-distilled in a pyrex, or a metallic, still and its conductivity and pH checked and recorded before use.

APPENDIX 1.

The Vibrating-reed Electrometer.

The ECKO vibrating-reed electrometer, type N616 B, is intended primarily for the measurement of very small currents in the range 10^{-8} to 10^{-16} amps from ionisation chambers but it may also be used for measuring currents and voltages from other sources.

The instrument comprises an electrometer head unit and an indicator unit coupled together by cables. The sealed and desiccated head unit contains three input resistors with a push button selector switch, a vibrating reed type dynamic capacitor and an A.C. amplifier with a cathode follower. The indicator unit houses the remainder of the electronics and controls.

The input current is passed through a known resistor, when the selector switch is in the "Ion Chamber" position, or is allowed to build up a charge on the capacitor, when the selector switch is in the "Voltage" position. The instrument then measures the voltage across either the resistor or the capacitor. The voltage is applied to the modulator, the capacity of which is changed cyclically at a frequency of approximately 450 hz, thus producing an A.C. signal proportional to the D.C. voltage across the capacitor. The A.C. voltage is amplified and rectified, the resultant D.C. voltage being sufficient to drive a meter and recorders. Overall feedback is provided to give gain stability.

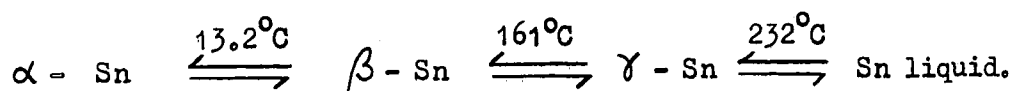
For the experiments described in this thesis the source impedance was less than 10 times the biggest input resistor and, therefore, the "Voltage" range was used. Any one of the three input resistors, 10^8 , 10^{10} or $10^{12} \Omega$ could be connected between the input and earth to shunt the applied voltage, or the Open Circuit push button on the head unit could be selected in which the shunting resistor was the leakage resistance of the unit to earth; under ideal conditions this should be around $10^{15} \Omega$.

The normal maximum full-scale deflection is for an input of 1 V but the meter can be switched to read a full-scale deflection of 300, 100, 30, 10 or 3 mV. With this "Range" switch in the "Check" position, voltages up to 3V can be measured and if a "back off" voltage is applied to the calibration socket on the front, voltages of up to 100 V can be measured.

APPENDIX 2.

The Effect of Low Temperatures on Solder.

Soft solder is an alloy of tin and lead in the proportions 33% tin and 67% lead. However, tin has three crystalline modifications. α - Tin is a non-metallic, low density form with a diamond structure. β - Tin and γ - tin are both metallic forms with close-packed arrangements of the atoms. The transitions are:-



Clearly, the most stable form of tin below 13°C is the non-metallic α - tin. However, the rate of transition of β - tin to α - tin is very slow at temperatures above 0°C , and as temperature falls, so the rate of transition increases. Therefore, at low temperatures, even well-soldered joints will become dry and brittle.

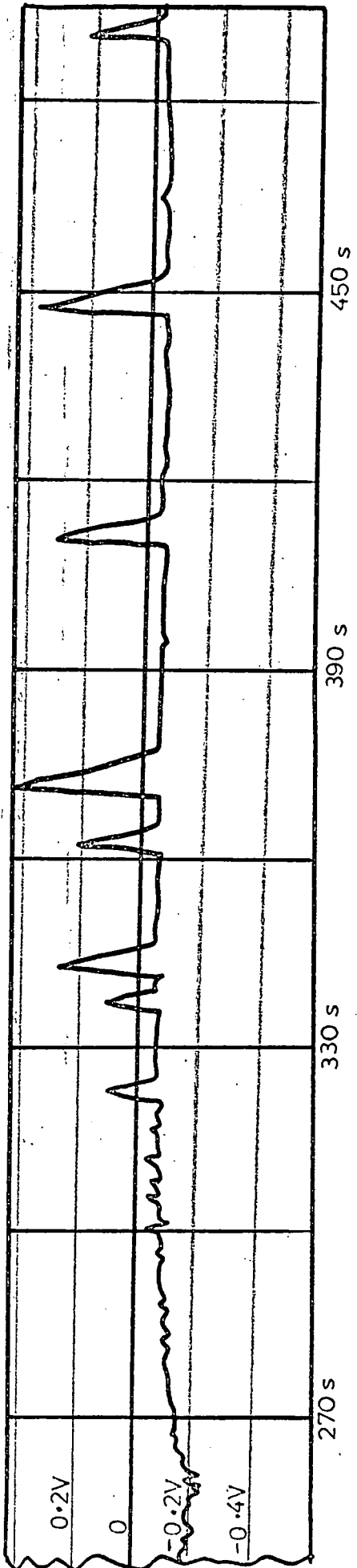
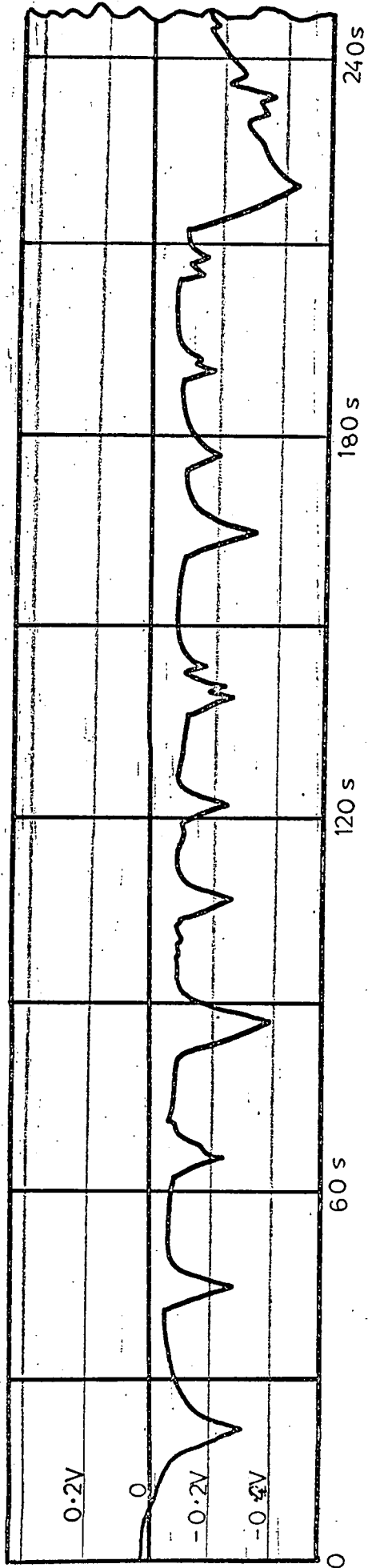
In order to ensure good electrical and mechanical joints at low temperatures, silver solder, which contains no tin, has been used throughout in the construction of the apparatus described in this thesis.

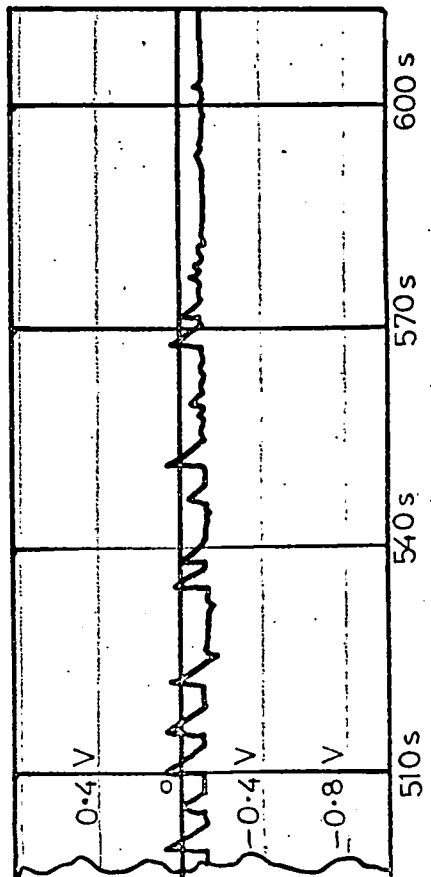
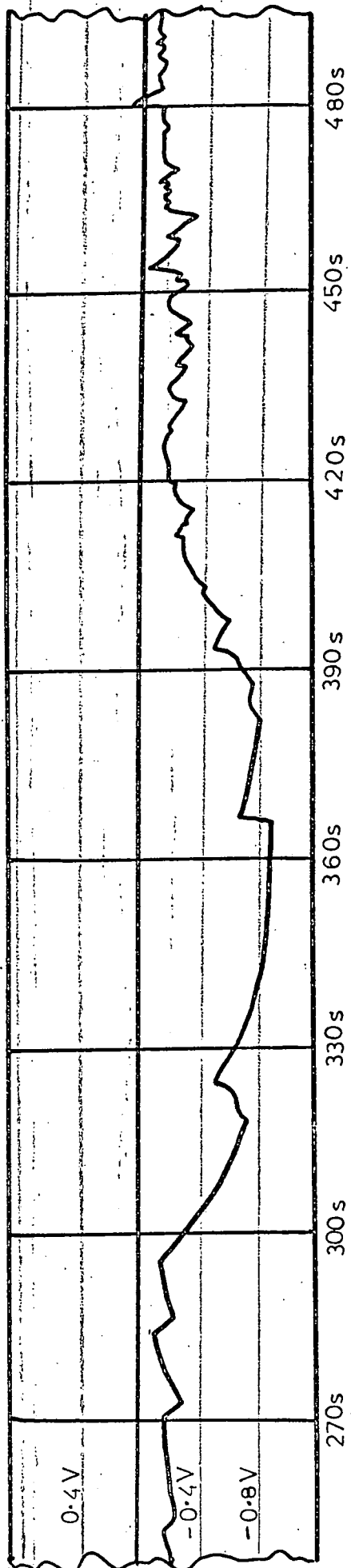
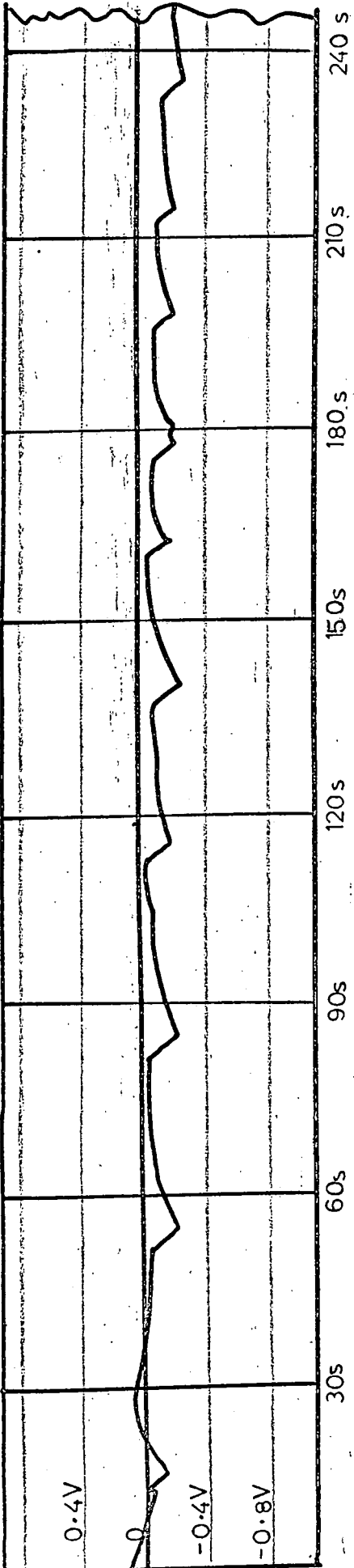
APPENDIX 3.

The Results of the Perspex Tube Experiments.

The graphs of voltage against time for the perspex tube experiments described in Chapter V. Section V. 3(b).

The electrometer input was not shunted and the voltages were measured between the ends of the tube using matched, brass electrodes. The same sample of de-mineralised water was used in all cases. A recorder speed of 10^{-3} m s^{-1} was used.





APPENDIX 4.

The Results of the Freezing Cell Experiments.

The graphs of voltage against time for the freezing cell experiments described in Chapter VI. Section VI.4(b).

The electrometer input was shunted with a $10^{10} \Omega$ resistor with the selector switch in the "Voltage" position. The same sample of de-mineralised distilled water was used for all the runs. A recorder speed of 10^{-3} m s^{-1} was used.

Initial Conductivity of Solution

$$= 1.555 \times 10^{-4} \Omega^{-1} \text{m}^{-1}$$

pH of solution

$$= 5.8$$

at 10.15 hrs B.S.T. on 25/2/69.

Run (1).

Time of starting = 13.58 hrs B.S.T. 25/2/69.

Time. (s)	Ice thickness (mm)	Freezing rate ($\mu\text{m s}^{-1}$)	Anti-freeze Temperature. ($^{\circ}\text{C}$)	Potential Difference. (V)
0	0		-16.3	
22.0	0.59			0.18
26.8	0.72	35.6		0.19
31.0	0.91		-19.5	0.19
39.8	1.19	28.8	-20.0	0.20
49.4	1.44		-20.1	0.20
61.2	1.76	27.3	-20.2	0.22
68.1	1.95		-20.2	0.22
81.0	2.20	24.5	-20.3	0.24
89.7	2.48		-20.3	0.26
102.0	2.75	21.2	-20.4	0.28
114.2	2.99		-20.4	0.26
127.9	3.24	20.9	-20.2	0.20
138.1	3.49		-20.2	0.20
154.3	3.74	19.3	-20.1	0.21
164.0	3.99		-20.1	0.22
		on stirring		-0.10

Run (2).

Time of starting = 14.16 hrs B.S.T. 25/2/69.

Time	Ice thickness.	Freezing rate.	Anti-freeze temperature	Potential Difference.
(s)	(mm)	($\mu\text{m s}^{-1}$)	($^{\circ}\text{C}$)	(V)
0	0			
39.0	0.59			0.19
44.0	0.72	23.7		0.18
52.5	0.91			0.18
59.6	1.19	23.8		0.21
74.8	1.44		-19.0	0.26
87.0	1.76	21.4	-19.0	0.32
98.6	1.95		-19.0	0.37
111	2.20	22.6	-19.0	0.39
122	2.48		-18.7	0.40
140	2.75	17.7	-18.9	0.41
150.8	2.99		-18.5	0.39
172.2	3.24	13.1	-18.4	0.40
189	3.49		-18.4	0.35
206.5	3.74	16.9	-18.3	0.30
218	3.99		-18.3	0.23
		on stirring		-0.08

Run (3).

Time of starting =

on 25/2/69,

Time (s)	Ice thickness (mm)	Freezing Rate ($\mu\text{m s}^{-1}$)	Anti-freeze Temperature ($^{\circ}\text{C}$)	Potential Difference. (V)
0	0		-16.0	
31	0.59			0.35
34	0.72	32.0		0.40
41	0.91			0.33
51	1.19	20.0	-18.3	0.24
67.5	1.44		-18.3	0.28
81	1.76	21.9	-18.4	0.41
90.8	1.95		-18.3	0.42
106.9	2.20	18.2	-18.3	0.43
120	2.48		-18.3	0.53
136.7	2.75	17.0	-18.2	0.58
152	2.99		-18.2	0.57
168.0	3.24	16.7	-18.1	0.58
182.0	3.49		-18.0	0.52
201	3.74	11.0	-17.8	0.50
227	3.99		-17.7	0.42
		on stirring		-0.075

Run (4).

Time of starting = 15.17 hrs B.S.T. 25/2/69.

Time (s)	Ice thickness (mm)	Freezing. rate ($\mu\text{m s}^{-1}$)	Anti-freeze temperature. ($^{\circ}\text{C}$)	Potential Difference. (V)
0	0		-17.0	
16.0	0.59			0.50
21	0.72	26.2	-18.0	0.8 +
28.2	0.91			0.8 +
36.0	1.19	24.3		0.8 +
50	1.44			0.70
61	1.76	24.3	-18.1	0.8 +
71	1.95		-18.2	0.78
84.0	2.20	18.9	-18.1	0.8 +
99	2.48		-18.0	0.70
114	2.75	17.0	-18.0	0.70
129	2.99		-17.9	0.60
147	3.24	14.7	-17.8	0.60
163	3.49		-17.7	0.55
184	3.74	13.1	-17.6	0.50
201	3.99		-17.4	0.55
		on stirring		-0.06

Run (5).

Time of starting = 16.38 hrs B.S.T. 25/2/69.

Time (s)	Ice Thickness. (mm)	Freezing Rate. ($\mu\text{m s}^{-1}$)	Anti-Freeze Temperature ($^{\circ}\text{C}$)	Potential difference. (v)
0	0		-16	
24.1	0.59			1.00
28.2	0.72	24.8	-17.4	1.3 +
37	0.91			1.3 +
50	1.19	25.5		1.3 +
57.8	1.44		-18.0	1.3 +
70.0	1.76	23.2		1.3 +
79.8	1.95			1.3 +
94.6	2.20	19.6	-18.4	1.3
106.8	2.48			1.2
122.3	2.75	16.4	-18.3	1.1
137	2.99		-18.2	1.0
154	3.24	17.9	-18.0	0.9
165	3.49		-18.0	0.9
186	3.74	13.6	-17.9	0.8
201.8	3.99		-17.7	0.75
		on stirring		-0.09

Run (6)

Time of starting = 16.53 hrs B.S.T. on 25/2/69.

Time (s)	Ice Thickness (mm)	Freezing Rate. ($\mu\text{m s}^{-1}$)	Anti-freeze Temperature ($^{\circ}\text{C}$)	Potential Difference. (V)
0	0		-15.5	
25	0.59			0.50
28	0.72	26.7	-16.8	1.00
37	0.91			1.00
49	1.19	2.52		0.98
58	1.44		-17.0	0.95
72	1.76	23.1	-17.0	0.70
80.1	1.95		-17.0	0.35
96.9	2.20	20.0	-17.0	0.30
106.6	2.48		-16.8	0.40
124.7	2.75	18.0	-16.7	0.40
135	2.99		-16.6	0.40
155.0	3.24	16.1	-16.5	0.40
166	3.49		-16.4	0.40
188.2	3.74	15.2	-16.3	0.42
199	3.99		-16.3	0.43
		on stirring		-0.065

Run (7).

Time of starting = 17.10 hrs B.S.T. 25/2/69.

Time.	Ice. Thickness	Freezing Rate.	Anti-freeze Temperature.	Potential Difference.
(s)	(mm)	($\mu\text{m s}^{-1}$)	($^{\circ}\text{C}$)	(V)
0	0		-14.5	
38	0.59			0.2
43.0	0.72 [‡]	16.6		0.5
57.3	0.91		-15.2	0.92
65.8	1.19	19.7	-15.3	0.97
84.2	1.44			1.0
96.3	1.76	22.4	-16.2	1.0
107	1.95		-16.2	1.0
125.0	2.20	16.6	-16.0	0.90
139	2.48		-16.0	0.90
157.8	2.75	12.8	-16.0	0.87
178.9	2.99		-15.9	0.85
193.6	3.24	16.8	-15.8	0.80
208.7	3.49		-15.7	0.75
231.9	3.74	11.5	-15.6	0.73
252	3.99		-15.5	0.65
		on stirring		-0.07

[‡] Freezing face completely covered with ice.

Run (8)

Time of starting = 17.28 hrs B.S.T. 25/2/69.

Time (s)	Ice Thickness. (mm)	Freezing Rate. ($\mu\text{m s}^{-1}$)	Anti-freeze Temperature ($^{\circ}\text{C}$)	Potential Difference. (V)
0	0		-13.8	
39	0.59			0.2
42.5	0.72 *	19.6	-15.5	0.5
55.3	0.91		-15.5	0.9
69	1.19	18.7	-15.6	0.9
83.7	1.44		-15.8	0.95
100	1.76	15.8	-15.7	1.0
116	1.91		-15.7	0.9
129.0	2.20	20.2	-15.6	0.9
142.2	2.48		-15.6	0.9
164.9	2.75	13.4	-15.5	0.85
180.4	2.99		-15.4	0.8
203.9	3.24	13.8	-15.3	0.8
216.6	3.49		-15.2	0.75
241.5	3.74	10.5	-15.1	0.7
264.3	3.99		-15.0	0.6
		on stirring		-0.07

* Freezing face completely covered with ice.

Run (9)

Time of starting = 10.20 hrs B.S.T. 26/2/69.

Time. (s)	Ice Thickness. (mm)	Freezing Rate ($\mu\text{m s}^{-1}$)	Anti-freeze Temperature. ($^{\circ}\text{C}$)	Potential Difference. (V)
0	0		-15.5	0.1
24.8	0.59			0.5
32	0.72	26.2		3.8 +
37	0.91			3.8 +
43.9	1.19			3.8 +
	1.44	27.3		3.8 +
64.3	1.75		-20.0	3.8 +
75.1	1.91			3.8 +
87.9	2.20	20.4		3.8 +
	2.48		-20.5	3.8 +
112.4	2.75			3.7
126.0	2.99	17.5	-20.4	3.5
140.3	3.24		-20.2	3.2
154.5	3.49			3.0
172	3.74	11.5	-19.7	3.0
197.8	3.99			3.8
		on stirring		-0.22

Run (10)

Time of starting = 10.40 hrs B.S.T. 26/2/69.

Time.	Ice Thickness.	Freezing Rate.	Anti-freeze Temperature.	Potential Difference.
(s)	(mm)	($\mu\text{m s}^{-1}$)	($^{\circ}\text{C}$)	(V)
0	0		-13.0	
20	0.59			3.2
23	0.72	32.7		2.5
29.8	0.91			1.95
40.1	1.19	28.5		1.10
48.4	1.44		-18.7	0.7
58.9	1.76	28.0		0.85
66.6	1.91		-19.0	0.90
77.3	2.20	26.0		1.0
87	2.48		-18.9	0.9
102	2.75	23.2	-18.7	0.8
109	2.99		-18.4	0.7
124.2	3.24	20.0	-18.3	0.8
134	3.49		-18.2	0.6
152.5	3.74	16.9		0.6
163.5	3.99			1.0
		on stirring		-0.11

Run (11).

Time of starting = 11.00 hrs B.S.T. 26/2/69.

Time.	Ice Thickness.	Freezing Rate.	Anti-freeze Temperature.	Potential Difference.
(s)	(mm)	($\mu\text{m s}^{-1}$)	($^{\circ}\text{C}$)	(V)
0	0		-15	4.2
16	0.59			3.9
19.1	0.72	39.0		3.2
24.2	0.91		-17.5	1.6
36.6	1.19		-17.7	0.9
	1.44	25.5		1.2
54.2	1.76		-18.0	1.2
65	1.91			1.2
76.2	2.20	26.5	-18.1	1.15
85	2.48			1.0
98.2	2.75	20.4	-17.8	1.0
110	2.99			1.0
124.3	3.24	18.5	-17.4	0.8
137	3.49		-17.0	1.0
153.4	3.74	16.7	-16.8	1.0
167	3.99		-17.0	1.0
		on stirring		-0.12

Run (12)

Time of starting = 12.04 hrs B.S.T. 26/2/69.

Time (s)	Ice Thickness (mm)	Freezing Rate. ($\mu\text{m s}^{-1}$)	Anti-freeze Temperature. ($^{\circ}\text{C}$)	Potential Difference. (V)
0	0			
15.5	0.59			5.6
18.0	0.72	35.6		6 +
24.5	0.91		-17.2	4.7
32.5	1.19	27.5		3.4
43.8	1.44			1.8
54.1	1.76	28.7	-18.0	1.2
61.6	1.95		-18.0	1.3
73.6	2.20	24.5	-18.2	1.25
83.2	2.48		-18.5	1.15
97.7	2.75	20.4	-18.5	1.0
108.2	2.99		-18.4	1.0
121.2	3.24	20.3	-18.1	1.0
132.8	3.49		-17.9	1.1
148.	3.74	18.4	-17.5	1.1
160	3.99			
		on stirring		-0.10

Run (13)

Time of starting = 14.10 hrs B.S.T. 26/2/69.

Time. (s)	Ice Thickness. (mm)	Freezing Rate. ($\mu\text{m s}^{-1}$)	Anti-freeze Temperature. ($^{\circ}\text{C}$)	Potential Difference. (V)
0	0		-15.5	
24	0.59			0.20
31	0.72	17.8		0.50
42	0.91		-17.0	4.8
	1.19			4.2
71	1.44	17.7	-17.5	3.6
86.2	1.76			3.35
100.9	1.95		-17.9	2.8
117.3	2.20	15.8	-18.0	2.6
134.4	2.48		-18.0	2.5
150	2.75	13.2	-17.8	2.5
173	2.99			2.5
184.4	3.24	15.7		2.6
204	3.49		-16.6	2.65
227	3.74	11.1	-16.4	2.65
249	3.99		-16.4	2.65
		on stirring		-0.10

Run (14).

Time of starting = 14.23 hrs B.S.T. 26/2/69.

Time	Ice Thickness.	Freezing Rate	Anti-freeze Temperature.	Potential Difference.
(s)	(mm)	($\mu\text{m s}^{-1}$)	($^{\circ}\text{C}$)	(V)
0	0		-14	
27	0.59			0.05
34	0.72	18.4		0.20
44.4	0.91		-16.2	1.70
61.2	1.19	22.6	-16.2	1.50
67.9	1.44		-16.2	1.41
82.5	1.76	19.2	-16.3	1.43
94.4	1.95		-16.4	1.51
109.5	2.20	17.5	-16.4	1.55
124.6	2.48		-16.4	1.60
144.3	2.75	14.3	-16.0	1.60
160.2	2.99		-16.0	1.50
180.1	3.24	13.7	-15.9	1.41
196.8	3.49		-15.7	1.52
220.2	3.74	12.7	-15.5	1.60
236.3	3.99		-15.5	1.65
		on stirring		-0.06

Run (15).

Time of starting = 14.38 hrs B.S.T. 26/2/69.

Time.	Ice Thickness	Freezing Rate.	Anti-freeze Temperature.	Potential Difference.
(s)	(mm)	($\mu\text{m s}^{-1}$)	($^{\circ}\text{C}$)	(V)
0	0		-13.5	
	0.59			0.5
40.8	0.72			0.20
49	0.91	*	-14.5	2.30
60.0	1.19	20.6	-14.5	2.28
74.7	1.44		-14.4	2.20
90.6	1.76	16.2	-14.3	2.10
106.2	1.95		-14.1	2.05
125.3	2.20	12.7	-14.3	2.03
147.8	2.48		-14.2	2.00
164.4	2.75	15.4	-14.2	2.05
181.0	2.99		-14.2	2.20
204.5	3.24	12.5	-14.1	2.20
221.1	3.49		-14.0	2.15
249.0	3.74	9.90	-13.9	2.15
271.6	3.99		-13.9	2.05
		on stirring		-0.05

*- Freezing face completely covered.

Run (16)

Time of starting = 14.51 hrs B.S.T. 26/2/69.

Time.	Ice Thickness.	Freezing Rate.	Anti-freeze Temperature.	Potential Difference.
(s)	(mm)	($\mu\text{m s}^{-1}$)	($^{\circ}\text{C}$)	(V)
0	0		-12.5	
26	0.59			0.20
35	0.72	17.8		0.80
44.0	0.91			1.95
53.1	1.19	23.7	-14.0	1.93
66.3	1.44			1.80
83.2	1.95		-13.6	1.80
94.5	1.95		-13.6	1.81
113.3	2.20	13.1	-13.5	1.90
135	2.48		-13.6	1.90
154.6	2.75	14.5	-13.4	1.82
170.2	2.99		-13.4	1.72
191.7	3.24	12.6	-13.3	1.62
209.8	3.49		-13.2	1.60
235.0	3.74	10.6	-13.2	1.50
257.1	3.99		-13.2	1.50
		on stirring		-0.04

Run (17)

Time of starting = 15.07 hrs B.S.T. 26/2/69.

Time	Ice Thickness.	Freezing Rate	Anti-freeze Temperature.	Potential Difference.
(s)	(mm)	($\mu\text{m s}^{-1}$)	($^{\circ}\text{C}$)	(V)
0	0		-11.5	
35	0.59		-13.0	0.20
40.5	0.72	22.5	-13.0	0.22
49.2	0.91		-12.9	2.0
63.1	1.19	16.2	-13.0	2.25
81.9	1.44		-12.9	2.20
95.2	1.76	16.5	-12.7	2.25
112.8	1.95		-12.6	2.10
132.7	2.20	13.7	-12.6	2.00
151.6	2.48		-12.6	1.98
171.8	2.75	13.7	-12.7	1.90
188.7	2.99			1.85
	3.24		-12.7	1.83
238	3.49	9.7	-12.7	2.00
265.7	3.74		-12.7	2.00
292.0	3.99		-12.7	1.80
		on stirring		-0.03

Run (18).

Time of starting = 14.27 hrs B.S.T. 27/2/69.

Time.	Ice Thickness.	Freezing. Rate	Anti-freeze Temperature.	Potential Difference.
(s)	(mm)	($\mu\text{m s}^{-1}$)	($^{\circ}\text{C}$)	(V)
0	0			
25.2	0.59			1.0
31	0.72	17.2		5.6
43.8	0.91		-9.0	6 +
58.1	1.19	14.1		6 +
81.3	1.44		-9.1	6 +
100.8	1.76		-9.2	5.4
	1.95		-9.3	4.7
139.0	2.20	13.8	-9.3	3.8
156.7	2.48		-9.5	2.6
	2.75		-9.5	2.0
202.2	2.99	10.9	-9.5	1.7
225.0	3.24		-9.5	1.7
249.1	3.49		-9.5	1.6
280.5	3.74	8.9		1.6
305.4	3.99			1.65
		on stirring		0

Run (19)

Time of starting = 14.49 hrs B.S.T. 27/2/69.

Time (s)	Ice Thickness. (mm)	Freezing Rate. ($\mu\text{m s}^{-1}$)	Anti-freeze Temperature. ($^{\circ}\text{C}$)	Potential Difference. (V)
0	0		-9.0	
12.0	0.59			5.2
16.8	0.72	14.2		4.8
34.6	0.91			5.2
45.5	1.19	25.7	-9.6	5.6
56.2	1.44			5.0
73.0	1.76	16.6		4.2
87	1.95			3.4
109.1	2.20			2.75
	2.48			2.2
149.4	2.75	13.5	-9.7	2.1
164	2.99		-9.7	2.1
194	3.24		-9.7	2.0
230	3.49		-9.7	1.95
	3.74	9.6	-9.7	1.90
267	3.99			1.80
		on stirring		-0.005

Run (20)

Time of starting = 15.05 hrs B.S.T. 27/2/69.

Time.	Ice Thickness	Freezing Rate.	Anti-freeze Temperature.	Potential Difference.
(s)	(mm)	($\mu\text{m s}^{-1}$)	($^{\circ}\text{C}$)	(V)
0	0			
18.0	0.59			5.6
21.4	0.72	32.7	-9.3	5.4
27.8	0.91			4.3
42.3	1.19	21.9		2.35
52.0	1.44			2.15
67.7	1.76	21.6	-9.7	1.0
75.8	1.95			0.80
91.4	2.20	17.0	-9.8	0.63
107.0	2.48	1	-9.8	0.60
129.3	2.75	16.5	-9.9	0.61
138	2.99		-9.9	0.62
165.9	3.24	10.0	-10.0	0.63
178.0	3.49		-10.0	0.70
205.0	3.74	11.2	-10.0	0.80
222.7	3.99			0.90
		on stirring		+0.005

Run (21).

Time of starting = 15.40 hrs B.S.T. 27/2/69.

Time. (s)	Ice Thickness. (mm)	Freezing Rate. ($\mu\text{m s}^{-1}$)	Anti-freeze Temperature. ($^{\circ}\text{C}$)	Potential Difference. (V)
0	0			
12.0	0.59			5.4
16.8	0.72	21.3		6.0
27.0	0.91			5.8
39.0	1.19	23.2	-10.1	4.2
49.8	1.44			2.8
69.0	1.76	17.8	-10.0	1.1
78.5	1.95		-10.0	1.1
101.9	2.20	13.1	-10.0	1.05
118	2.40		-10.0	1.1
135.7	2.75	14.8	-10.0	1.15
152.4	2.99		-10.0	1.2
175.4	3.24	12.0	-10.0	1.2
194.0	3.49		-10.0	1.2
215.4	3.77	11.4	-10.0	1.1
237.8	3.99			
		on stirring		0

Final Conductivity of solution = $9.50 \times 10^{-4} \Omega^{-1} \text{m}^{-1}$

pH of solution = 6.8

at 16.05 hrs B.S.T. 27/2/69.

APPENDIX 5.

The Results of the Freezing Tube Experiments.

The graphs of voltage against time for the freezing tube experiments described in Chapter VII. Section VII. 2(c).

The same sample of de-mineralised, distilled water was used for all the runs and it was the same as those used for the freezing cell experiments described in Chapter VI and set out in Appendix 4. A recorder speed of 10^{-3} m s⁻¹ was used.

All the voltages are recorded taking the value of the standing potential across the tube, just before the onset of freezing, as zero. The potential is that of the upper electrode with respect to the lower, earthed electrode. Normally the water flowed in through the lower, earthed female electrode, but, when reversed, it entered the tube through the upper, male electrode. The anti-freeze solution normally entered the cooling jacket through the lower tube.

	Size of initial peak. (mV)	Maximum size of final, broad peak. (mV)	Observations.
Run(1)	-2	-42	initial ice shell appeared to melt completely and was then re-formed
Run(2)	+2	-25	dendrites grew out of the top of the tube when freezing commenced.
Run(3)	0	-40	
Run(4)	0	-30	
Run(5)	+9	-15	dendrites initially grew out of the tube. A characteristic supercooled Workman and Reynolds-type potential-against-time graph was obtained, with a secondary peak minimum of +4 mV.
Run(6)	+5	-11	dendrites grew out of the top of the tube when freezing commenced.

	Size of initial peak (mV)	Maximum size of final, broad peak. (mV)	Observations.
Run(7)	+3	-14	initially dendrites grew out of the tube. The same water flow rate as in Run(6) was used.
Run(8)	+7	-20	initially dendrites grew out of the tube. The same water flow rate as in Run(6) was used.
Run(9)	+6	-10	the same water flow rate as Run(6) was used, but the anti-freeze flow direction was reversed.
Run(10)	+4	-7	water and anti-freeze directions normal, but a very slow freezing rate was used. (Same water flow rate as Run (6)).
Run(11)	+7	+20	direction of the water flow rate was reversed.
Run(12)	+7	-25	direction of water flow rate was initially reversed and finally normal.
Run(13)	+4	0 but going positive.	direction of water flow rate was initially normal and finally reversed.

(See also Fig. VII. 9.)

REFERENCES

- Alty, T. (1924) The cataphoresis of gas bubbles in water. Proc. Roy. Soc. London, Vol.106, page 622.
- Alty, T and Currie, B.W. (1929) Absorption at a water surface. Proc. Roy. Soc. Vol.122, page 622.
- Bent, R.B. and Hutchinson, W.C.A., (1965) Electric space charge over melting snow on the ground. J. Atmos. Terr. Phys. Vol. 27, page 91.
- Bernal, J.D. and Fowler, R.H. (1933) Theory of water and ionic solution, with particular reference to hydrogen and hydroxyl ions. J. Chem. Phys. Vol.1, page 515.
- Bjerrum, N. (1951) K. Danske Vid. Selsk. fys. Medd. Vol. 27, page 56.
- Blanchard, D.C. (1951) A verification of the Balley-Dorsey theory of spicule formation on sleet pellets. J. Met. Vol. 8, page 268.
- Blanchard, D.C. (1955) The supercooling, freezing and melting of giant water-drops at terminal velocity in air. "Artificial Stimulation of Rain", Pergamon Press, page 233.
- Bradley, R.S. (1959) Trans. Faraday Soc. Vol. 53, pt. 5, page 687.
- Braham, R.R. and Byers, H.R. (1949) Thunderstorm structure and circulation. J. Met. Vol. 5, page 71.
- Brook, M. (1958) Laboratory studies of charge separation during ice-ice contact. "Recent Advances in Atmospheric Electricity, " Pergamon Press, page 383.

- Brook, M. (1969) Unpublished communication, Durham University Atmospheric Physics Senior Colloquium, May 1969.
- Browning, K.A. (1968) The organisation of severe local storms. Weather Vol. 23, No. 10, page 429.
- Brownscombe, J.L. and Hallett, J. (1967) Experimental and field studies of precipitation particles formed by the freezing of supercooled water. Quart. J. Royal Met. Soc. Vol. 93, page 455.
- Butler, J.A.V. (c 1932) "Electrocapillarity", Chapter IV.
- Chalmers, J.A. (1965A) "Atmospheric Electricity", 2nd Edition. Pergamon Press.
- Chalmers, J.A. (1965B) The role of melting in atmospheric electricity. Proc. Int. Conf. Cloud Phys., Suppl. Tokyo. Met. Soc. Japan, page 152-156.
- Church, C.R. (1966) Unpublished Durham Ph.D. thesis.
- Costa Ribeiro, J. (1945) Anais. Acad. Bras. Cienc. Vol. 17, page 2.
- Cotton, F.A. and Wilkinson, G. (1962) "Advanced Inorganic Chemistry", 1st Ed. Interscience, J. Wiley and Sons.
- Coulson, C.A. (1961) "Valence", 2nd Ed. Oxford University Press.
- Coulson, C.A. and Danielsson, O. (1954) Ark. Fys. Vol. 8, page 239 and 245.
- Cross, J.D. (1969) Scanning electron microscopy of evaporating ice. Science Vol. 164, page 174.
- Decroly, J.C., Graenicher, H. and Jaccard, C. (1957) Helv. Phys. acta Vol. 30, page 466.

- Dinger, J.E. (1964) Quart. J. Royal Met. Soc. Vol. 90, page 208.
- Dinger, J.E. (1965) Electrification associated with the melting of snow and ice. J. Atmos. Sciences Vol. 22, page 162.
- Dinger, J.E. and Gunn, R. (1946) Electrical effects associated with a change of state of water. Terr. Magn. Atmos. Elect. Vol. 51, page 477.
- Dorsey, N.E. (1948) The freezing of supercooled water. Trans. Amer. Phil. Soc. Vol. 38, page 247.
- Drake, J.C. (1968) Electrification accompanying the melting of ice particles. Quart. J. Royal Met. Soc. Vol. 94, page 176.
- Eigen, M. and De Maeyer, L. (1958) Self-dissociation and protonic charge transfer in water and ice. Proc. Roy. Soc. A. Vol. 247, page 505.
- Evans, D.G. and Hutchinson, W.C.A. (1963) The electrification of freezing water drops and of colliding ice particles. Quart. J. Royal Met. Soc. Vol. 89, page 370.
- Fitzgerald, D.R. (1956) Theoretical and experimental studies of convective cloud electrification. Report contract AF 19 (604), 1552. University of Chicago.
- Fitzgerald, D.R. and Byers, H.R. (1958) Aircraft observations of convective cloud electrification. "Recent Advances in Atmospheric Electricity", Pergamon Press, page 245. J. Atmos. Terr. Phys. Vol. 15, page 254.
- Frank, H.S. (1958) Covalency in the hydrogen bond and the properties of water and ice. Proc. Roy. Soc. A. Vol. 247 page

- Giauque, W.F. and Ashley, M. (1933) Molecular rotation in ice at 10 °K. Free energy of formation and entropy of water. Phys. Rev. Vol. 43, page 81.
- Gierer, A. and Wirtz, K. (1949) Ann. Phys. Lpz. (6) Vol. 6, page 257.
- Glasstone, S. (1962) "Handbook of Physical Chemistry", 2nd Edition.
- Graenicher, H., Jaccard, C., Sherrer, P. and Steinmann, A. (1957) Disc. Faraday Soc. Vol. 23, page 50.
- Henry, P.S.M. (1952) Brit. J. App. Phys. Supplement 2, page 31.
- Hueckel, E. Z. Elektrochem. Vol. 34, page 596.
- Iribarne, J.V. and Mason, B.J. (1967) Electrification accompanying the bursting of bubbles in water and dilute aqueous solutions. Trans. Faraday Soc. Vol. 163, page 537, part 9.
- Jaccard, C. (1963) Thermoelectric effects in ice crystals. Physik Der Kondens Materie, Vol. 2, page 143.
- Johnson, D.A. and Hallett, J. (1968) Freezing and shattering of supercooled water drops. Quart. J. Royal Met. Soc. Vol. 94, page 468.
- Kachurin, L.G. and Bekryaev, V.I. (1960) Investigation of the electrification of crystallizing water. Dokl. Akad. Nauk. SSSR. No.1, page 57.
- Kuettner, J. (1950) The electrical and meteorological conditions inside thunderclouds. J. Met. Vol. 7, page 322.
- Latham, J. (1963) The electrification of frost deposits. Quart. J. Royal Met. Soc. Vol. 89, page 265.

- Latham, J. (1964A) Charge transfer associated with temperature gradients in ice crystals grown in a diffusion chamber. Quart. J. Royal Met. Soc. Vol. 90, page 266.
- Latham, J. (1964B) Charge transfer associated with temperature gradients in ionic solutions. Nature. Vol. 202, page 686.
- Latham, J. and Mason, B.J. (1961A) Electric charge transfer associated with temperature gradients in ice. Proc. Roy. Soc. Vol. 260, No. 1303, page 523.
- Latham, J and Mason, B.J. (1961B) Generation of electric charge associated with the formation of soft hail in thunderclouds. Proc. Roy. Soc. A. Vol. 260, page 537.
- Latham, J. and Stow, C.D. (1965) Electrification associated with the evaporation of ice. J. Atmos. Sciences, Vol. 22, page 320.
- List, R. (1960) Growth and structure of graupel and hailstones. "Physics of Precipitation", Geophysical monograph 5, page 317, Am. Geophys. Union, Washington, D.C.
- Loeb, L.B. (1958) "Static Electrification".
- Lueder, H. (1951) Ein neuer elektrischer Effekt bei der Eisbildung durch Vergraupelung in natuerlichen unterkuehlten Nebeln. Zeit. fur Angewandte Physik, Vol. 3, page 247 and Vergraupelungselektroskopierung als eine Ursache der Gewitterelektrizitaet. Zeit fur Angewandte Physik, Vol. 3, page 288.
- MacCready, P.B. and Proudfit, A. (1965) Observations of hydrometer charge evolution in thunderstorms. Quart. J. Royal Met. Soc. Vol, 91, page 44.

- Macklin, W.C. (1961) Accretion in mixed clouds.
Quart. J. Royal Met. Soc.,
Vol. 87, page 413.
- Macklin, W.C. and
Ryan, B.F. (1962) On the formation of spongy ice.
Quart. J. Royal Met. Soc.,
Vol. 88, page 548.
- Macklin, W.C., and
Ryan, B.F. (1965) The structure of ice grown in
bulk supercooled water.
J. Atmos. Sciences, Vol.22, page 452.
- Magono, C. and
Takahashi, T. (1963) On the electrical phenomena
during riming and glazing in natural
supercooled cloud droplets.
J. Met. Soc. Japan. Series, II.
Vol. 41, page 71.
- Malan, D.J. and
Schonland, B.J.F. (1951) The distribution of electricity
in thunderclouds.
Proc. Roy. Soc. A. Vol. 209,
page 158.
- Mason, B.J. (1956) The nucleation of supercooled
water clouds.
Sci. Prog. Vol. 175, page 494.
- Mason, B.J. (1957) "The Physics of Clouds",
Oxford University Press.
- Mason, B.J. and
Maybank, J. (1960) The fragmentation and electrific-
ation of freezing water drops.
Quart. J. Royal Met. Soc.,
Vol. 86, page 176.
- McTaggart, H.A. (1914) The electrification at liquid-gas
surfaces.
Phil. Mag. Vol. 27, page 297.
- McTaggart, H.A. (1914) Electrification at liquid-gas
surfaces.
Phil. Mag. Vol. 28, page 367.
- McTaggart, H.A. (1922) On the electrification at the
boundary between a liquid and a
gas.
Phil. Mag. Vol. 44, page 386.

- Moore, C.B. (1965A) "Problems in Atmospheric and Space Electricity", page 255.
- Moore, C.B. (1965B) Lightning discharge and precipitation. Quart. J. Royal Met. Soc., Vol. 91, page 363.
- Pauling, L. (1935) Structure and entropy of ice and other crystals. J. Amer. Chem. Soc. Vol 56, page 2680.
- Pauling, L. (1960) "Nature of the Chemical Bond", 3rd Ed. page 466.
- Perram, J.W. and Levine, S. (1968) A statistical treatment of hydrogen bonding in water. "Hydrogen Bonded Solvent System", ed. Covington and Jones. Taylor and Francis.
- Pople, J.A. (1951) Proc. Roy. Soc. A. Vol. 205, page 163.
- Pruppacher, H.R. (1967) Growth modes of ice crystals in supercooled water and aqueous solutions. J. Glaciol. Vol. 6, page 657 and
On the growth of ice crystals in supercooled water and aqueous solution drops. Pure and Appl. Geophysics. Vol. 66, page 186.
- Reynolds, S.E., Brook, M., and Gourley, M.F. (1957) Thunderstorm charge separation. Journal of Meteorology, Vol. 14, page 425.
- Rogers, L.N. (1967) Unpublished Durham Ph.D. thesis.
- Siksna, R. (1957) Conduction of electricity through ice and snow. Arkiv for Fysik Vol. 11, No.43, page 495.
- Simpson, G.C. and Robinson, G.D. (1940) The distribution of electricity in thunderclouds, II. Proc. Roy. Soc. A. Vol. 161, page 309.
- Stern, O. (1924) Z. Elek. Vol. 30, page 507.

- Stott, D. and
Hutchinson, W.C.A. (1965) The electrification of freezing water drops. Quart. J. Royal Met. Soc. Vol. 91, page 80.
- Tamura, Y. (1956) Electrification of minor shower clouds.
Report on N.S. contract, AF.62 (502)1219.
- Van Panthaleon van Eck, C.L.,
Mendel, H. and
Fahrenfort, J. (1958) A tentative interpretation of the results of recent X-ray and infra-red studies of liquid water and H₂ O-D₂ O mixtures.
Proc. Roy. Soc. A. Vol. 247, page 472.
- Wall, T.T. and
Hornig, D.F. (1965) J. Chem. Phys. Vol. 43, page 2079.
- Walrafen, G.E. (1968) Structure of Water.
"Hydrogen Bonded Solvent Systems", ed. Covington and Jones. Taylor and Francis.
- Weickmann, H.K. and
Aufm Kampe, H.J. (1950) Preliminary experimental results concerning charge generation in thunderstorms concurrent with the formation of hailstones.
J. Met. Vol. 7, page 404.
- Williams, J.C. (1958) Some properties of the lower positive charge in thunderclouds.
"Recent Advances in Atmospheric Electricity", Pergamon Press, page 425.
- Wilson, C.T.R. (1925) The electric field of a thundercloud and some of its effects.
Proc. Phys. Soc. London, Vol. 37., 32 D - 37 D.
- Workman, E.J. and
Holzer, R.E. (1942) N.A.C.A., Washington.
Tech. Note No. 850.
- Workman, E.J. and
Reynolds, S.E. (1949) Electrical activity as related to thunderstorm cell growth.
Bull. Amer. Met. Soc. Vol. 30, page 142.
- Workman, E.J. and
Reynolds, S.E. (1950) Electrical phenomena occurring during the freezing of dilute aqueous solutions and their possible relationship to thunderstorm electricity.
Physical Review, Vol.78, No.3, page 254.

ix.

Workman, E.J. and
Reynolds, S.E. (1953)

"Thunderstorm Electricity", ed.
Byers, H.R.
University of Chicago Press.

